

Evaporative Loss From External Floating–Roof Tanks

API PUBLICATION 2517
THIRD EDITION, FEBRUARY 1989

American Petroleum Institute
1220 L Street, Northwest
Washington, D.C. 20005



Evaporative Loss From External Floating-Roof Tanks

Measurement Coordination Department

API PUBLICATION 2517
THIRD EDITION, FEBRUARY 1989

American
Petroleum
Institute



SPECIAL NOTES

1. API PUBLICATIONS NECESSARILY ADDRESS PROBLEMS OF A GENERAL NATURE. WITH RESPECT TO PARTICULAR CIRCUMSTANCES, LOCAL, STATE, AND FEDERAL LAWS AND REGULATIONS SHOULD BE REVIEWED.

2. API IS NOT UNDERTAKING TO MEET THE DUTIES OF EMPLOYERS, MANUFACTURERS, OR SUPPLIERS TO WARN AND PROPERLY TRAIN AND EQUIP THEIR EMPLOYEES, AND OTHERS EXPOSED, CONCERNING HEALTH AND SAFETY RISKS AND PRECAUTIONS, NOR UNDERTAKING THEIR OBLIGATIONS UNDER LOCAL, STATE, OR FEDERAL LAWS.

3. INFORMATION CONCERNING SAFETY AND HEALTH RISKS AND PROPER PRECAUTIONS WITH RESPECT TO PARTICULAR MATERIALS AND CONDITIONS SHOULD BE OBTAINED FROM THE EMPLOYER, THE MANUFACTURER OR SUPPLIER OF THAT MATERIAL, OR THE MATERIAL SAFETY DATA SHEET.

4. NOTHING CONTAINED IN ANY API PUBLICATION IS TO BE CONSTRUED AS GRANTING ANY RIGHT, BY IMPLICATION OR OTHERWISE, FOR THE MANUFACTURE, SALE, OR USE OF ANY METHOD, APPARATUS, OR PRODUCT COVERED BY LETTERS PATENT. NEITHER SHOULD ANYTHING CONTAINED IN THE PUBLICATION BE CONSTRUED AS INSURING ANYONE AGAINST LIABILITY FOR INFRINGEMENT OF LETTERS PATENT.

5. GENERALLY, API STANDARDS ARE REVIEWED AND REVISED, REAFFIRMED, OR WITHDRAWN AT LEAST EVERY FIVE YEARS. SOMETIMES A ONE-TIME EXTENSION OF UP TO TWO YEARS WILL BE ADDED TO THIS REVIEW CYCLE. THIS PUBLICATION WILL NO LONGER BE IN EFFECT FIVE YEARS AFTER ITS PUBLICATION DATE AS AN OPERATIVE API STANDARD OR, WHERE AN EXTENSION HAS BEEN GRANTED, UPON REPUBLICATION. STATUS OF THE PUBLICATION CAN BE ASCERTAINED FROM THE API AUTHORIZING DEPARTMENT [TELEPHONE (202) 682-8000]. A CATALOG OF API PUBLICATIONS AND MATERIALS IS PUBLISHED ANNUALLY AND UPDATED QUARTERLY BY API, 1220 L STREET, N.W., WASHINGTON, D.C. 20005.

FOREWORD

In 1957, the API Evaporation Loss Committee initiated an extensive effort to collect available petroleum industry data on evaporative losses from external floating-roof tanks. An intensive study was made of these data and resulted in correlations for estimating evaporative losses from external floating-roof tanks. These results were published in February 1962 as API Publication 2517.

By the mid-1970s, as a result of the national energy crisis and increased concern for the environment, additional emphasis was placed on the need to reduce evaporative losses from petroleum storage tanks. Accordingly, in 1976 the API Committee on Evaporation Loss Measurement began a review and analysis of the prior API work and of more recent work performed by oil companies, manufacturers, industry groups, and regulatory agencies. From this analysis, and in view of the considerable improvements that had been made in both the technology of floating-roof tank seals and the methods for measuring evaporative losses, the committee recommended that the evaporative-loss data be updated and combined with new data obtained from an extensive test program. API responded by sponsoring a broad program that included laboratory, test-tank, and field-tank studies. From this intensive effort, the mechanisms of evaporative loss were identified, and the effects of the relevant variables were more precisely quantified. The results were published in February 1980 as the second edition of API Publication 2517.

The second edition of API Publication 2517 dealt with evaporative loss from the floating-roof rim seal and the shell-wetting loss from lowering the stock level in external floating-roof tanks. In 1984, as the result of other related API test programs, the Committee on Evaporation Loss Measurement believed that sufficient evidence existed to warrant an additional test program to determine the magnitude of evaporative losses from floating-roof fittings. A survey of tank manufacturers and owners was conducted to establish the type and number of typical roof fittings used on tanks of various diameters. From this survey and an API-sponsored test program performed in 1984, methods were developed for calculating the evaporative loss from the various external floating-roof fittings. As a result, API Publication 2517 was updated with this information, and this third edition was published.

This edition contains the following information:

- a. Section 2 contains the equations necessary for estimating the evaporative loss or the equivalent atmospheric hydrocarbon emissions from the general types of external floating-roof tanks currently available.
- b. Section 3 describes current typical external floating-roof tanks, including types of floating roofs, rim-seal systems, and roof fittings.
- c. Section 4 discusses the mechanisms of evaporative loss and the development of the loss correlations.

The entire data base and the details of the data analysis are on file at API. This third edition supersedes all previous editions of API Publication 2517.

API publications may be used by anyone desiring to do so. Every effort has been made by the Institute to assure the accuracy and reliability of the data contained in them; however, the Institute makes no representation, warranty, or guarantee in connection with this publication and hereby expressly disclaims any liability or responsibility for loss or damage resulting from its use or for the violation of any federal, state, or municipal regulation with which this publication may conflict.

Suggested revisions are invited and should be submitted to the director of the Measurement Coordination Department, American Petroleum Institute, 1220 L Street, N.W., Washington, D.C. 20005.

API COMMITTEE ON EVAPORATION LOSS MEASUREMENT (1988)

Brian J. Lewis, Chairman
Texaco Trading & Transportation Inc.
Denver, Colorado

James K. Walters, Secretary
American Petroleum Institute
Washington, D.C.

James R. Arnold
Colonial Pipeline Company
Atlanta, Georgia

F. L. (Bill) Blumquist
Petrex
Warren, Pennsylvania

J. Mike Braden
Pitt-Des Moines, Inc.
Des Moines, Iowa

Michael Butchello
Chevron Corporation
Richmond, California

Rob Ferry
Conservatek
Conroe, Texas

Richard E. Hills
Pitt-Des Moines, Inc.
Pittsburgh, Pennsylvania

Ronald C. Kern
Ultraflote Corporation
Houston, Texas

Royce J. Laverman
CBI Industries, Inc.
Plainfield, Illinois

Robert W. Powell
Exxon Research & Engineering
Company
Florham Park, New Jersey

Richard Rodack
Mobil Research & Development
Company
Princeton, New Jersey

Ann M. Ruebush
Chevron Research Corporation
Richmond, California

Hayden J. Silver
Texaco Inc.
Beacon, New York

Paul C. Tranquill
BP America Inc.
Cleveland, Ohio

Robert B. Wagoner
Matrix Service, Inc.
Tulsa, Oklahoma

Wesley S. Watkins
Williams Pipe Line Company
Tulsa, Oklahoma

Eugene Wittner
Shell Oil Company
Houston, Texas

Ellen H. Zampello
Conoco Inc.
Houston, Texas

COORDINATING COMMITTEE

James R. Arnold
Colonial Pipeline Company
Atlanta, Georgia

Brian J. Lewis
Texaco Trading & Transportation Inc.
Denver, Colorado

Wesley S. Watkins
Williams Pipe Line Company
Tulsa, Oklahoma

Eugene Wittner
Shell Oil Company
Houston, Texas

STANDARD 2517 (FITTINGS) WORKING GROUP

James R. Arnold, Chairman
Colonial Pipeline Company
Atlanta, Georgia

James K. Walters, Secretary
American Petroleum Institute
Washington, D.C.

J. Mike Braden
Pitt-Des Moines, Inc.
Des Moines, Iowa

Rob Ferry
Conservatek
Conroe, Texas

Richard E. Hills
Pitt-Des Moines, Inc.
Pittsburgh, Pennsylvania

Ronald C. Kern
Ultraflote Corporation
Houston, Texas

Royce J. Laverman
CBI Industries, Inc.
Plainfield, Illinois

Brian J. Lewis
Texaco Trading & Transportation Inc.
Denver, Colorado

Richard Rodack
Mobil Research & Development
Company
Princeton, New Jersey

Robert L. Russell
Unocal
Brea, California

Wesley S. Watkins
Williams Pipe Line Company
Tulsa, Oklahoma

Ellen H. Zampello
Conoco Inc.
Houston, Texas

CONTENTS

	Page
SECTION 1—SCOPE	1
SECTION 2—PROCEDURES FOR CALCULATING LOSSES	2
2.1 Loss Equations	2
2.1.1 General	2
2.1.2 Standing Storage Loss	2
2.1.3 Withdrawal Loss	2
2.1.4 Total Loss	3
2.2 Discussion of Variables	4
2.2.1 General	4
2.2.2 Standing Storage Loss Factors	4
2.2.2.1 Rim-Seal Loss Factor	4
2.2.2.2 Total Roof-Fitting Loss Factor	6
2.2.2.3 Vapor Pressure Function	6
2.2.2.4 Vapor Molecular Weight	12
2.2.2.5 Product Factor	13
2.2.2.6 Density of Condensed Vapor	13
2.2.3 Withdrawal Loss Factors	14
2.2.3.1 Significance	14
2.2.3.2 Annual Net Throughput	14
2.2.3.3 Clingage	14
2.2.3.4 Average Liquid Stock Density	15
2.3 Summary of Calculation Procedure	15
2.4 Sample Problem	15
2.4.1 Problem	15
2.4.2 Solution	16
2.4.2.1 Standing Storage Loss	16
2.4.2.2 Withdrawal Loss	18
2.4.2.3 Total Loss	19
SECTION 3—COMPONENTS OF EXTERNAL FLOATING-ROOF TANKS	34
3.1 External Floating-Roof Tanks	34
3.2 Floating Roofs	34
3.3 Rim Seals	34
3.3.1 General	34
3.3.2 Mechanical-Shoe Primary Seals	35
3.3.3 Resilient-Filled Primary Seals	37
3.3.4 Flexible-Wiper Primary Seals	38
3.3.5 Secondary Seals	38
3.3.6 Weather Shields	39
3.4 Roof Fittings	39
3.4.1 General	39
3.4.2 Access Hatches	39
3.4.3 Unslotted Guide-Pole Wells	39
3.4.4 Slotted Guide-Pole/Sample Wells	40
3.4.5 Gauge-Float Wells	40
3.4.6 Gauge-Hatch/Sample Wells	40
3.4.7 Vacuum Breakers	40
3.4.8 Roof Drains	41

3.4.9	Roof Legs.....	42
3.4.10	Rim Vents	43
SECTION 4—DETAILS OF LOSS ANALYSIS.....		43
4.1	Introduction	43
4.2	Loss Mechanisms	43
4.2.1	General.....	43
4.2.2	Rim-Seal Loss	44
4.2.3	Roof-Fitting Loss	45
4.2.4	Withdrawal Loss	45
4.3	Data Base for Loss Correlations.....	45
4.3.1	Standing Storage Loss Data	45
4.3.2	Withdrawal Loss Data	46
4.4	Development of Standing Storage Loss Correlation	46
4.4.1	General.....	46
4.4.2	Rim-Seal Loss Factors	46
4.4.3	Tank Diameter	46
4.4.4	Roof-Fitting Loss Factors	47
4.4.5	Vapor Pressure Function	47
4.4.6	Product Factors	47
4.4.7	Tank Paint Color.....	47
4.5	Development of Withdrawal Loss Correlation	47
SECTION 5—REFERENCES		48
APPENDIX A—DEVELOPMENT OF RIM-SEAL LOSS FACTORS		49
APPENDIX B—DEVELOPMENT OF RELATIONSHIP BETWEEN		
AIRFLOW RATE AND WIND SPEED		51
APPENDIX C—DEVELOPMENT OF DIAMETER FUNCTION		53
APPENDIX D—DEVELOPMENT OF ROOF-FITTING LOSS		
FACTORS		55
APPENDIX E—DEVELOPMENT OF VAPOR PRESSURE		
FUNCTION.....		57
APPENDIX F—DEVELOPMENT OF PRODUCT FACTORS.....		59
APPENDIX G—DEVELOPMENT OF CLINGAGE FACTORS		61
APPENDIX H—DOCUMENTATION RECORDS		63

Figures

1—Rim-Seal Loss Factor for a Welded Tank With a Mechanical-Shoe Primary Seal.....	7
2—Rim-Seal Loss Factor for a Welded Tank With a Liquid-Mounted Resilient-Filled Primary Seal.....	8
3—Rim-Seal Loss Factor for a Welded Tank With a Vapor-Mounted Resilient-Filled Primary Seal.....	9
4—Rim-Seal Loss Factor for a Riveted Tank With a Mechanical-Shoe Primary Seal.....	10
5—Roof-Fitting Loss Factor for Access Hatches.....	14
6—Roof-Fitting Loss Factor for Unslotted Guide-Pole Wells.....	15
7—Roof-Fitting Loss Factor for Slotted Guide-Pole/Sample Wells	16
8—Roof-Fitting Loss Factor for Gauge-Float Wells	17
9—Roof-Fitting Loss Factor for Gauge Hatch/Sample Wells	18
10—Roof-Fitting Loss Factor for Vacuum Breakers	19
11—Roof-Fitting Loss Factor for Roof Drains.....	20
12—Roof-Fitting Loss Factor for Adjustable Roof Legs	21

13—Roof-Fitting Loss Factor for Rim Vents	22
14—Total Roof-Fitting Loss Factor for Typical Fittings on Pontoon Floating Roofs	24
15—Total Roof-Fitting Loss Factor for Typical Fittings on Double-Deck Floating Roofs	25
16—Vapor Pressure Function	26
17A—True Vapor Pressure of Refined Petroleum Stocks With a Reid Vapor Pressure of 1–20 Pounds per Square Inch.....	27
17B—Equation for True Vapor Pressure of Refined Petroleum Stocks With a Reid Vapor Pressure of 1–20 Pounds per Square Inch	29
18A—True Vapor Pressure of Crude Oils With a Reid Vapor Pressure of 2–15 Pounds per Square Inch	28
18B—Equation for True Vapor Pressure of Crude Oils With a Reid Vapor Pressure of 2–15 Pounds per Square Inch.....	29
19—External Floating-Roof Tank With Pontoon Floating Roof.....	35
20—External Floating-Roof Tank With Double-Deck Floating Roof	36
21—Mechanical-Shoe Primary Seal	37
22—Resilient-Filled Primary Seal.....	37
23—Flexible-Wiper Primary Seal	38
24—Mechanical-Shoe Primary Seal With Shoe-Mounted Secondary Seal.....	38
25—Resilient-Filled Primary Seal With Rim-Mounted Secondary Seal....	39
26—Access Hatch	39
27—Unslotted Guide-Pole Well	39
28—Slotted Guide-Pole/Sample Well.....	40
29—Gauge-Float Well	40
30—Gauge-Hatch/Sample Well.....	41
31—Vacuum Breaker	41
32—Overflow Roof Drain	42
33—Roof Leg.....	42
34—Rim Vent	43
C-1—Calculated Losses as a Function of Diameter Exponent	54

Tables

1—Summary of Procedure for Calculating Standing Storage Loss	3
2—Summary of Procedure for Calculating Withdrawal Loss	5
3—Rim-Seal Loss Factors, K_r and n	5
4—Average Annual Wind Speed (V) for Selected U.S. Locations	11
5—Roof-Fitting Loss Factors, K_{f6} , K_{f7} , and m , and Typical Number of Roof Fittings, N_f	13
6—Typical Number of Vacuum Breakers, N_{f6} , and Roof Drains, N_{f7}	23
7—Typical Number of Roof Legs, N_{f8}	23
8—Physical Properties of Selected Petrochemicals	30
9—Average Annual Ambient Temperature (T_a) for Selected U.S. Locations.....	32
10—Average Annual Stock Storage Temperature (T_s) as a Function of Tank Paint Color.....	34
11—Average Clingage Factors, C	34

Evaporative Loss From External Floating-Roof Tanks

SECTION 1—SCOPE

This publication contains an improved method for estimating the total evaporative losses or the equivalent atmospheric hydrocarbon emissions from external floating-roof tanks that contain multicomponent hydrocarbon mixtures (such as crude oils and gasolines) or single-component stocks (such as petrochemicals). This publication was developed by the API Committee on Evaporation Loss Measurement. The equations presented are based on recent laboratory, test-tank, and field-tank data. These equations are intended to provide loss estimates for general equipment types, since it is not within the scope of this publication to address specific proprietary equipment designs.

Typical currently available types of floating roofs, rim-seal systems, and roof fittings are described for information only. This publication is not intended to be used as a guide for equipment design, selection, or operation.

The equations are intended to be used to estimate annual losses from external floating-roof tanks for various types of tank construction, floating roofs, rim-seal systems, and roof fittings, as well as for various liquid stocks, stock vapor pressures, tank sizes, and wind speeds. The equations are applicable to properly maintained equipment under normal working conditions. The equations were developed for liquids that are not boiling, stocks with a true vapor pressure ranging from approximately 1.5 to less than 14.7 pounds per square inch absolute, average wind speeds ranging from 2 to 15 miles per hour, and tank diameters greater than 20 feet. Without detailed field information, the estimation techniques become more approximate when used to calculate losses for time periods shorter than 1 year.

The equations are not intended to be used in the following applications:

- a. To estimate losses from unstable or boiling stocks or from mixtures of hydrocarbons or petrochemicals for which the vapor pressure is not known or cannot readily be predicted.
- b. To estimate losses from tanks in which the materials used in the rim seal, roof fittings, or both have either

deteriorated or been significantly permeated by the stored stock.

Section 2 includes a complete guide for estimating evaporative stock loss or the equivalent total atmospheric emissions from volatile stocks stored in external floating-roof tanks.

Note: The calculated pounds per year of total hydrocarbon losses may include both reactive and nonreactive compounds. To obtain reactive hydrocarbon emissions, the weight fraction of reactive hydrocarbons in the vapor must be applied.

Detailed equations are given in 2.1, and a description of how to determine specific values for the variables included in the equations is given in 2.2. References are made to tables and figures that include information about the most common (typical) values to use when specific information is not available. The loss-estimation procedures are summarized in 2.3 (Tables 1 and 2), and a sample problem is presented in 2.4.

Section 3 describes the typical equipment types covered in Section 2.

Section 4 describes the bases and development of the loss-estimation procedures presented in Section 2. The estimation procedures were developed to provide estimates of typical losses from external floating-roof tanks that are properly maintained and in normal working condition. Losses from poorly maintained equipment may be greater. Because the loss equations are based on equipment conditions that represent a large population of tanks, a loss estimate for a group of external floating-roof tanks will be more accurate than a loss estimate for an individual tank. It is difficult to determine precise values of the loss-related parameters for any individual tank.

Equipment should not be selected for use based solely on evaporative-loss considerations. Many other factors not addressed in this publication, such as tank operation, maintenance, and safety, are important in designing and selecting tank equipment for a given application.

SECTION 2—PROCEDURES FOR CALCULATING LOSSES

2.1 Loss Equations

2.1.1 GENERAL

This section outlines procedures for estimating the total annual evaporative stock loss or the equivalent atmospheric hydrocarbon vapor emissions from volatile stocks stored in external floating-roof tanks. The total loss, L_t , is the sum of the standing storage loss, L_s , and the withdrawal loss, L_w . In some cases, the withdrawal loss may be negligible (see 2.2.3.1); in these cases, the total loss is approximately equal to the standing storage loss.

2.1.2 STANDING STORAGE LOSS

The following minimum information is needed to calculate the standing storage loss, L_s :

- The true vapor pressure of the stock (or the Reid vapor pressure and average storage temperature of the stock).
- The type of stock.
- The tank diameter.
- The average wind speed at the tank site.

Improved estimates of the standing storage loss can be obtained through a knowledge of some or all of the following additional information:

- The type of tank construction (welded or riveted).
- The type of rim-seal system.
- The type and number of roof fittings.
- The type of floating-roof construction (pontoon or double-deck).
- The molecular weight of the stock vapor.

The standing storage loss, L_s , includes losses from the rim seal and the roof fittings. The standing storage loss can be estimated as follows:

$$L_s = (F_r D + F_t) P^* M_v K_c \quad (1)$$

Where:

- L_s = standing storage loss, in pounds per year.
- F_r = rim-seal loss factor, in pound-moles per foot-year.
- D = tank diameter, in feet.
- F_t = total roof-fitting loss factor, in pound-moles per year.
- P^* = vapor pressure function (dimensionless).
- M_v = average molecular weight of stock vapor, in pounds per pound-mole.
- K_c = product factor (dimensionless).

The standing storage loss is converted from pounds per year to barrels per year as follows:

$$L_s \text{ (barrels per year)} = \frac{L_s \text{ (pounds per year)}}{42W_v} \quad (2)$$

Where:

- W_v = density of the condensed vapor, in pounds per gallon.

The procedures used to calculate the standing storage loss are summarized in Table 1.

Equation 1 was derived by adding together the two equations that represent the independent loss contributions of the rim seal and the roof fittings. The following equations can be used to estimate the independent contributions:

$$L_r = F_r D P^* M_v K_c \quad (3)$$

$$L_t = F_t P^* M_v K_c \quad (4)$$

Where:

- L_r = rim-seal loss, in pounds per year.
- L_t = total roof-fitting loss, in pounds per year.

The other variables are as defined for Equation 1.

2.1.3 WITHDRAWAL LOSS

The withdrawal loss, L_w , can be calculated from the following information:

- The annual net throughput (associated with lowering the liquid stock level in the tank).
- The type of stock.
- The average liquid stock density.
- The tank diameter.
- The condition of the tank shell.

The withdrawal loss, L_w , pertains to the evaporation of liquid stock that clings to the tank shell while the stock is withdrawn. The withdrawal loss can be estimated as follows:

$$L_w = \frac{0.943 Q C W_1}{D} \quad (5)$$

Where:

- L_w = withdrawal loss, in pounds per year.
- Q = annual net throughput (associated with lowering the liquid stock level in the tank), in barrels per year.
- C = clingage factor, in barrels per 1000 square feet.

Table 1—Summary of Procedure for Calculating Standing Storage Loss

Standing Storage Loss Equations			
		L_s (pounds per year) = $[(F_r D) + (F_f)]P^*M_sK_s$	(1)
		L_s (barrels per year) = $\frac{L_s \text{ (pounds per year)}}{42W_1}$	(2)
Variable	Definition	Units of Measurement	Source
F_r	= Rim-seal loss factor = $K_r V^n$ (Equation 9)	Pound-moles per foot-year	Figures 1–4 or Equation 9
K_r	= Rim-seal loss factor	Pound-moles per (miles per hour) ⁿ -foot-year	Table 3
V	= Average wind speed	Miles per hour	User specified or Table 4
n	= Rim-seal-related wind-speed exponent	(Dimensionless)	Table 3
D	= Tank diameter	Feet	User specified
F_f	= Total roof-fitting loss factor = $[(N_0 K_0) + (N_1 K_1) + \dots + (N_k K_k)]$ (Equation 10)	Pound-moles per year	If no specific information about the type and number of fittings is available: Figure 14 for a pontoon floating roof Figure 15 for a double-deck floating roof If specific information about the type and number of fittings is available: Equations 10 and 11, using values from Tables 5–7 or Figures 5–13
N_0	= Number of roof fittings of a particular type	(Dimensionless)	
K_0	= Roof-fitting loss factor for a particular type of fitting = $K_{0a} + K_{0b} V^m$ (Equation 11)	Pound-moles per year	
K_{0a}	= Roof-fitting loss factor	Pound-moles per year	
K_{0b}	= Roof-fitting loss factor	Pound-moles per (miles per hour) ^m -year	
m	= Roof-fitting loss factor	(Dimensionless)	
i	= 1, 2, . . . , k	(Dimensionless)	
V	= Average wind speed	Miles per hour	
k	= Total number of different types of roof fittings	(Dimensionless)	

W_1 = average liquid stock density at the average storage temperature, in pounds per gallon.

D = tank diameter, in feet.

The constant, 0.943, has dimensions of (1000 cubic feet) × [gallons per (barrel squared)].

The withdrawal loss is converted from pounds per year to barrels per year as follows:

$$L_w \text{ (barrels per year)} = \frac{L_w \text{ (pounds per year)}}{42W_1} \quad (6)$$

Where:

W_1 = average liquid stock density at 60°F, in pounds per gallon.

The procedures used to calculate withdrawal loss are summarized in Table 2.

2.1.4 TOTAL LOSS

The total loss, L_t , in pounds per year and barrels per year, can be estimated as follows:

Table 1—Continued

Standing Storage Loss Equations			
		L_s (pounds per year) = $[(F_r D) + (F_r)]P^*M,K_c$	(1)
		L_s (barrels per year) = $\frac{L_s \text{ (pounds per year)}}{42W_c}$	(2)
Variable	Definition	Units of Measurement	Source
P^*	= Vapor pressure function	(Dimensionless)	Figure 16 (or Equation 12)
P	= True vapor pressure	Pounds per square inch absolute	Figure 17 for refined petroleum stocks Figure 18 for crude oils Table 8 for selected petrochemicals
RVP	= Reid vapor pressure (Figures 17 and 18)	Pounds per square inch	User specified
T_s	= average storage temperature of stock (Figures 17 and 18)	Degrees Fahrenheit	User specified or Tables 9 and 10
M_c	= Average molecular weight of stock vapor	Pounds per pound-mole	User specified or 64 for gasoline 50 for U.S. midcontinent crude oil Table 8 for selected petrochemicals
K_c	= Product factor	(Dimensionless)	1.0 for refined stocks 0.4 for crude oil 1.0 for single-component stocks
W_c	= Density of condensed vapor = Liquid stock density for pure compounds	Pounds per gallon	User specified or 0.08 M_c for refined petroleum stocks and crude oils Table 8 for selected petrochemicals

$$L_t \text{ (pounds per year)} = (L_s + L_w) \text{ (pounds per year)} \quad (7)$$

$$L_t \text{ (barrels per year)} = (L_s + L_w) \text{ (barrels per year)} \quad (8)$$

Where:

L_t = total loss.

L_s = standing storage loss.

L_w = withdrawal loss.

2.2 Discussion of Variables

2.2.1 GENERAL

Information is summarized below on how to determine specific values for the variables in the loss equations given in 2.1. Tables, figures, and the range of values of the variables for which the loss equations are applicable are cited for reference.

To obtain the most accurate estimate, the detailed quantities, sizes, and other information pertinent to the specific tank or tanks under consideration should be used. The typical quantities and sizes included in the tables and figures should be used only when actual detailed information is not available. More detailed discussions of the development, definition, and effects of these variables are given in Section 4 and the appendixes.

2.2.2 STANDING STORAGE LOSS FACTORS

2.2.2.1 Rim-Seal Loss Factor

The rim-seal loss factor, F_r , can be estimated as follows:

$$F_r = K_r V^n \quad (9)$$

Where:

K_r = rim-seal loss factor, in pound-moles per (miles per hour) ^{n} -foot-year.

V = average wind speed, in miles per hour.

n = rim-seal-related wind-speed exponent (dimensionless).

The rim-seal loss factors, K_r and n , are given in Table 3 as a function of tank construction and rim-seal system. There are three basic types of primary seals: mechanical shoe, resilient filled, and flexible wiper. Resilient-filled primary seals can be either vapor mounted or liquid mounted. Vapor-mounted primary seals are mounted on the floating roof so that a vapor space exists between the liquid stock and the bottom of the primary seal. Liquid-mounted primary seals are mounted so that the bottom of the primary seal touches the liquid. In addition to the primary seal, some rim-seal systems are also equipped

Table 2—Summary of Procedure for Calculating Withdrawal Loss

Withdrawal Loss Equations			
		$L_w \text{ (pounds per year)} = \frac{0.943QCW_1}{D}$	(5)
		$L_w \text{ (barrels per year)} = \frac{L_w \text{ (pounds per year)}}{42W_1}$	(6)
Variable	Definition	Units of Measurement	Source
Q	= Annual net throughput (associated with lowering the liquid stock level in the tank)	Barrels per year	User specified
C	= Clingage factor	Barrels per 1000 square feet	Table 11
W_1	= Average liquid stock density at average stock storage temperature (Equation 5)	Pounds per gallon	User specified or 6.1 for gasoline Table 8 for selected petrochemicals
D	= Tank diameter	Feet	User specified
W_2	= Average liquid stock density at 60°F (Equation 6)	Pounds per gallon	User specified or 6.1 for gasoline Table 8 for selected petrochemicals

with a secondary seal. For mechanical-shoe primary seals, the secondary seal can be either shoe mounted or rim mounted. For resilient-filled primary seals, the secondary seal is only rim mounted.

The factors for average-fitting seals are applicable for typical rim-seal conditions and should be used except

when a rim-seal system is known to be consistently tight fitting (that is, when there are no gaps more than 1/8 inch wide between the rim seal and the tank shell), in which case the factors for tight-fitting seals are applicable.

The development of these average and tight factors is described in Appendix A. Average factors were devel-

 Table 3—Rim-Seal Loss Factors, K_r , and n

Tank Construction and Rim-Seal System	Average-Fitting Seals		Tight-Fitting Seals ^a	
	K_r [lb-mole/(mi/hr) ² -ft-yr]	n (dimensionless)	K_r [lb-mole/(mi/hr) ² -ft-yr]	n (dimensionless)
Welded Tanks				
Mechanical-shoe seal				
Primary only	1.2 ^b	1.5 ^b	0.8	1.6
Shoe-mounted secondary	0.8	1.2	0.8	1.1
Rim-mounted secondary	0.2	1.0	0.2	0.9
Liquid-mounted resilient-filled seal				
Primary only	1.1	1.0	0.5	1.1
Weather shield	0.8	0.9	0.5	1.0
Rim-mounted secondary	0.7	0.4	0.5	0.5
Vapor-mounted resilient-filled seal				
Primary only	1.2	2.3	1.0	1.7
Weather shield	0.9	2.2	1.1	1.6
Rim-mounted secondary	0.2	2.6	0.4	1.5
Riveted Tanks				
Mechanical-shoe seal				
Primary only	1.3	1.5	c	c
Shoe-mounted secondary	1.4	1.2	c	c
Rim-mounted secondary	0.2	1.6	c	c

Note: The rim-seal loss factors K_r and n may only be used for wind speeds from 2 to 15 miles per hour.

^aCriteria for seal tightness are defined in 2.2.2.1.

^bIf no specific information is available, a welded tank with an average-

fitting mechanical-shoe primary seal only can be assumed to represent the most common or typical construction and rim-seal system in use.

^cNo evaporative-loss information is available for riveted tanks with consistently tight fitting rim-seal systems.

oped because it was not possible to quantify parameters for all rim-seal conditions that affect loss. It was thus not possible to determine an exact relationship between the rim-seal loss and rim-seal conditions.

The rim-seal loss factor, F_r , can be calculated using Equation 9 or read directly from Figures 1–4.

The rim-seal loss factors are only applicable for wind speeds from 2 to 15 miles per hour. If the average wind speed, V , at the tank site is not available, wind-speed data from the nearest local weather station or values from Table 4 may be used as an approximation.

If no information is available on the specific type of tank construction and rim-seal system, a welded tank with a mechanical-shoe primary seal may be assumed to represent the most common type currently in use. However, calculations based on such assumed data should be used only as a preliminary indication of evaporative losses. Losses from specific tanks must be based on the actual tank characteristics.

2.2.2.2 Total Roof-Fitting Loss Factor

If information is available on the specific type and number of roof fittings, the total roof-fitting loss factor, F_t , can be estimated as follows:

$$F_t = [(N_{t1}K_{t1}) + (N_{t2}K_{t2}) + \dots + (N_{tk}K_{tk})] \quad (10)$$

Where:

F_t = total roof-fitting loss factor, in pound-moles per year.

N_{ti} = number of roof fittings of a particular type (dimensionless).

K_{ti} = loss factor for a particular type of roof fitting, in pound-moles per year.

$i = 1, 2, \dots, k$ (dimensionless).

k = total number of different types of roof fittings (dimensionless).

The loss factor for a particular type of roof fitting, K_{ti} , can be estimated as follows:

$$K_{ti} = K_{tbi} + K_{tvi}V^{m_i} \quad (11)$$

Where:

K_{tbi} = loss factor for a particular type of roof fitting, in pound-moles per year.

K_{tvi} = loss factor for a particular type of roof fitting, in pound-moles per (miles per hour) ^{m_i} -year.

m_i = loss factor for a particular type of roof fitting (dimensionless).

$i = 1, 2, \dots, k$ (dimensionless).

V = average wind speed, in miles per hour.

The most common roof fittings are listed in Table 5, along with the associated roof-fitting-related loss fac-

tors, K_{t1} , K_{t2} , and m_i , for various types of construction details. These factors are applicable for typical roof-fitting conditions. The roof-fitting loss factors may only be used for wind speeds from 2 to 15 miles per hour. The loss factor for a particular type of roof fitting may be calculated using Equation 11 or read directly from Figures 5–13.

Since the number of each type of roof fitting can vary significantly from tank to tank, N_{ti} values for each type of roof fitting should be determined for the tank under consideration. If this information is not available, typical N_{ti} values are given in Tables 5, 6, and 7.

If no information is available about the specific type and number of roof fittings, a typical total roof-fitting loss factor, F_t , can be read from Figure 14 or 15. These figures show the total roof-fitting loss factor, F_t , as a function of tank diameter, D , for pontoon and double-deck floating roofs, respectively.

2.2.2.3 Vapor Pressure Function

The vapor pressure function, P^* , can be determined as follows:

$$P^* = \frac{P/P_a}{\{1 + [1 - (P/P_a)]^{0.5}\}^2} \quad (12)$$

Where:

P = true vapor pressure at the average stock storage temperature, in pounds per square inch absolute.

P_a = average atmospheric pressure at the tank location, in pounds per square inch absolute.

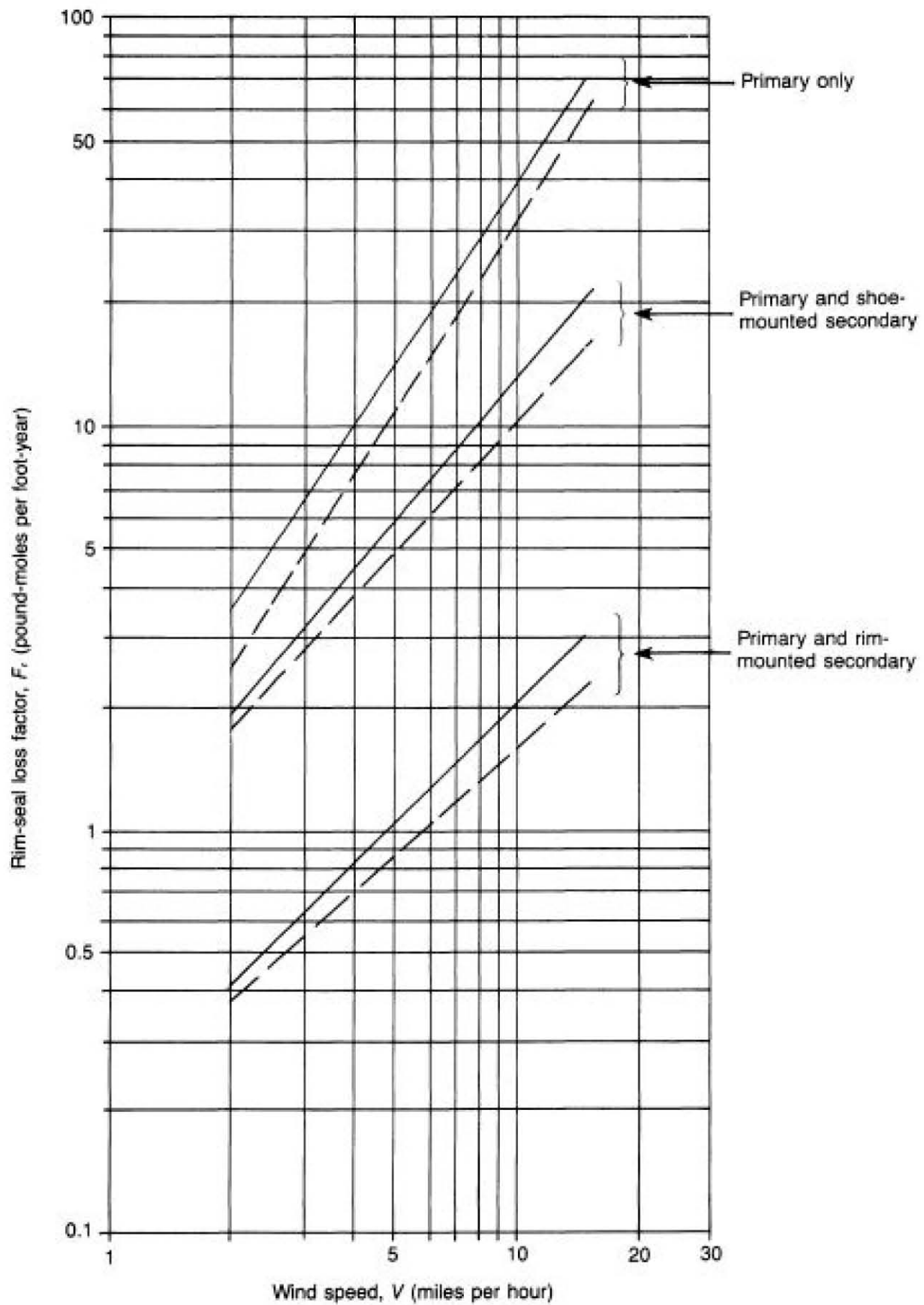
Alternatively, P^* can be read directly from Figure 16, which is based on an atmospheric pressure, P_a , of 14.7 pounds per square inch absolute.

True vapor pressures can be determined from Figures 17A and 17B for refined stocks (gasolines and naphthas) and from Figures 18A and 18B for crude oils by knowing the Reid vapor pressure, RVP , and the average stock storage temperature, T_s , in degrees Fahrenheit. Vapor pressures of selected petrochemical stocks are given in Table 8.

If the average stock storage temperature, T_s , is not known, it can be estimated from the average annual ambient temperature, T_a , in degrees Fahrenheit (given for selected U.S. locations in Table 9), and the tank paint color, using Table 10.

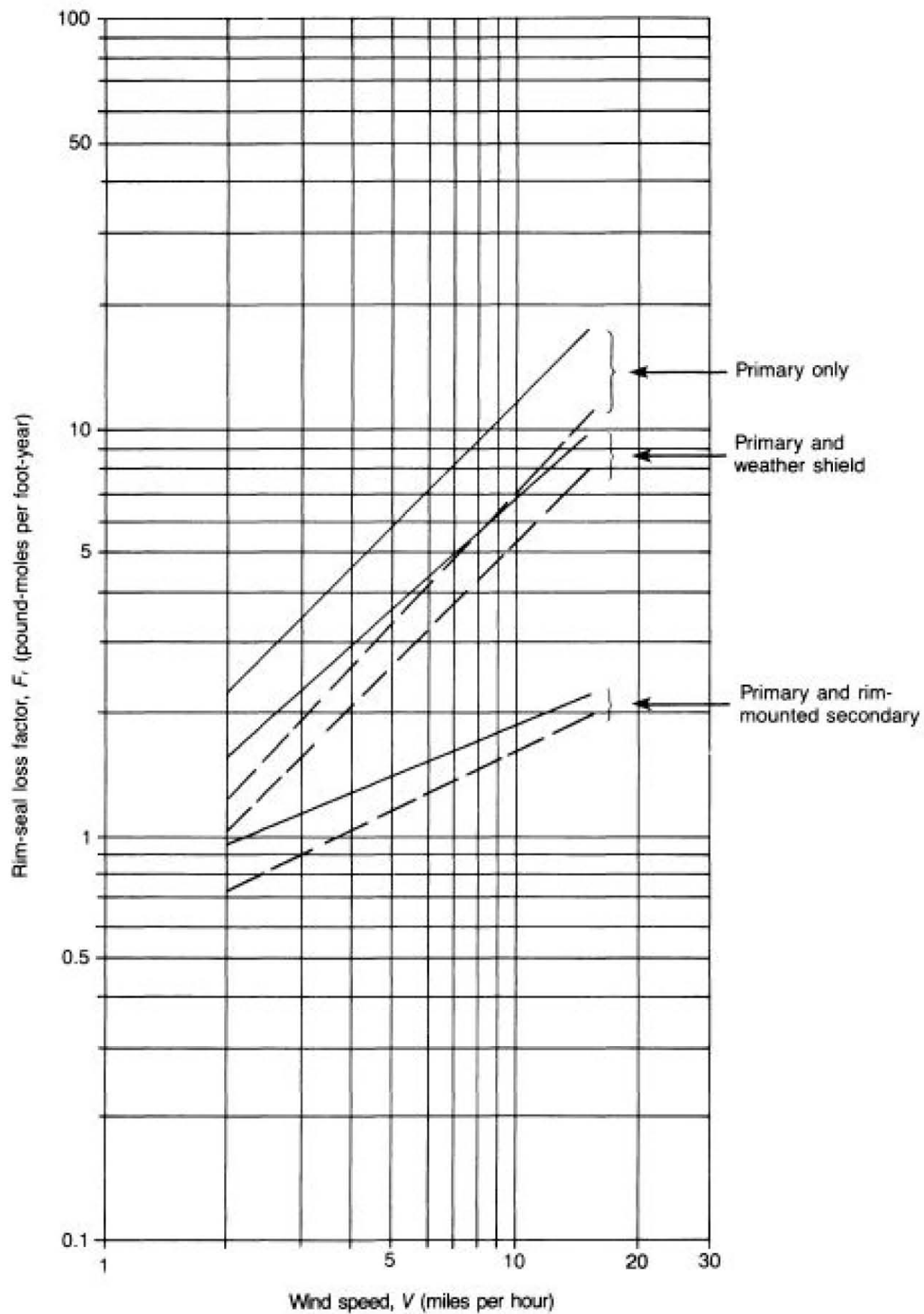
The loss equations are applicable for nonboiling stocks down to a true vapor pressure of at least 1.5 pounds per square inch absolute. The loss equations can be applied at lower vapor pressures with some small loss

(text continued on page 12)



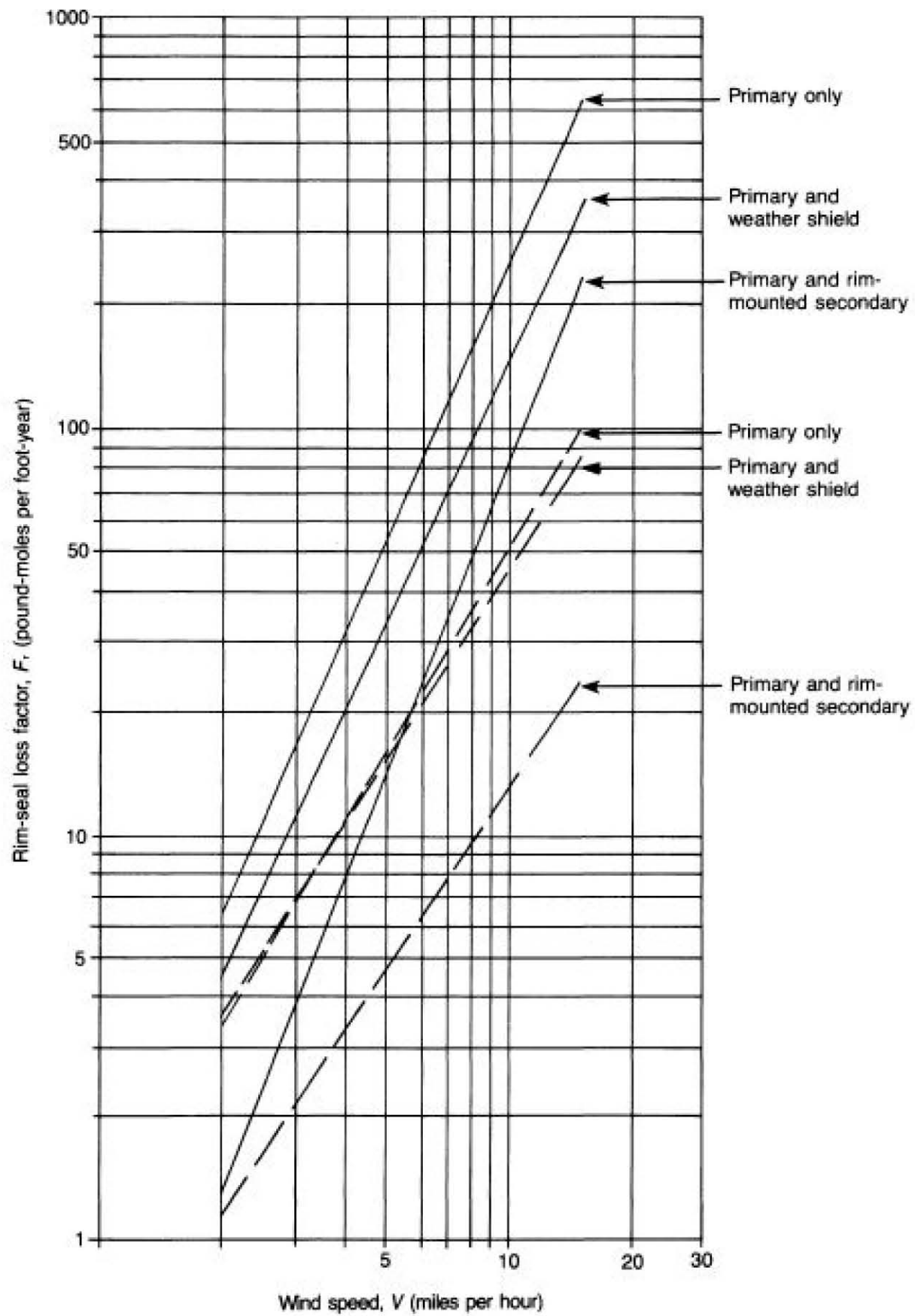
Note: Solid line indicates average-fitting seal; broken line indicates tight-fitting seal; $F_r = K_r V^n$.

Figure 1—Rim-Seal Loss Factor for a Welded Tank With a Mechanical-Shoe Primary Seal



Note: Solid line indicates average-fitting seal; broken line indicates tight-fitting seal; $F_r = K_r V^n$.

Figure 2—Rim-Seal Loss Factor for a Welded Tank With a Liquid-Mounted Resilient-Filled Primary Seal



Note: Solid line indicates average-fitting seal; broken line indicates tight-fitting seal; $F_r = K_r V^n$.

Figure 3—Rim-Seal Loss Factor for a Welded Tank With a Vapor-Mounted Resilient-Filled Primary Seal

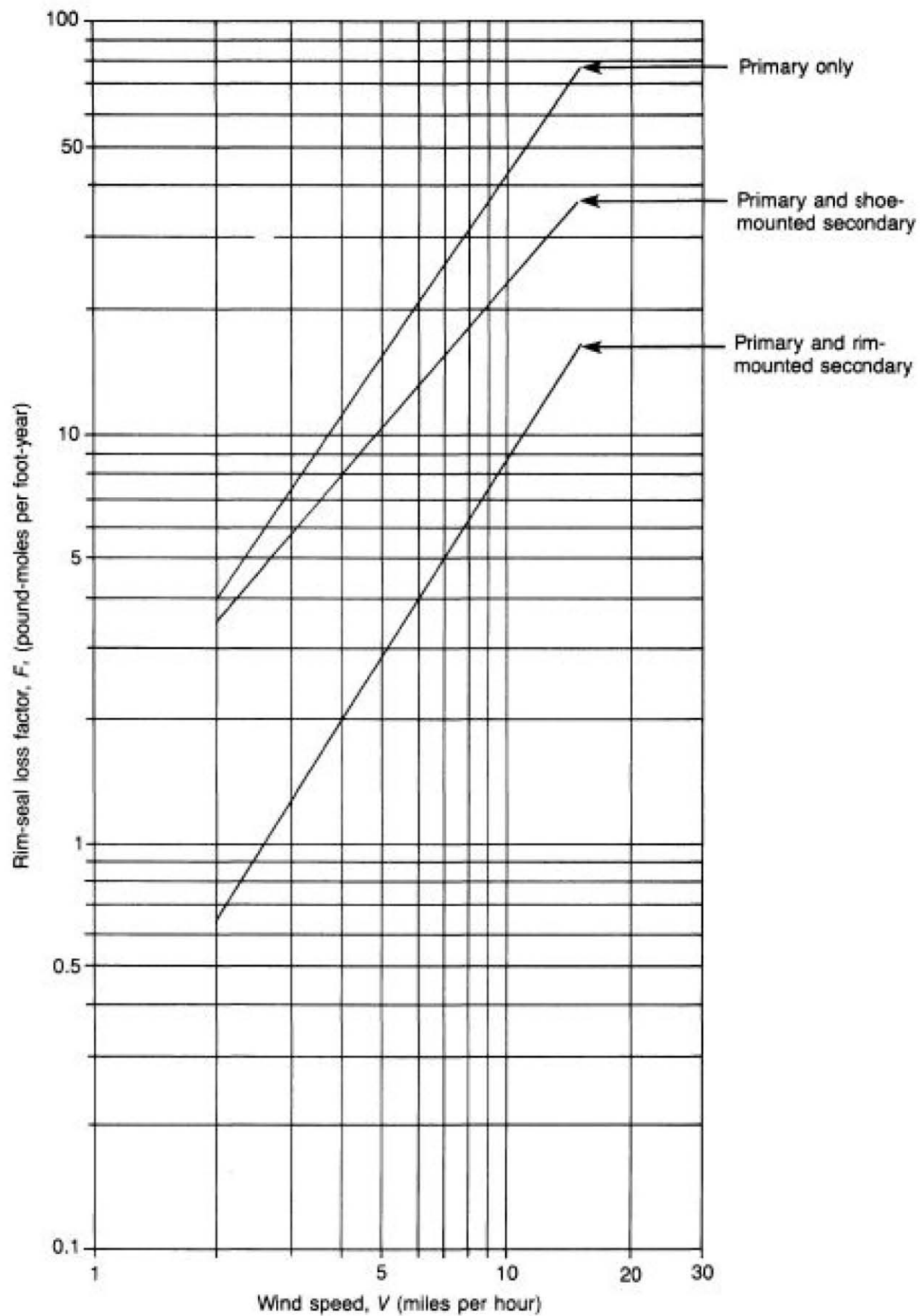


Figure 4—Rim-Seal Loss Factor for a Riveted Tank With a Mechanical-Shoe Primary Seal

Table 4—Average Annual Wind Speed (V) for Selected U.S. Locations

Location	Wind Speed (miles per hour)	Location	Wind Speed (miles per hour)	Location	Wind Speed (miles per hour)
Alabama		Delaware		Louisiana (continued)	
Birmingham	7.3	Wilmington	9.2	New Orleans	8.2
Huntsville	8.1	District of Columbia		Shreveport	8.6
Mobile	9.0	Dulles Airport	7.5	Maine	
Montgomery	6.7	National Airport	9.3	Caribou	11.2
Alaska		Florida		Portland	8.7
Anchorage	6.8	Apalachicola	7.9	Maryland	
Annette	10.6	Daytona Beach	8.8	Baltimore	9.2
Barrow	11.8	Fort Myers	8.2	Massachusetts	
Barter Island	13.2	Jacksonville	8.2	Blue Hill Observatory	15.4
Bethel	12.8	Key West	11.2	Boston	12.4
Bettles	6.7	Miami	9.2	Worcester	10.2
Big Delta	8.2	Orlando	8.6	Michigan	
Cold Bay	16.9	Pensacola	8.4	Alpena	7.9
Fairbanks	5.4	Tallahassee	6.5	Detroit	10.2
Gulkana	6.8	Tampa	8.6	Flint	10.3
Homer	7.2	West Palm Beach	9.5	Grand Rapids	9.8
Juneau	8.4	Georgia		Houghton Lake	8.9
King Salmon	10.7	Athens	7.4	Lansing	10.1
Kodiak	10.6	Atlanta	9.1	Muskegon	10.7
Kotzebue	13.0	Augusta	6.5	Sault Sainte Marie	9.4
McGrath	5.1	Columbus	6.7	Minnesota	
Nome	10.7	Macon	7.7	Duluth	11.2
St. Paul Island	18.3	Savannah	7.9	International Falls	9.0
Talkeetna	4.5	Hawaii		Minneapolis-Saint Paul	10.5
Valdez	6.0	Hilo	7.1	Rochester	12.9
Yakutat	7.4	Honolulu	11.6	Saint Cloud	8.0
Arizona		Kahului	12.8	Mississippi	
Flagstaff	7.3	Lihue	11.9	Jackson	7.4
Phoenix	6.3	Idaho		Meridian	6.0
Tucson	8.2	Boise	8.9	Missouri	
Winslow	8.9	Pocatello	10.2	Columbia	9.8
Yuma	7.8	Illinois		Kansas City (City)	9.9
Arkansas		Cairo	8.5	Kansas City Airport	10.7
Fort Smith	7.6	Chicago	10.3	Saint Louis	9.7
Little Rock	8.0	Moline	10.0	Springfield	10.9
California		Peoria	10.1	Montana	
Bakersfield	6.4	Rockford	9.9	Billings	11.3
Blue Canyon	7.7	Springfield	11.3	Glasgow	10.8
Eureka	6.8	Indiana		Great Falls	12.8
Fresno	6.4	Evansville	8.2	Havre	9.9
Long Beach	6.4	Fort Wayne	10.2	Helena	7.8
Los Angeles (City)	6.2	Indianapolis	9.6	Kalispell	6.6
Los Angeles International Airport	7.5	South Bend	10.4	Miles City	10.2
Mount Shasta	5.1	Iowa		Missoula	6.1
Oakland	8.2	Des Moines	10.9	Nebraska	
Red Bluff	8.6	Sioux City	11.0	Grand Island	12.0
Sacramento	8.1	Waterloo	10.7	Lincoln	10.4
San Diego	6.8	Kansas		Norfolk	11.8
San Francisco (City)	8.7	Concordia	12.3	North Platte	10.3
San Francisco International Airport	10.5	Dodge City	13.9	Omaha	10.6
Santa Maria	7.0	Goodland	12.6	Scotts Bluff	10.6
Stockton	7.5	Topeka	10.2	Valentine	10.0
Colorado		Wichita	12.4	Nevada	
Colorado Springs	10.1	Kentucky		Elko	6.0
Denver	8.8	Cincinnati Airport	9.1	Ely	10.4
Grand Junction	8.1	Jackson	7.0	Las Vegas	9.2
Pueblo	8.7	Lexington	9.5	Reno	6.5
Connecticut		Louisville	8.3	Winnemucca	7.9
Bridgeport	12.0	Louisiana		New Hampshire	
Hartford	8.5	Baton Rouge	7.7	Concord	6.7
		Lake Charles	8.7	Mount Washington	35.1

Table 4—Continued

Location	Wind Speed (miles per hour)	Location	Wind Speed (miles per hour)	Location	Wind Speed (miles per hour)
New Jersey		Oregon (continued)		Texas (continued)	
Atlantic City	10.2	Portland	7.9	Houston	7.8
Newark	10.2	Salem	7.0	Lubbock	12.4
New Mexico		Sexton Summit	11.8	Midland–Odessa	11.1
Albuquerque	9.1	Pennsylvania		Port Arthur	9.9
Roswell	8.7	Allentown	9.2	San Angelo	10.4
New York		Avoca	8.4	San Antonio	9.4
Albany	8.9	Erie	11.2	Victoria	10.0
Binghamton	10.3	Harrisburg	7.7	Waco	11.3
Buffalo	12.1	Philadelphia	9.5	Wichita Falls	11.7
New York (Central Park)	9.4	Pittsburgh International		Utah	
New York (JFK Airport)	12.2	Airport	9.2	Salt Lake City	8.8
New York (La Guardia		Williamsport	7.9	Vermont	
Airport)	12.3	Puerto Rico		Burlington	8.8
Rochester	9.8	San Juan	8.5	Virginia	
Syracuse	9.7	Rhode Island		Lynchburg	7.8
North Carolina		Providence	10.6	Norfolk	10.5
Asheville	7.6	South Carolina		Richmond	7.5
Cape Hatteras	11.4	Charleston	8.7	Roanoke	8.3
Charlotte	7.5	Columbia	6.9	Washington	
Greensboro–High Point	7.6	Greenville–Spartanburg	6.7	Olympia	6.7
Raleigh	7.8	South Dakota		Quillayute	6.1
Wilmington	8.9	Aberdeen	11.2	Seattle International	
North Dakota		Huron	11.7	Airport	9.1
Bismarck	10.3	Rapid City	11.2	Spokane	8.7
Fargo	12.5	Sioux Falls	11.1	Walla Walla	5.3
Williston	10.1	Tennessee		Yakima	7.1
Ohio		Bristol–Johnson City	5.6	West Virginia	
Akron	9.8	Chattanooga	6.2	Beckley	9.3
Cleveland	10.7	Knoxville	7.1	Charleston	6.4
Columbus	8.7	Memphis	9.0	Elkins	6.2
Dayton	10.1	Nashville	8.0	Huntington	6.5
Mansfield	11.0	Oak Ridge	4.4	Wisconsin	
Toledo	9.4	Texas		Green Bay	10.1
Youngstown	10.0	Abilene	12.2	La Crosse	8.8
Oklahoma		Amarillo	13.7	Madison	9.8
Oklahoma City	12.5	Austin	9.3	Milwaukee	11.6
Tulsa	10.4	Brownsville	11.6	Wyoming	
Oregon		Corpus Christi	12.0	Casper	12.9
Astoria	8.5	Dallas–Fort Worth	10.8	Cheyenne	12.9
Eugene	7.6	Del Rio	9.9	Lander	6.9
Medford	4.8	El Paso	9.2	Sheridan	8.1
Pendleton	9.0	Galveston	11.0		

Note: The data in this table are taken from *Comparative Climatic Data Through 1984*, National Oceanic and Atmospheric Administration, Asheville, North Carolina, 1986.

in accuracy, but they should not be applied at vapor pressures at which it is possible for the stock to reach a boiling state at the liquid surface. The vapor pressure of some mixtures of hydrocarbons or petrochemicals cannot be readily predicted; in these cases, the loss equations cannot be applied.

2.2.2.4 Vapor Molecular Weight

The molecular weight of the vapor, M_v , can be determined by analysis of vapor samples or by calculation

from the composition of the liquid. In the absence of this information, a typical value of 64 pounds per pound-mole can be assumed for gasoline, and a value of 50 pounds per pound-mole can be assumed for U.S. mid-continent crude oils (including both reactive and non-reactive fractions). Since a large variability in molecular weights has been observed in foreign crude oils, no average value has been developed for these stocks. For single-component stocks, the molecular weight of the vapor is equal to the molecular weight of the liquid stock, which is given in Table 8 for selected petrochemicals.

Table 5—Roof-Fitting Loss Factors, K_{fs} , K_{fb} , and m , and Typical Number of Roof Fittings, N_f

Fitting Type and Construction Details	Loss Factors			Typical Number of Fittings, N_f
	K_{fs} (lb-mole/yr)	K_{fb} [lb-mole/(mi/hr) ² -yr]	m (dimensionless)	
Access hatch (24-inch-diameter well)				1
Bolted cover, gasketed	0	0	0 ^a	
Unbolted cover, ungasketed	2.7	7.1	1.0	
Unbolted cover, gasketed	2.9	0.41	1.0	
Unslotted guide-pole well (8-inch-diameter unslotted pole, 21-inch-diameter well)				1
Ungasketed sliding cover	0	67	0.98 ^a	
Gasketed sliding cover	0	3.0	1.4	
Slotted guide-pole/sample well (8-inch-diameter slotted pole, 21-inch-diameter well)				^b
Ungasketed sliding cover, without float	0	310	1.2	
Ungasketed sliding cover, with float	0	29	2.0	
Gasketed sliding cover, without float	0	260	1.2	
Gasketed sliding cover, with float	0	8.5	2.4	
Gauge-float well (20-inch diameter)				1
Unbolted cover, ungasketed	2.3	5.9	1.0 ^a	
Unbolted cover, gasketed	2.4	0.34	1.0	
Bolted cover, gasketed	0	0	0	
Gauge-hatch/sample well (8-inch diameter)				1
Weighted mechanical actuation, gasketed	0.95	0.14	1.0 ^a	
Weighted mechanical actuation, ungasketed	0.91	2.4	1.0	
Vacuum breaker (10-inch-diameter well)				N_{fb} (Table 6)
Weighted mechanical actuation, gasketed	1.2	0.17	1.0 ^a	
Weighted mechanical actuation, ungasketed	1.1	3.0	1.0	
Roof drain (3-inch diameter)				N_{fr} (Table 6)
Open	0	7.0	1.4 ^c	
90% closed	0.51	0.81	1.0	
Roof leg (3-inch diameter)				N_{fb} (Table 7) ^d
Adjustable, pontoon area	1.5	0.20	1.0 ^a	
Adjustable, center area	0.25	0.067	1.0 ^a	
Adjustable, double-deck roofs	0.25	0.067	1.0	
Fixed	0	0	0	
Roof leg (2½-inch diameter)				N_{fb} (Table 7) ^d
Adjustable, pontoon area	1.7	0	0	
Adjustable, center area	0.41	0	0	
Adjustable, double-deck roofs	0.41	0	0	
Fixed	0	0	0	
Rim vent (6-inch diameter)				1 ^e
Weighted mechanical actuation, gasketed	0.71	0.10	1.0 ^a	
Weighted mechanical actuation, ungasketed	0.68	1.8	1.0	

Note: The roof-fitting loss factors, K_{fs} , K_{fb} , and m , may only be used for wind speeds from 2 to 15 miles per hour.

^aIf no specific information is available, this value can be assumed to represent the most common or typical roof fittings currently in use.

^bA slotted guide-pole/sample well is an optional fitting and is not typically used.

^cRoof drains that drain excess rainwater into the product are not used on pontoon floating roofs. They are, however, used on double-deck floating roofs and are typically left open.

^dThe most common roof leg diameter is 3 inches. The loss factors for 2½-inch-diameter roof legs are provided for use if this smaller size roof leg is used on a particular floating roof.

^eRim vents are used only with mechanical-shoe primary seals.

2.2.2.5 Product Factor

The product factor, K_c , accounts for the effect of different types of liquid stocks on evaporative loss. Product factors have been developed for multicomponent hydrocarbon mixtures, including refined stocks (such as gasolines and naphthas) and crude oils, as well as single-component stocks (such as petrochemicals):

$$\begin{aligned}
 K_c &= 1.0 \text{ for refined stocks} \\
 &= 0.4 \text{ for crude oils} \\
 &= 1.0 \text{ for single-component stocks}
 \end{aligned}$$

2.2.2.6 Density of Condensed Vapor

For refined petroleum stocks and crude oils, the density of the condensed vapor, W_v , is lower than the density

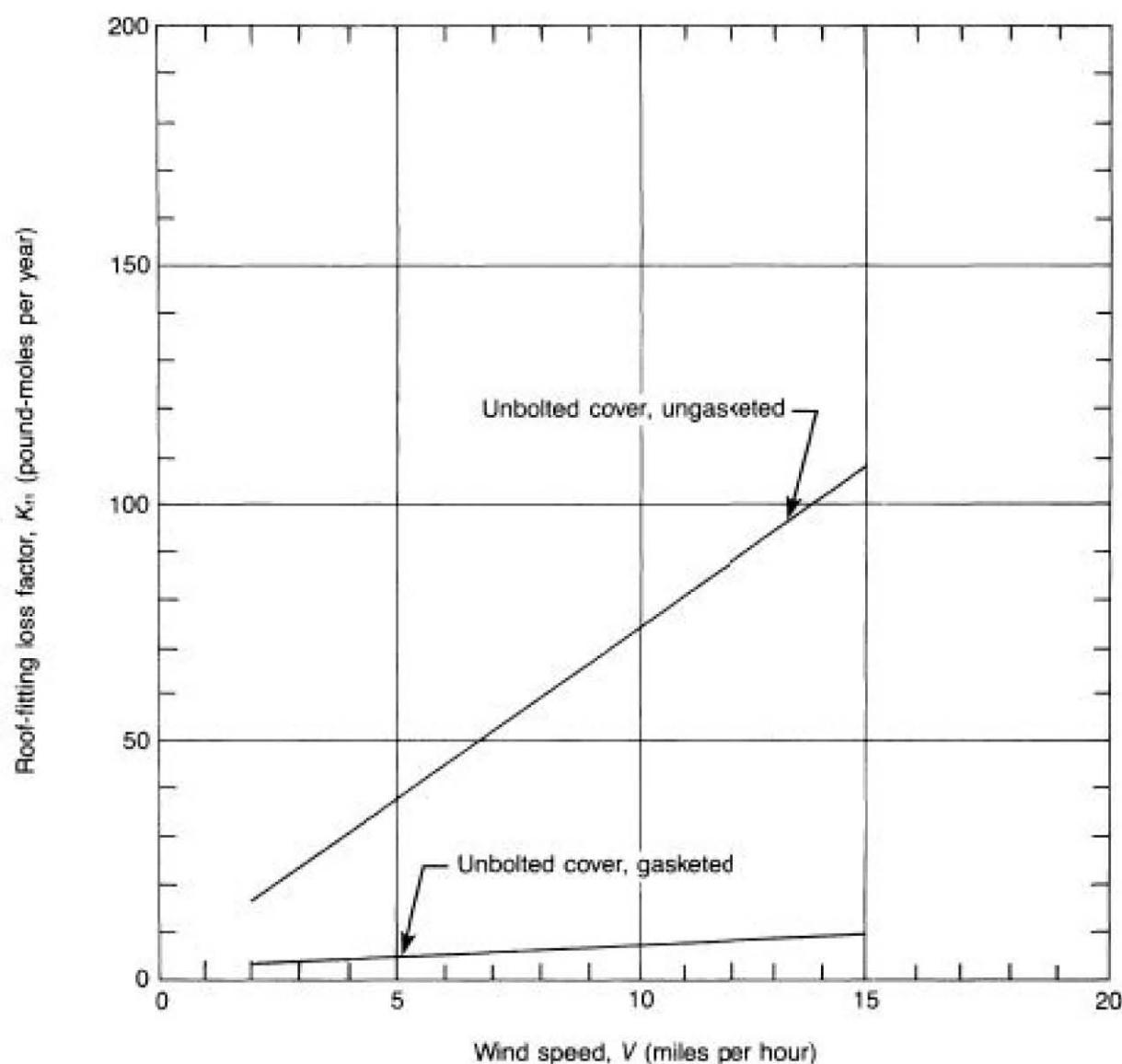


Figure 5—Roof-Fitting Loss Factor for Access Hatches

of the stored liquid stock. If the density of the condensed vapor is not known, it can be approximated from Equation 13, which was developed primarily for gasoline:

$$W_v = 0.08M_v \quad (13)$$

Where:

W_v = density of condensed vapor, in pounds per gallon.

M_v = vapor molecular weight, in pounds per pound-mole.

For single-component stocks, the density of the condensed vapor is equal to the density of the liquid stock, W_l . This information is given in Table 8 for selected petrochemicals.

2.2.3 WITHDRAWAL LOSS FACTORS

2.2.3.1 Significance

The significance of the withdrawal loss, L_w , will vary with tank operating practices. Industry-wide, with-

drawal loss can typically be assumed to be negligible relative to the standing storage loss, L_s . However, in cases of extremely high throughput that result in frequent tank turnovers, the withdrawal loss may become so significant that it should be included in a calculation of the total loss.

2.2.3.2 Annual Net Throughput

As used in this publication, annual net throughput, Q , is the total volume of stock withdrawn from the tank per year that results in a decrease in the level of the liquid in the tank. If filling and withdrawal occur equally and simultaneously so that the liquid level does not change, the net throughput is zero.

2.2.3.3 Clingage

Table 11 gives clingage factors, C , for steel tanks with light rust, dense rust, and gunite lining in gasoline, single-component stock, and crude oil service.

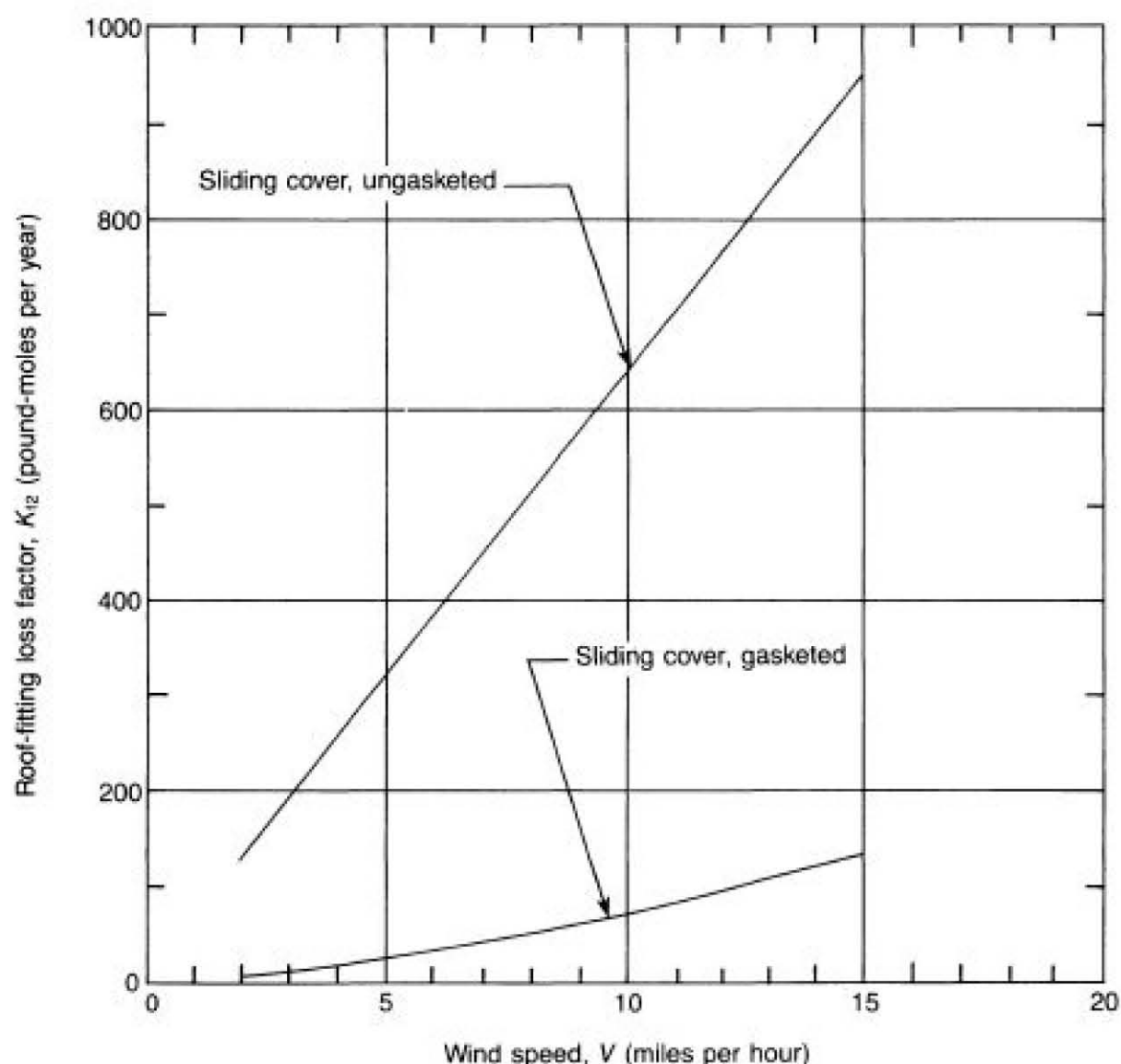


Figure 6—Roof-Fitting Loss Factor for Unslotted Guide-Pole Wells

2.2.3.4 Average Liquid Stock Density

The density of liquid stocks, W_1 , can vary significantly, particularly for crude oils and single-component stocks. This information is given in Table 8 for selected petrochemical stocks. For gasoline, the density is generally consistent enough that a typical value of 6.1 pounds per gallon can be assumed.

2.3 Summary of Calculation Procedure

Tables 1 and 2 summarize the equations and information necessary to estimate the total evaporative loss, including the standing storage loss and the withdrawal loss, respectively. The information in these tables is the same as that presented in 2.1 and 2.2, but without all of the important descriptive qualifiers presented in those sections. Therefore, questions about the information in Tables 1 and 2 should be answered by referring to 2.1 and 2.2 for more detailed information.

The total evaporative loss is the sum of the standing storage loss (Table 1) and the withdrawal loss (Table 2).

However, as noted in 2.2.3.1, the withdrawal loss can often be assumed to be negligible, in which case the total loss can be assumed to be approximately equal to the standing storage loss.

2.4 Sample Problem

2.4.1 PROBLEM

Estimate the total annual evaporative loss, in pounds per year and barrels per year, given the following information.

A welded, external floating-roof tank in good condition has the following characteristics:

- A diameter of 100 feet.
- A shell painted an aluminum color.
- A pontoon floating roof.
- A mechanical-shoe primary seal.
- Typical roof fittings.

The motor gasoline stored in the tank has the following characteristics (no vapor or liquid composition is given):

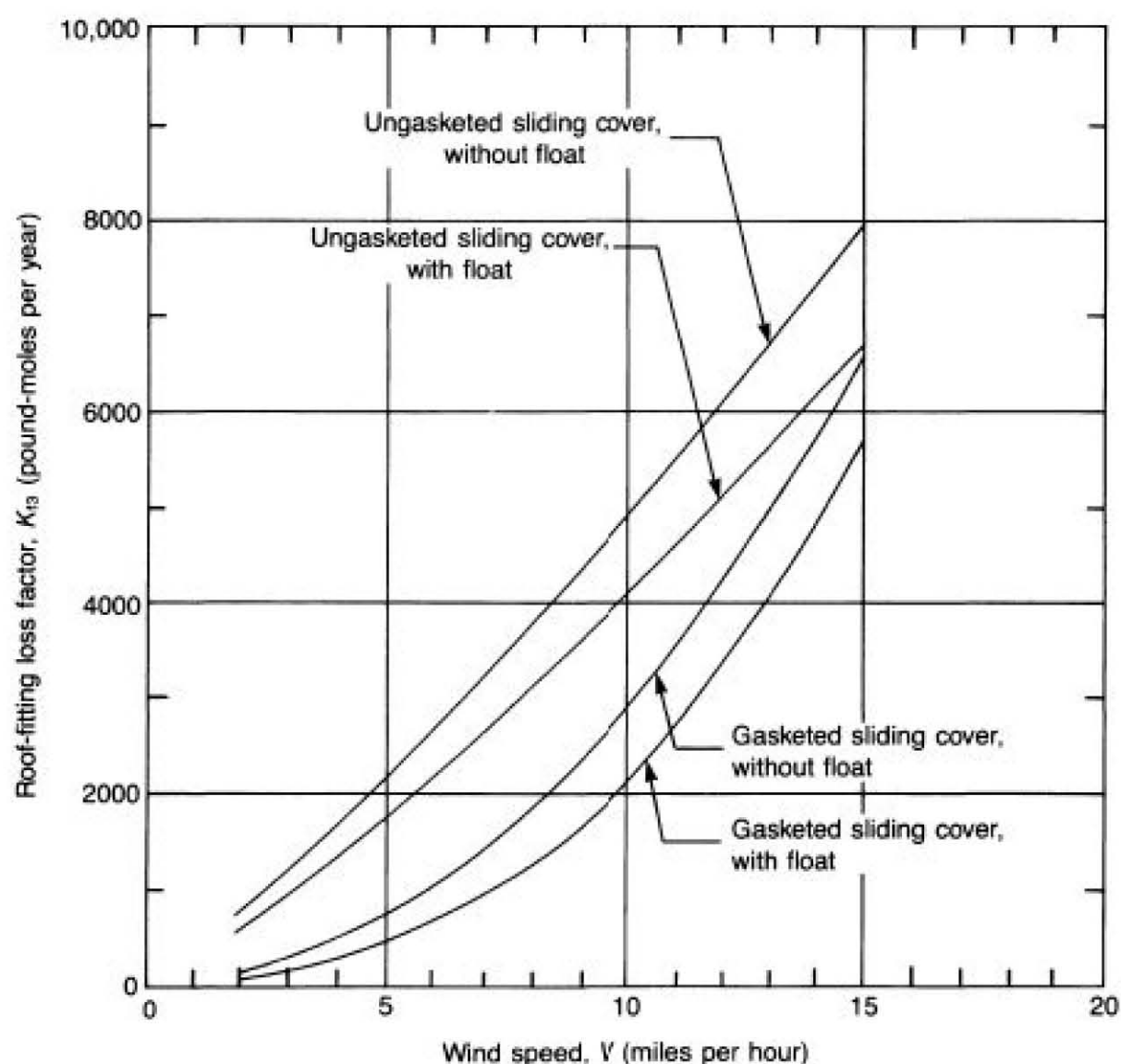


Figure 7—Roof-Fitting Loss Factor for Slotted Guide-Pole/Sample Wells

- A Reid vapor pressure of 10 pounds per square inch.
- A liquid stock density of 6.1 pounds per gallon.
- An average net throughput of 1.5 million barrels per year.

The ambient conditions are as follows:

- An average annual ambient temperature of 60°F.
- An atmospheric pressure of 14.7 pounds per square inch absolute.
- An average annual wind speed of 10 miles per hour.

2.4.2 SOLUTION

2.4.2.1 Standing Storage Loss

Calculate the standing storage loss from Equations 1 and 2:

$$L_s \text{ (pounds per year)} = [F_r D + F_t] P^* M_s K_c \quad (1)$$

$$L_s \text{ (barrels per year)} = \frac{L_s \text{ (pounds per year)}}{42 W_v} \quad (2)$$

The variables in Equations 1 and 2 can be determined as follows:

$$\begin{aligned} F_r &= K_r V^n \\ &= 38 \text{ pound-moles per foot-year (from Equation 9} \\ &\text{or from Figure 1 for an average-fitting primary} \\ &\text{seal only, with } V = 10 \text{ miles per hour).} \end{aligned}$$

Where:

$$K_r = 1.2 \text{ pound-moles per (miles per hour)}^{1.5}\text{-foot-year (from Table 3 for a welded tank with a mechanical-shoe primary seal).}$$

$$V = 10 \text{ miles per hour (given).}$$

$$n = 1.5 \text{ (from Table 3 for a welded tank with a mechanical-shoe primary seal).}$$

$$D = 100 \text{ feet (given).}$$

$$\begin{aligned} F_t &= [(N_{t1} K_{t1}) + (N_{t2} K_{t2}) + \dots + (N_{tk} K_{tk})] \\ &= 782 \text{ pound-moles per year (from Equation 10 or} \\ &\text{from Figure 14, with } V = 10 \text{ miles per hour).} \end{aligned}$$

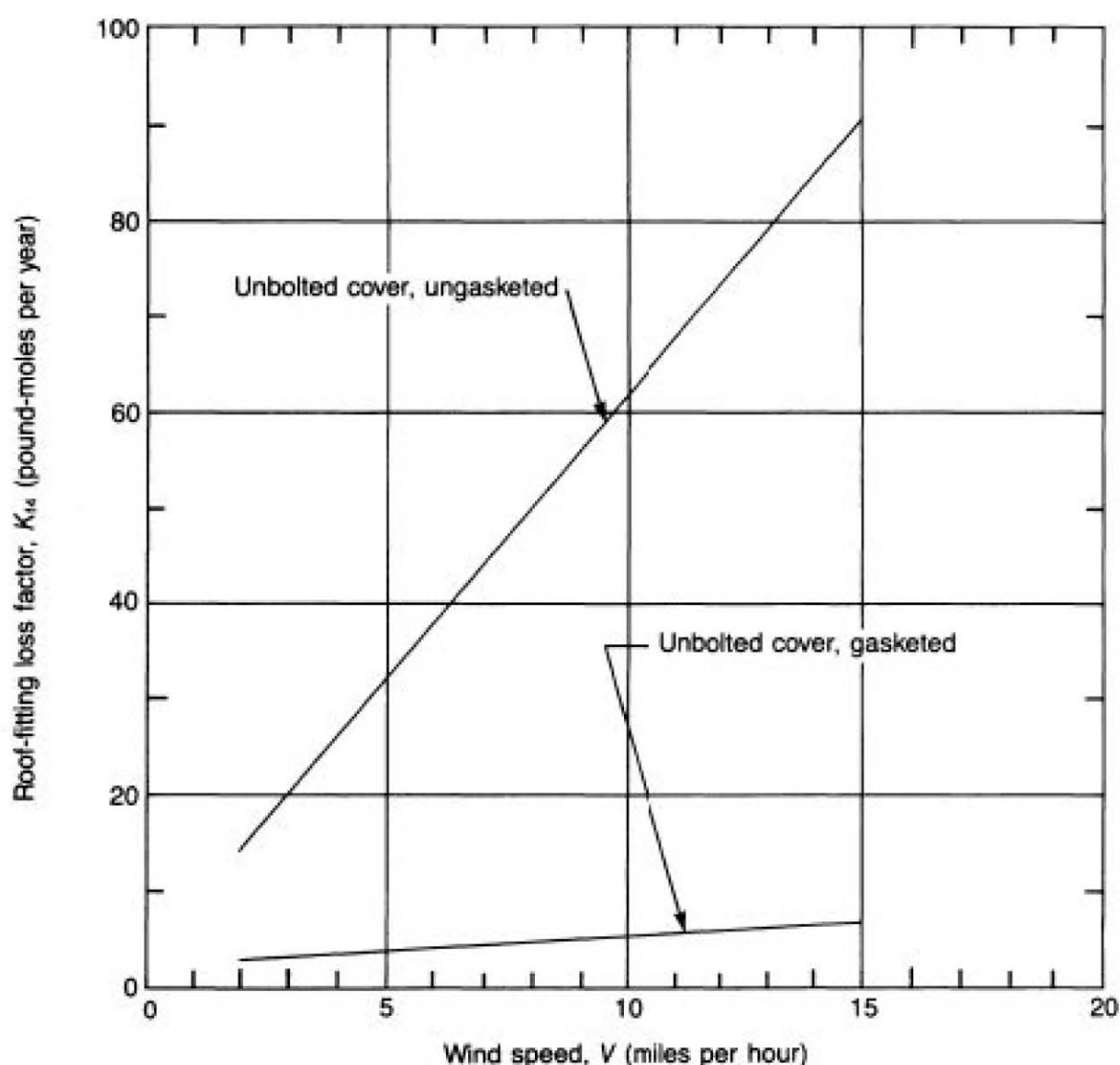


Figure 8—Roof-Fitting Loss Factor for Gauge-Float Wells

Where:

$$N_{f1}K_{f1} = (1)[(0) + (0)(10)^0]$$

= 0 pound-moles per year (for access hatches, from Equation 11 and Table 5 or from Figure 5).

$$N_{f2}K_{f2} = (1)[(0) + (67)(10)^{0.98}]$$

= 640 pound-moles per year (for unslotted guide-pole wells, from Equation 11 and Table 5 or from Figure 6).

$$N_{f3}K_{f3} = (\text{not typically used})$$

= 0 pound-moles per year (for slotted guide-pole/sample wells, from Equation 11 and Table 5 or from Figure 7).

$$N_{f4}K_{f4} = (1)[(2.3) + (5.9)(10)^{1.0}]$$

= 61.3 pound-moles per year (for gauge-float wells, from Equation 11 and Table 5 or from Figure 8).

$$N_{f5}K_{f5} = (1)[(0.95) + (0.14)(10)^{1.0}]$$

= 2.35 pound-moles per year (for gauge-

hatch/sample wells, from Equation 11 and Table 5 or from Figure 9).

$$N_{f6}K_{f6} = (1)[(1.2) + (0.17)(10)^{1.0}]$$

= 2.90 pound-moles per year (for vacuum breakers, from Equation 11 and Tables 5 and 6 or from Figure 10).

$$N_{f7}K_{f7} = (\text{not typically used})$$

= 0 pound-moles per year (for roof drains, from Equation 11 and Tables 5 and 6 or from Figure 11).

$$N_{f8}K_{f8} = (17)[(1.5) + (0.20)(10)^{1.0}] + (16)[(0.25) + (0.067)(10)^{1.0}]$$

= 74.2 pound-moles per year (for roof legs, from Equation 11 and Tables 5 and 7 or from Figure 12).

$$N_{f9}K_{f9} = (1)[(0.71) + (0.10)(10)^{1.0}]$$

= 1.71 pound-moles per year (for rim vents, from Equation 11 and Table 5 or from Figure 13).

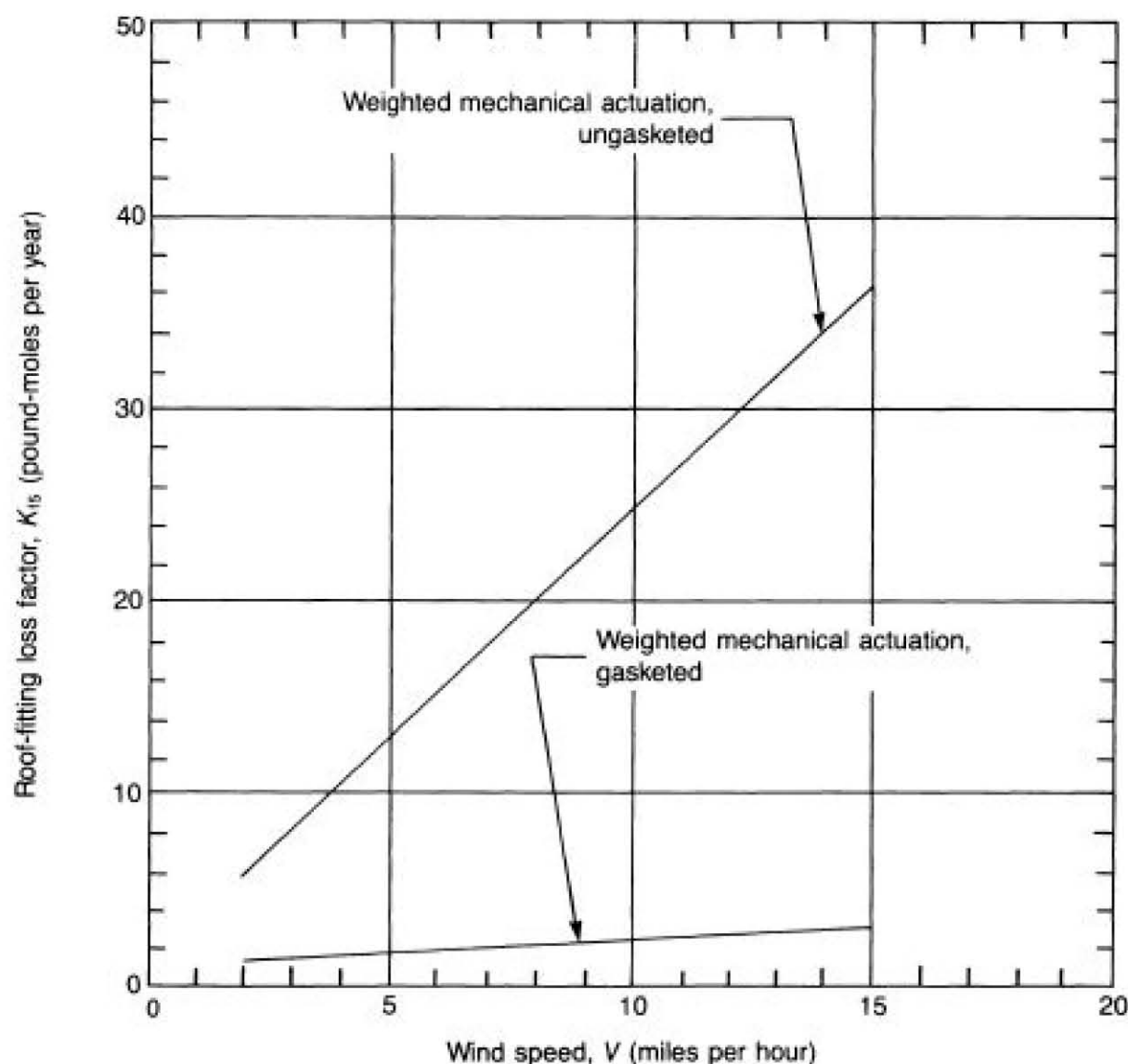


Figure 9—Roof-Fitting Loss Factor for Gauge-Hatch/Sample Wells

$$P^* = \frac{P/P_a}{\{1 + [1 - (P/P_a)]^{0.5}\}^2}$$

$$= \frac{5.4/14.7}{\{1 + [1 - (5.4/14.7)]^{0.5}\}^2}$$

$$= 0.114 \text{ (for } P = 5.4 \text{ pounds per square inch absolute, from Equation 12 or from Figure 16).}$$

Where:

$T_a = 60^\circ\text{F}$ (given).

$T_s = 62.5^\circ\text{F}$ (from Table 10 for an aluminum-colored tank).

$RVP =$ Reid vapor pressure.
 $= 10$ pounds per square inch (given).

$P = 5.4$ pounds per square inch absolute (for gasoline with $RVP = 10$ pounds per square inch and $T_s = 62.5^\circ\text{F}$, from Figure 17).

$P_a = 14.7$ pounds per square inch absolute (given).

$M_v = 64$ pounds per pound-mole (for gasoline, from 2.2.2.4).

$K_c = 1.0$ (for refined stocks, from 2.2.2.5).

$W_v = 5.1$ pounds per gallon (from Equation 13).

To calculate the standing storage loss in pounds per year, substitute the values above into Equation 1:

$$L_s = [(38)(100) + 782](0.114)(64)(1.0)$$

$$= 33,400 \text{ pounds per year}$$

To calculate the standing storage loss in barrels per year, substitute the values above into Equation 2:

$$L_s = 33,400/[(42)(5.1)]$$

$$= 156 \text{ barrels per year}$$

2.4.2.2 Withdrawal Loss

Calculate the withdrawal loss from Equations 5 and 6:

$$L_w \text{ (pounds per year)} = \frac{0.943QCW_1}{D} \quad (5)$$

$$L_w \text{ (barrels per year)} = \frac{L_w \text{ (pounds per year)}}{42W_1} \quad (6)$$

The variables in Equations 5 and 6 can be determined as follows:

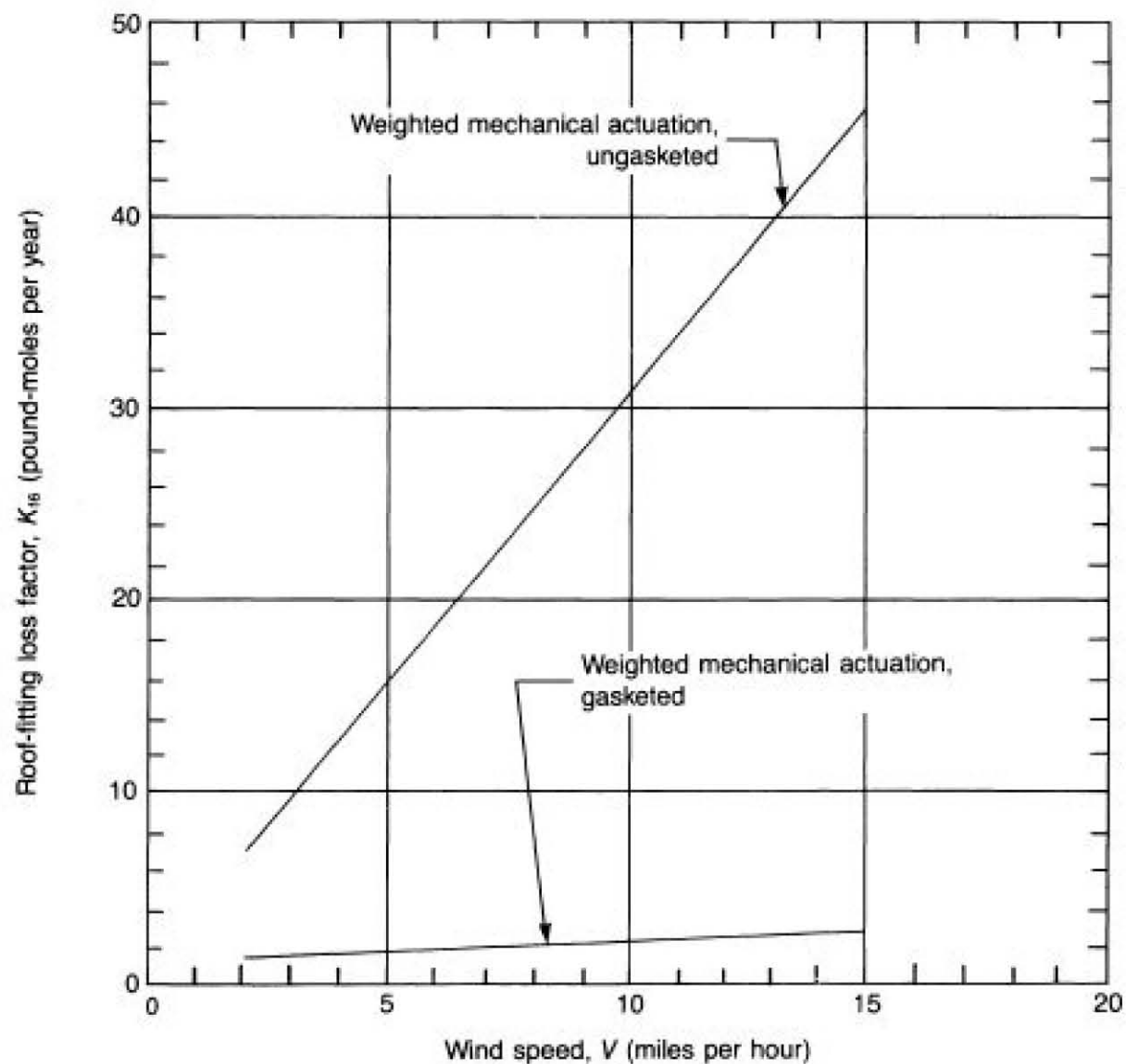


Figure 10—Roof-Fitting Loss Factor for Vacuum Breakers

$Q = 1.5 \times 10^6$ barrels per year (given).

$C = 0.0015$ barrel per 1000 square feet (for gasoline in a lightly rusted tank, from Table 11).

$W_1 = 6.1$ pounds per gallon (given).

$D = 100$ feet (given).

To calculate the withdrawal loss in pounds per year, substitute the values above into Equation 5:

$$L_w = [(0.943)(1.5 \times 10^6)(0.0015)(6.1)]/100 \\ = 129 \text{ pounds per year}$$

To calculate withdrawal loss in barrels per year, substitute the values above into Equation 6:

$$L_w = 129/[(42)(6.1)] \\ = 0.5 \text{ barrel per year}$$

2.4.2.3 Total Loss

Calculate the total loss from Equations 7 and 8:

$$L_t \text{ (pounds per year)} = (L_s + L_w) \text{ (pounds per year)} \quad (7) \\ = 33,400 + 129 \\ = 33,500 \text{ pounds per year}$$

$$L_t \text{ (barrels per year)} = (L_s + L_w) \text{ (barrels per year)} \quad (8) \\ = 156 + 0.5 \\ = 157 \text{ barrels per year}$$

(text continued on page 34)

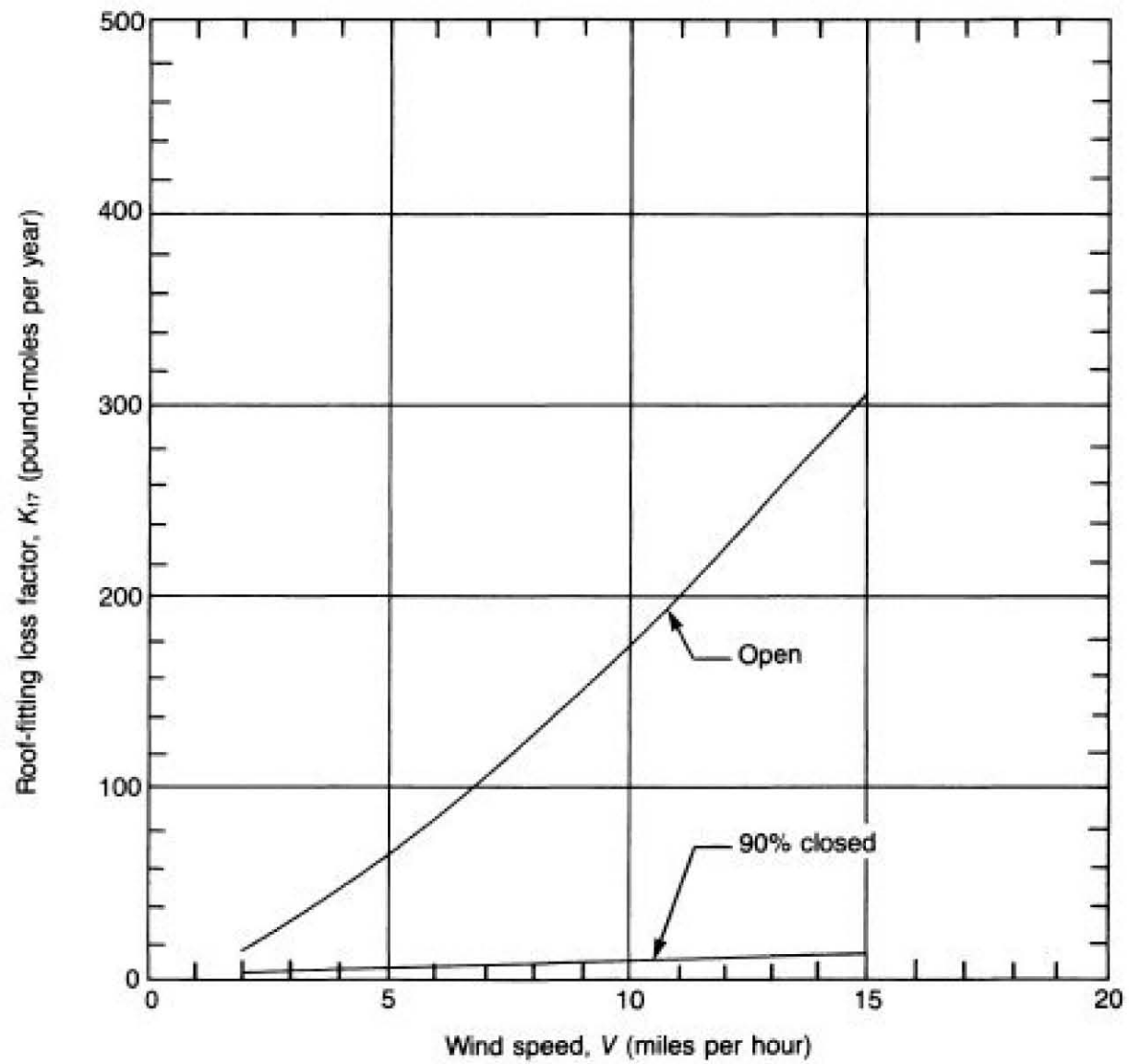


Figure 11—Roof-Fitting Loss Factor for Roof Drains

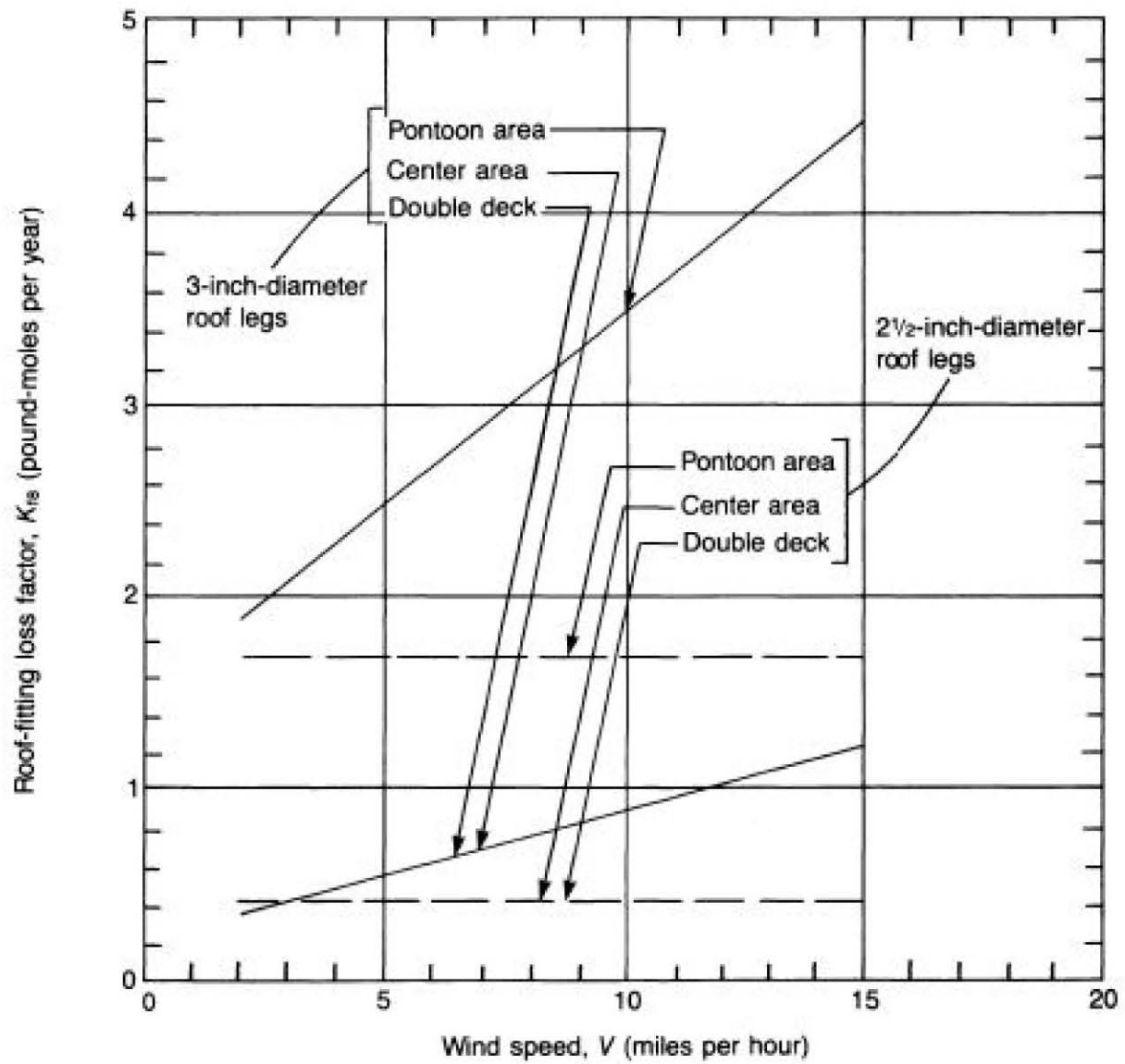


Figure 12—Roof-Fitting Loss Factor for Adjustable Roof Legs

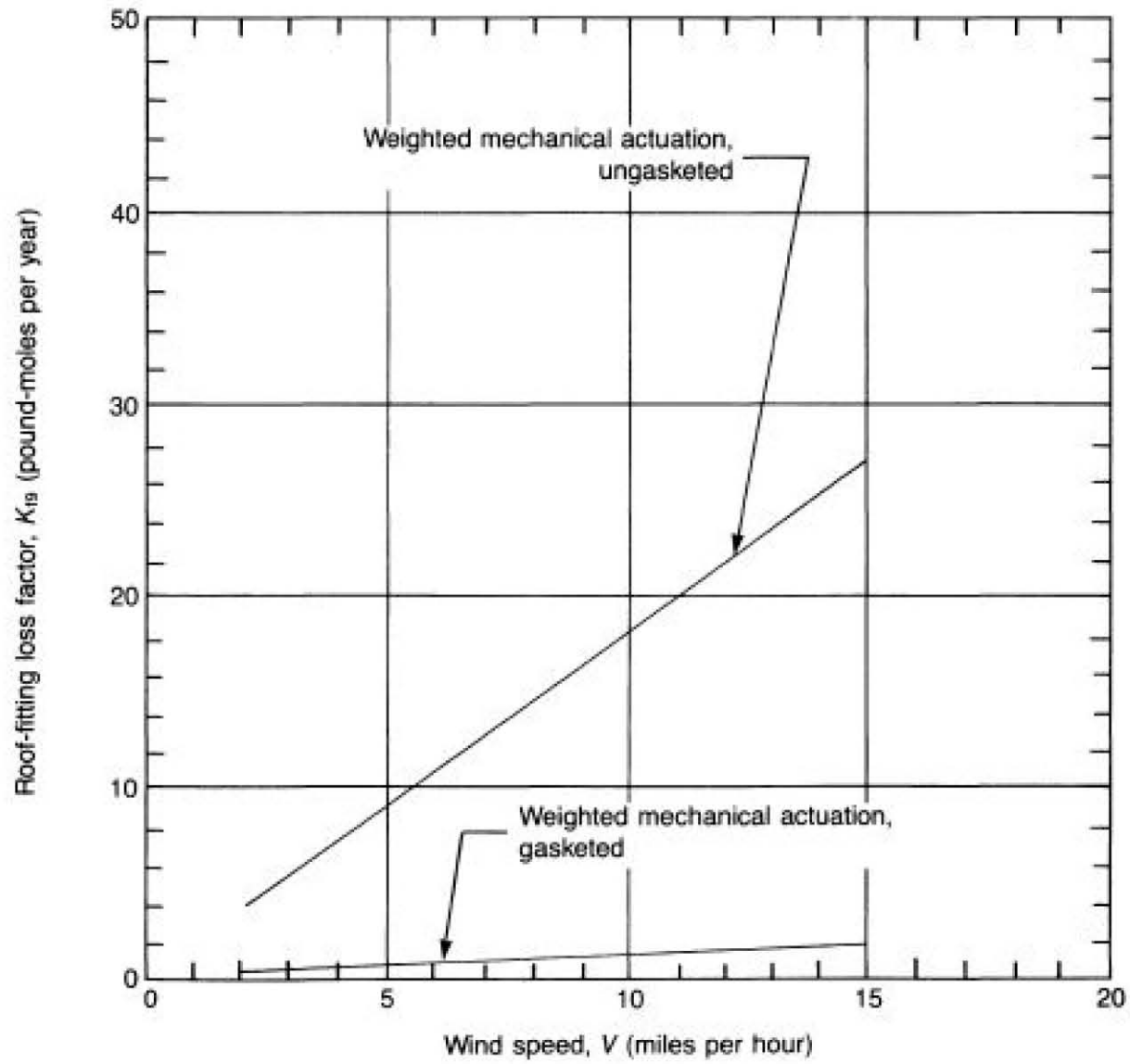


Figure 13—Roof-Fitting Loss Factor for Rim Vents

Table 6—Typical Number of Vacuum Breakers, N_{16} , and Roof Drains, N_{17}

Tank Diameter, D (feet) ^a	Number of Vacuum Breakers, N_{16}		Number of Roof Drains, N_{17} (Double-Deck Roof) ^b
	Pontoon Roof	Double-Deck Roof	
50	1	1	1
100	1	1	1
150	2	2	2
200	3	2	3
250	4	3	5
300	5	3	7
350	6	4	—
400	7	4	—

Note: This table was derived from a survey of users and manufacturers. The actual number of vacuum breakers may vary greatly depending on throughput and manufacturing prerogatives. The actual number of roof drains may also vary greatly depending on the design rainfall and manufacturing prerogatives. For tanks more than 300 feet in diameter, actual tank data or the manufacturer's recommendations may be needed for the number of roof drains. This table should not supersede information based on actual tank data.

^aIf the actual diameter is between the diameters listed, the closest diameter listed should be used. If the actual diameter is midway between the diameters listed, the next larger diameter should be used.

^bRoof drains that drain excess rainwater into the product are not used on pontoon floating roofs. They are, however, used on double-deck floating roofs and are typically left open.

Table 7—Typical Number of Roof Legs, N_{18}

Tank Diameter, D (feet) ^a	Pontoon Roof		Number of Legs on Double-Deck Roof
	Number of Pontoon Legs	Number of Center Legs	
30	4	2	6
40	4	4	7
50	6	6	8
60	9	7	10
70	13	9	13
80	15	10	16
90	16	12	20
100	17	16	25
110	18	20	29
120	19	24	34
130	20	28	40
140	21	33	46
150	23	38	52
160	26	42	58
170	27	49	66
180	28	56	74
190	29	62	82
200	30	69	90
210	31	77	98
220	32	83	107
230	33	92	115
240	34	101	127
250	35	109	138
260	36	118	149
270	36	128	162
280	37	138	173
290	38	148	186
300	38	156	200
310	39	168	213
320	39	179	226
330	40	190	240
340	41	202	255
350	42	213	270
360	44	226	285
370	45	238	300
380	46	252	315
390	47	266	330
400	48	281	345

Note: This table was derived from a survey of users and manufacturers. The actual number of roof legs may vary greatly depending on age, style of floating roof, loading specifications, and manufacturing prerogatives. This table should not supersede information based on actual tank data.

^aIf the actual diameter is between the diameters listed, the closest diameter listed should be used. If the actual diameter is midway between the diameters listed, the next larger diameter should be used.

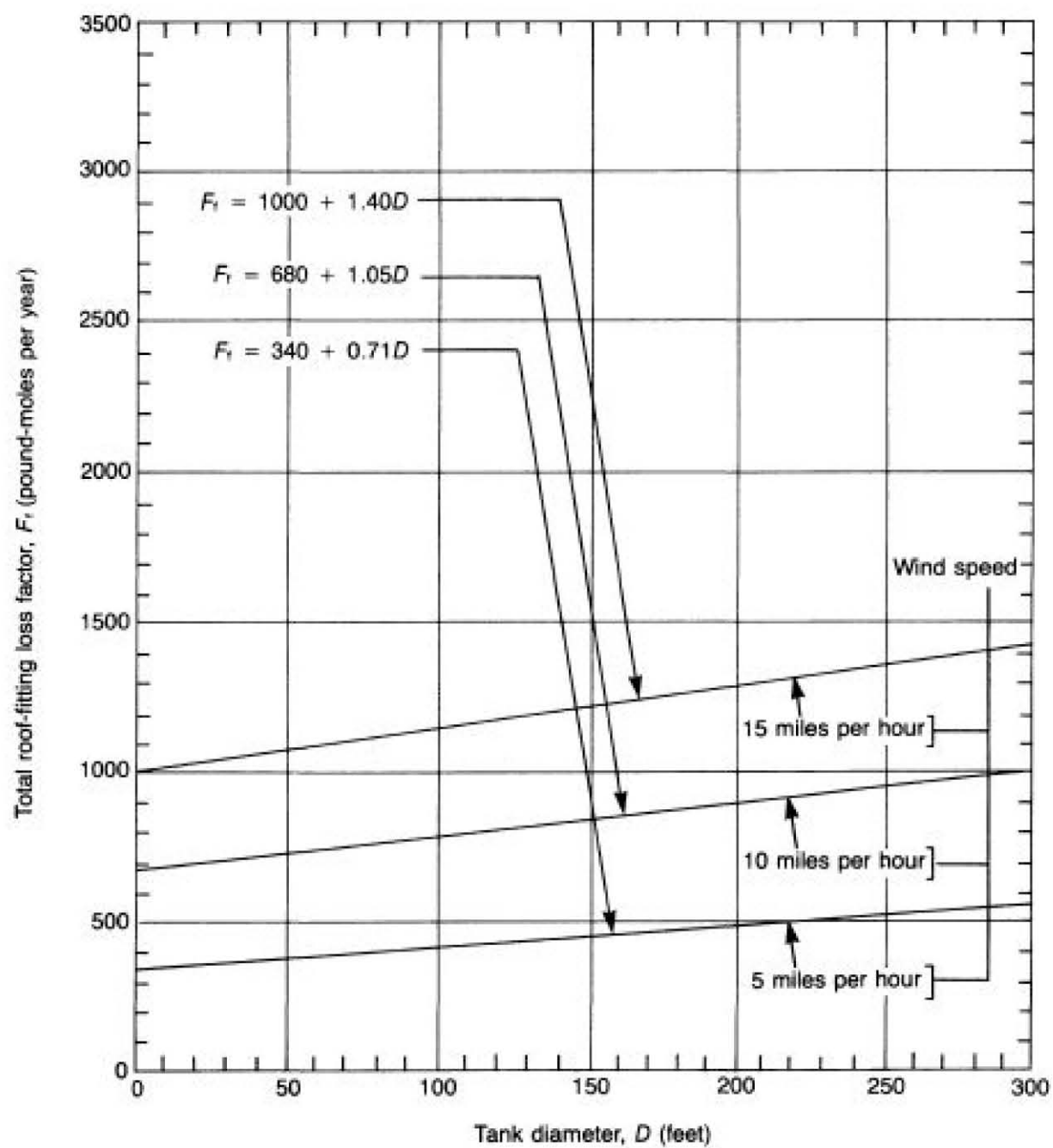


Figure 14—Total Roof-Fitting Loss Factor for Typical Fittings on Pontoon Floating Roofs

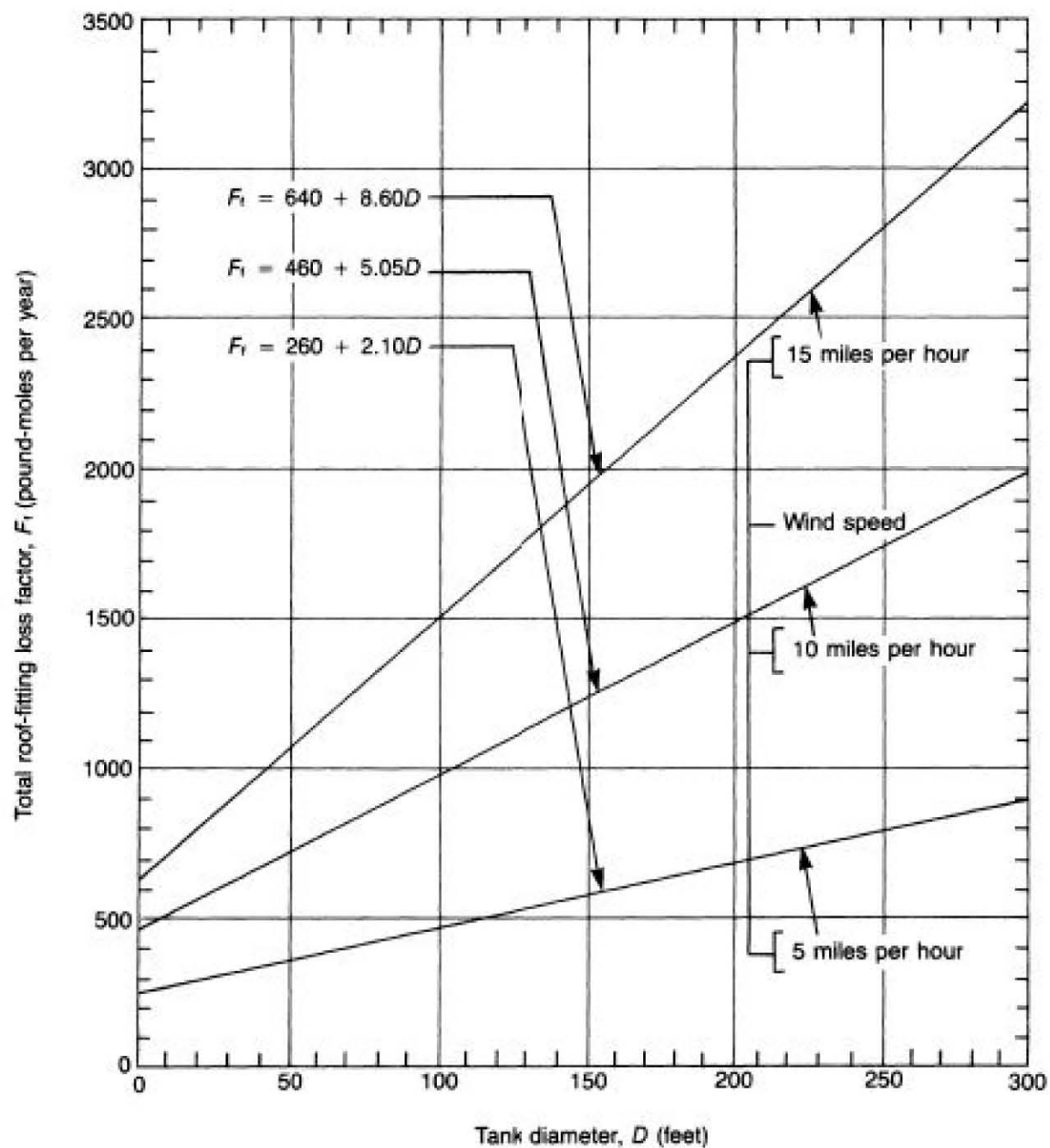
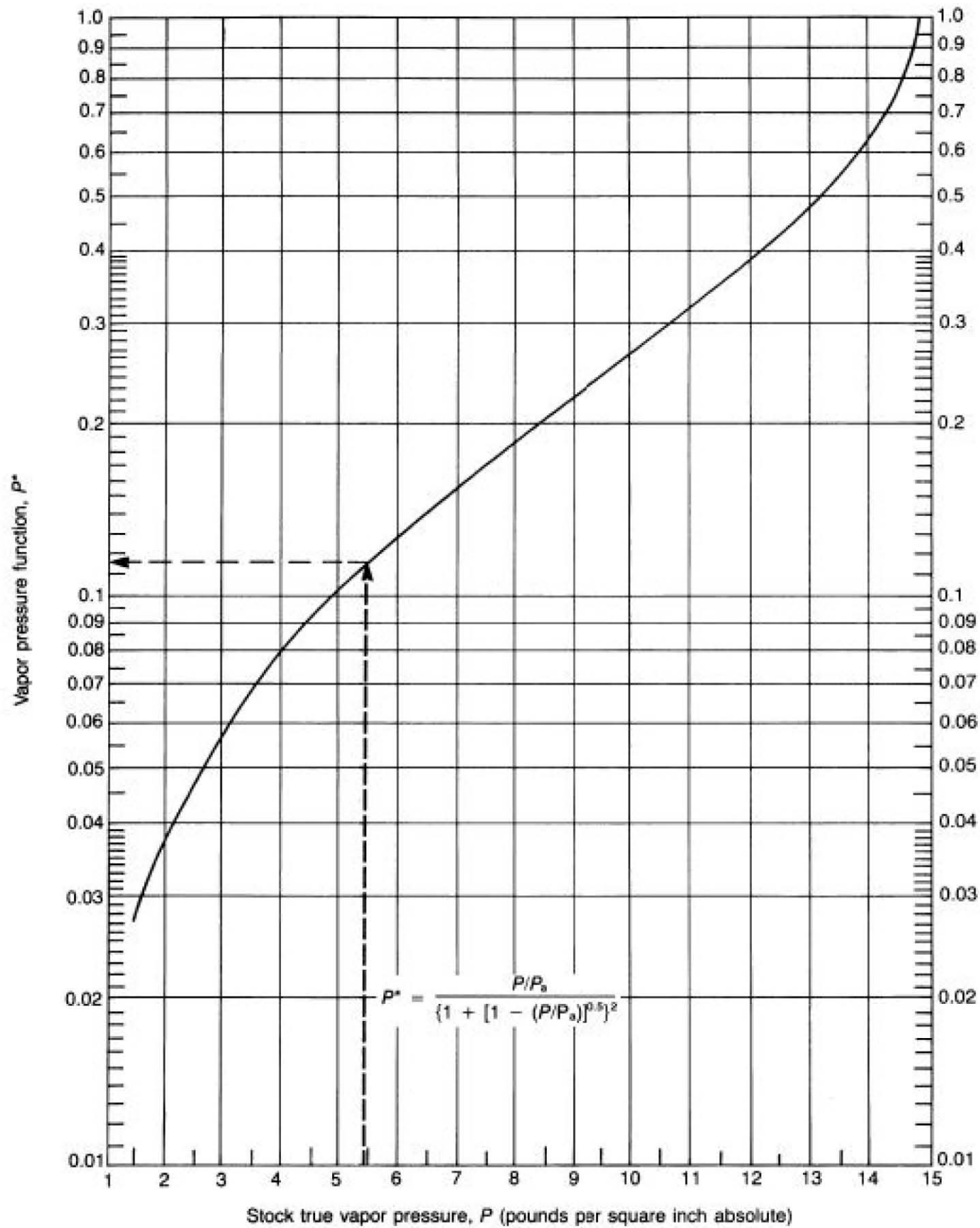


Figure 15—Total Roof-Fitting Loss Factor for Typical Fittings on Double-Deck Floating Roofs



Notes:

1. Broken line illustrates sample problem for $P = 5.4$ pounds per square inch absolute.

2. Curve is for atmospheric pressure, P_s , equal to 14.7 pounds per square inch absolute.

Figure 16—Vapor Pressure Function

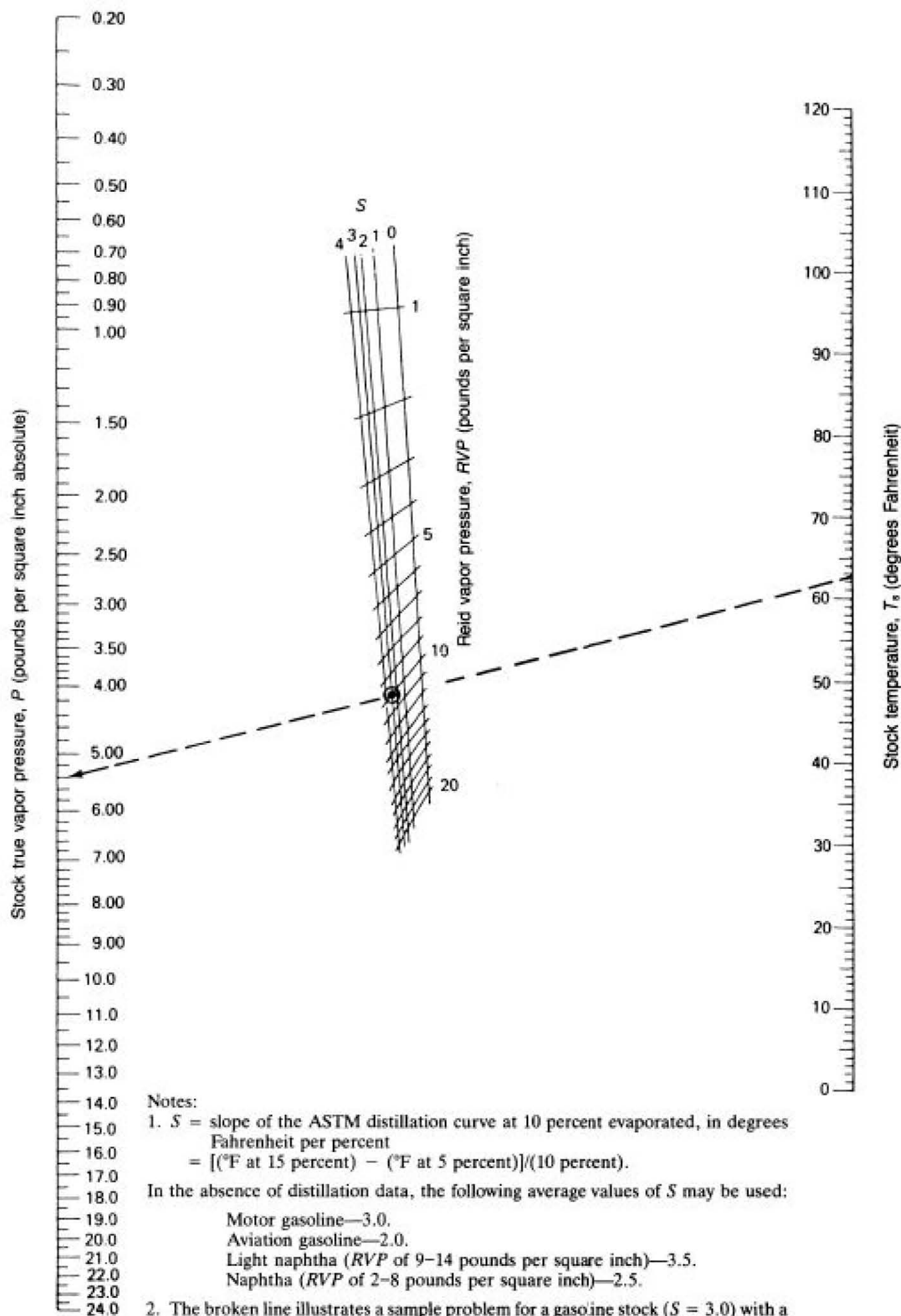
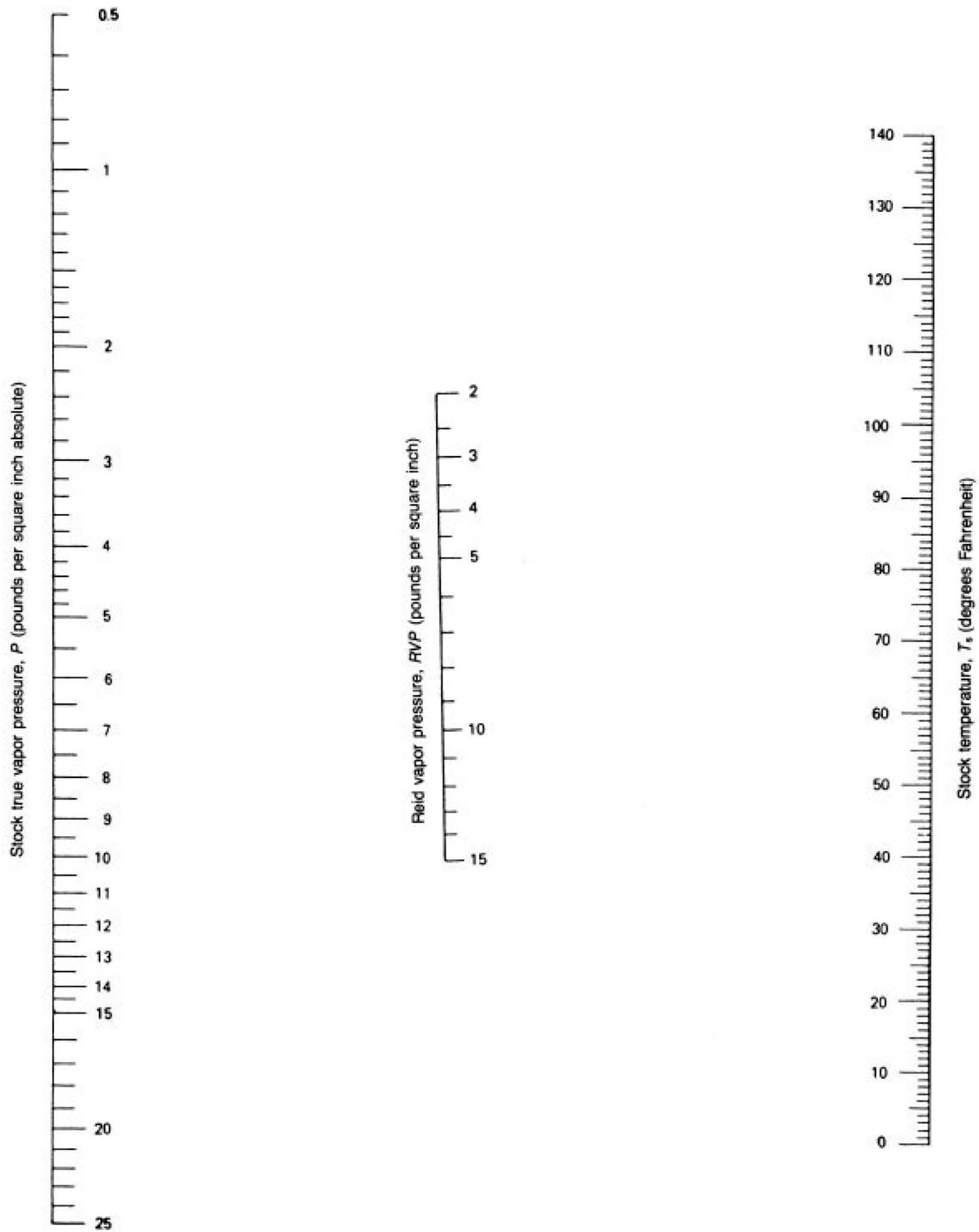


Figure 17A—True Vapor Pressure of Refined Petroleum Stocks With a Reid Vapor Pressure of 1–20 Pounds per Square Inch



Note: See Figure 18B for the equation for stock true vapor pressure, P .

Figure 18A—True Vapor Pressure of Crude Oils With a Reid Vapor Pressure of 2–15 Pounds per Square Inch

$$P = \exp \left\{ \left[0.7553 - \left(\frac{413.0}{T + 459.6} \right) \right] S^{0.5} \log_{10}(RVP) - \left[1.854 - \left(\frac{1042}{T + 459.6} \right) \right] S^{0.5} + \left[\left(\frac{2416}{T + 459.6} \right) - 2.013 \right] \log_{10}(RVP) - \left(\frac{8742}{T + 459.6} \right) + 15.64 \right\}$$

Where:

- P = stock true vapor pressure, in pounds per square inch absolute.
- T = stock temperature, in degrees Fahrenheit.
- RVP = Reid vapor pressure, in pounds per square inch.
- S = slope of the ASTM distillation curve at 10 percent evaporated, in degrees Fahrenheit per percent.

Note: This equation was derived from a regression analysis of points read off Figure 17A over the full range of Reid vapor pressures, slopes of the ASTM distillation curve at 10 percent evaporated, and stock temperatures. In general, the equation yields P values that are within ± 0.05 pound per square inch absolute of the values obtained directly from the nomograph.

Figure 17B—Equation for True Vapor Pressure of Refined Petroleum Stocks With a Reid Vapor Pressure of 1–20 Pounds per Square Inch

$$P = \exp \left\{ \left[\left(\frac{2799}{T + 459.6} \right) - 2.227 \right] \log_{10}(RVP) - \left(\frac{7261}{T + 459.6} \right) + 12.82 \right\}$$

Where:

- P = stock true vapor pressure, in pounds per square inch absolute.
- T = stock temperature, in degrees Fahrenheit.
- RVP = Reid vapor pressure, in pounds per square inch.

Note: This equation was derived from a regression analysis of points read off Figure 18A over the full range of Reid vapor pressures, slopes of the ASTM distillation curve at 10 percent evaporated, and stock temperatures. In general, the equation yields P values that are within ± 0.05 pound per square inch absolute of the values obtained directly from the nomograph.

Figure 18B—Equation for True Vapor Pressure of Crude Oils With a Reid Vapor Pressure of 2–15 Pounds per Square Inch

Table 8—Physical Properties of Selected Petrochemicals

Name	Formula	Molecular Weight	Boiling Point at 1 Atmosphere (degrees Fahrenheit)	Liquid Density at 60°F (pounds per gallon)	Vapor Pressure (pounds per square inch absolute) at						
					40°F	50°F	60°F	70°F	80°F	90°F	100°F
Acetone	CH ₃ COCH ₃	58.08	133.0	6.628	1.682	2.185	2.862	3.713	4.699	5.917	7.251
Acetonitrile	CH ₃ CN	41.05	178.9	6.558	0.638	0.831	1.083	1.412	1.876	2.456	3.133
Acrylonitrile	CH ₂ =CHCN	53.06	173.5	6.758	0.812	0.967	1.373	1.779	2.378	3.133	4.022
Allyl alcohol	CH ₂ =CHCH ₂ OH	58.08	206.6	7.125	0.135	0.193	0.261	0.387	0.522	0.716	1.006
Allyl chloride	CH ₂ =CHCH ₂ Cl	76.53	113.2	7.864	2.998	3.772	4.797	6.015	7.447	9.110	11.025
Ammonium hydroxide (28.8% solution)	NH ₄ OH—H ₂ O	35.05	83.0	7.481	5.130	6.630	8.480	10.760	13.520	16.760	20.680
Benzene	C ₆ H ₆	78.11	176.2	7.365	0.638	0.870	1.160	1.508	1.972	2.610	3.287
<i>iso</i> -Butyl alcohol	(CH ₃) ₂ CHCH ₂ OH	74.12	227.1	6.712	0.058	0.097	0.135	0.193	0.271	0.387	0.541
<i>tert</i> -Butyl alcohol	(CH ₃) ₃ COH	74.12	180.5	6.595	0.174	0.290	0.425	0.638	0.909	1.238	1.702
<i>n</i> -Butyl chloride	CH ₃ CH ₂ CH ₂ CH ₂ Cl	92.57	172.0	7.430	0.715	1.006	1.320	1.740	2.185	2.684	3.481
Carbon disulfide	CS ₂	76.13	115.3	10.588	3.036	3.867	4.834	6.014	7.387	9.185	11.215
Carbon tetrachloride	CCl ₄	153.84	170.2	13.366	0.793	1.064	1.412	1.798	2.301	2.997	3.771
Chloroform	CHCl ₃	119.39	142.7	12.488	1.528	1.934	2.475	3.191	4.061	5.163	6.342
Chloroprene	CH ₂ =CCl-CH=CH ₂	88.54	138.9	8.046	1.760	2.320	2.901	3.655	4.563	5.685	6.981
Cyclohexane	C ₆ H ₁₂	84.16	177.3	6.522	0.677	0.928	1.218	1.605	2.069	2.610	3.249
Cyclopentane	C ₅ H ₁₀	70.13	120.7	6.248	2.514	3.287	4.177	5.240	6.517	8.063	9.668
1,1-Dichloroethane	CH ₃ CHCl ₂	98.97	135.1	9.861	1.682	2.243	2.901	3.771	4.738	5.840	7.193
1,2-Dichloroethane	CH ₂ ClCH ₂ Cl	98.97	182.5	10.500	0.561	0.773	1.025	1.431	1.740	2.243	2.804
<i>cis</i> -1,2-Dichloroethylene	CHCl=CHCl	96.95	140.2	10.763	1.450	2.011	2.668	3.461	4.409	5.646	6.807
<i>trans</i> -1,2-Dichloroethylene	CHCl=CHCl	96.95	119.1	10.524	2.552	3.384	4.351	5.530	6.807	8.315	10.016
Diethylamine	(C ₂ H ₅) ₂ NH	73.14	131.9	5.906	1.644	1.992	2.862	3.867	4.892	6.130	7.541
Diethyl ether	C ₂ H ₅ OC ₂ H ₅	74.12	94.3	5.988	4.215	5.666	7.019	8.702	10.442	13.342	16.760
Di- <i>iso</i> -propyl ether	(CH ₃) ₂ CHOCH(CH ₃) ₂	102.17	153.5	6.075	1.199	1.586	2.127	2.746	3.481	4.254	5.298
1,4-Dioxane	O-CH ₂ CH ₂ OCH ₂ CH ₂	88.10	214.7	8.659	0.232	0.329	0.425	0.619	0.831	1.141	1.508
Dipropyl ether	CH ₃ CH ₂ CH ₂ OCH ₂ CH ₂ CH ₃	102.17	195.8	6.260	0.425	0.619	0.831	1.102	1.431	1.876	2.320
Ethyl acetate	C ₂ H ₅ COOCH ₃	88.10	170.9	7.551	0.580	0.831	1.102	1.489	1.934	2.514	3.191
Ethyl acrylate	C ₂ H ₅ COOCC=CH ₂	100.11	211.8	7.750	0.213	0.290	0.425	0.599	0.831	1.122	1.470

Table 8—Continued

Name	Formula	Molecular Weight	Boiling Point at 1 Atmosphere (degrees Fahrenheit)	Liquid Density at 60°F (pounds per gallon)	Vapor Pressure (pounds per square inch absolute) at						
					40°F	50°F	60°F	70°F	80°F	90°F	100°F
Ethyl alcohol	C_2H_5OH	46.07	173.1	6.610	0.193	0.406	0.619	0.870	1.218	1.682	2.320
Freon 11	CCl_3F	137.38	75.4	12.480	7.032	8.804	10.900	13.40	16.31	19.69	23.60
n-Heptane	$CH_3(CH_2)_5CH_3$	100.20	209.2	5.727	0.290	0.406	0.541	0.735	0.967	1.238	1.586
n-Hexane	$CH_3(CH_2)_4CH_3$	86.17	155.7	5.527	1.102	1.450	1.876	2.436	3.055	3.906	4.892
Hydrogen cyanide	HCN	27.03	78.3	5.772	6.284	7.831	9.514	11.853	15.392	18.563	22.237
Isooctane	$(CH_3)_3CCH_2CH(CH_3)_2$	114.22	210.6	5.794	0.213	0.387	0.580	0.812	1.093	1.392	1.740
Isopentane	$(CH_3)_2CHCH_2CH_3$	72.15	82.1	5.199	5.878	7.889	10.005	12.530	15.334	18.370	21.657
Isoprene	$(CH_2)=C(CH_3)CH=CH_2$	68.11	93.5	5.707	4.757	6.130	7.677	9.668	11.699	14.503	17.113
Isopropyl alcohol	$(CH_3)_2CHOH$	60.09	180.1	6.573	0.213	0.329	0.483	0.677	0.928	1.296	1.779
Methacrylonitrile	$CH_2=C(CH_3)CN$	67.09	194.5	6.738	0.483	0.657	0.870	1.160	1.470	1.934	2.456
Methyl acetate	CH_3COOCH_3	74.08	134.8	7.831	1.489	2.011	2.746	3.693	4.699	5.762	6.961
Methyl acrylate	$CH_2=OOCCH_2CH_3$	86.09	176.9	7.996	0.599	0.773	1.025	1.354	1.798	2.398	3.055
Methyl alcohol	CH_3OH	32.04	148.4	6.630	0.735	1.006	1.412	1.953	2.610	3.461	4.525
Methylcyclohexane	$CH_3-C_6H_{11}$	98.18	213.7	6.441	0.309	0.425	0.541	0.735	0.986	1.315	1.721
Methylcyclopentane	$CH_3-C_5H_9$	84.16	161.3	6.274	0.909	1.160	1.644	2.224	2.862	3.616	4.544
Methylene chloride	CH_2Cl_2	84.94	104.2	11.122	3.094	4.254	5.434	6.787	8.702	10.329	13.342
Methyl ethyl ketone	$CH_3COC_2H_5$	72.10	175.3	6.747	0.715	0.928	1.199	1.489	2.069	2.668	3.345
Methyl methacrylate	$CH_3OOCCH_2CH_2CH_3$	100.11	212.0*	7.909	0.116	0.213	0.348	0.541	0.773	1.064	1.373
Methyl propyl ether	$CH_3OCC_2H_5$	74.12	102.1	6.166	3.674	4.738	6.091	7.058	9.417	11.602	13.729
Nitromethane	CH_3NO_2	61.04	214.2	9.538	0.213	0.251	0.348	0.503	0.715	1.006	1.334
n-Pentane	$CH_3(CH_2)_3CH_3$	72.15	96.9	5.253	4.293	5.454	6.828	8.433	10.445	12.959	15.474
n-Propylamine	$C_3H_7NH_2$	59.11	119.7	6.030	2.456	3.191	4.157	5.250	6.536	8.044	9.572
1,1,1-Trichloroethane	CH_3CCl_3	133.42	165.2	11.216	0.909	1.218	1.586	2.030	2.610	3.307	4.199
Trichloroethylene	$CHCl=CCl_2$	131.40	188.6	12.272	0.503	0.677	0.889	1.180	1.508	2.030	2.610
Toluene	$CH_3-C_6H_5$	92.13	231.1	7.261	0.174	0.213	0.309	0.425	0.580	0.773	1.006
Vinyl acetate	$CH_2=CHOOCCCH_3$	86.09	162.5	7.817	0.735	0.986	1.296	1.721	2.262	3.113	4.022
Vinylidene chloride	$CH_2=CCl_2$	96.5	89.1	10.383	4.990	6.344	7.930	9.806	11.799	15.280	23.210

Note: Most of the values in this table were taken or calculated from data given in J. Timmermanns, *Physico-Chemical Constants of Pure Organic Compounds*, Elsevier, New York, 1950, and in R. H. Perry, C. H. Chilton, and S. D. Kirkpatrick (Eds.), *Chemical Engineers Handbook* (4th ed.), McGraw-Hill, New York, 1963.

Table 9—Average Annual Ambient Temperature (T_a) for Selected U.S. Locations

Location	Ambient Temperature (degrees Fahrenheit)	Location	Ambient Temperature (degrees Fahrenheit)	Location	Ambient Temperature (degrees Fahrenheit)
Alabama		Colorado (continued)		Kansas	
Birmingham	62.0	Denver	50.3	Concordia	53.2
Huntsville	60.6	Grand Junction	52.7	Dodge City	55.1
Mobile	67.5	Pueblo	52.8	Goodland	50.7
Montgomery	64.9	Connecticut		Topeka	54.1
Alaska		Bridgeport	51.8	Wichita	56.4
Anchorage	35.3	Hartford	49.8	Kentucky	
Annette	45.4	Delaware		Cincinnati Airport	53.4
Barrow	9.1	Wilmington	54.0	Jackson	52.6
Barter Island	9.6	District of Columbia		Lexington	54.9
Bethel	28.4	Dulles Airport	53.9	Louisville	56.2
Bettles	21.2	National Airport	57.5	Paducah	57.2
Big Delta	27.4	Florida		Louisiana	
Cold Bay	37.9	Apalachicola	68.2	Baton Rouge	67.5
Fairbanks	25.9	Daytona Beach	70.3	Lake Charles	68.0
Gulkana	26.5	Fort Myers	73.9	New Orleans	68.2
Homer	36.6	Gainesville	68.6	Shreveport	68.4
Juneau	40.0	Jacksonville	68.0	Maine	
King Salmon	32.8	Key West	77.7	Caribou	38.9
Kodiak	40.7	Miami	75.7	Portland	45.0
Kotzebue	20.9	Orlando	72.4	Maryland	
McGrath	25.0	Pensacola	68.0	Baltimore	55.1
Nome	25.5	Tallahassee	67.2	Massachusetts	
St. Paul Island	34.3	Tampa	72.0	Blue Hill Observatory	48.6
Talkeetna	32.6	Vero Beach	72.4	Boston	51.5
Unalakleet	26.4	West Palm Beach	74.6	Worcester	46.8
Valdez	38.3	Georgia		Michigan	
Yakutat	38.6	Athens	61.4	Alpena	42.2
Arizona		Atlanta	61.2	Detroit	48.6
Flagstaff	45.4	Augusta	63.2	Flint	46.8
Phoenix	71.2	Columbus	64.3	Grand Rapids	47.5
Tucson	68.0	Macon	64.7	Houghton Lake	42.9
Winslow	54.9	Savannah	65.9	Lansing	47.2
Yuma	73.8	Hawaii		Marquette	39.2
Arkansas		Hilo	73.6	Muskegon	47.2
Fort Smith	60.8	Honolulu	77.0	Sault Sainte Marie	39.7
Little Rock	61.9	Kahului	75.5	Minnesota	
North Little Rock	61.7	Lihue	75.2	Duluth	38.2
California		Idaho		International Falls	36.4
Bakersfield	65.5	Boise	51.1	Minneapolis-Saint Paul	44.7
Bishop	56.0	Lewiston	52.1	Rochester	43.5
Blue Canyon	50.4	Pocatello	46.6	Saint Cloud	41.4
Eureka	52.0	Illinois		Mississippi	
Fresno	62.6	Cairo	59.1	Jackson	64.6
Long Beach	63.9	Chicago (O'Hare Airport)	49.2	Meridian	64.1
Los Angeles (City)	65.3	Moline	49.5	Tupelo	61.9
Los Angeles International Airport	62.6	Peoria	50.4	Missouri	
Mount Shasta	49.5	Rockford	47.8	Columbia	34.1
Red Bluff	62.9	Springfield	52.6	Kansas City (City)	59.1
Sacramento	60.6	Indiana		Kansas City Airport	56.3
San Diego	63.8	Evansville	55.7	Saint Louis	55.4
San Francisco (City)	56.8	Fort Wayne	49.7	Springfield	55.9
San Francisco International Airport	56.6	Indianapolis	52.1	Montana	
Santa Barbara	58.9	South Bend	49.4	Billings	46.7
Santa Maria	56.8	Iowa		Glasgow	41.6
Stockton	61.6	Des Moines	49.7	Great Falls	44.7
Colorado		Dubuque	46.3	Havre	42.3
Alamosa	41.2	Sioux City	48.4	Helena	43.3
Colorado Springs	48.9	Waterloo	46.1	Kalispell	42.5

Table 9—Continued

Location	Ambient Temperature (degrees Fahrenheit)	Location	Ambient Temperature (degrees Fahrenheit)	Location	Ambient Temperature (degrees Fahrenheit)
Montana (continued)		Ohio (continued)		Texas (continued)	
Miles City	45.4	Cleveland	49.6	Amarillo	57.3
Missoula	44.1	Columbus	51.7	Austin	68.1
Nebraska		Dayton	51.9	Brownsville	73.6
Grand Island	49.9	Mansfield	49.5	Corpus Christi	72.1
Lincoln	50.5	Toledo	48.6	Dallas-Fort Worth	66.0
Norfolk	48.3	Youngstown	48.2	Del Rio	69.8
North Platte	48.1	Oklahoma		El Paso	63.4
Omaha (City)	49.5	Oklahoma City	59.9	Galveston	69.6
Omaha (Eppley Airport)	51.1	Tulsa	60.3	Houston	68.3
Scotts Bluff	48.5	Oregon		Lubbock	59.9
Valentine	46.8	Astoria	50.6	Midland-Odessa	63.5
Nevada		Burns	46.6	Port Arthur	68.7
Elko	46.2	Eugene	52.5	San Angelo	65.7
Ely	44.4	Medford	53.6	San Antonio	68.7
Las Vegas	66.2	Pendleton	52.5	Victoria	70.1
Reno	49.4	Portland	53.0	Waco	67.0
Winnemucca	48.8	Salem	52.0	Wichita Falls	63.5
New Hampshire		Sexton Summit	47.7	Utah	
Concord	45.3	Pacific Islands		Milford	49.1
Mount Washington	26.6	Guam	78.8	Salt Lake City	51.7
New Jersey		Johnston Island	78.9	Vermont	
Atlantic City (City)	54.1	Pennsylvania		Burlington	44.1
Atlantic City (Airport)	53.1	Allentown	51.0	Virginia	
Newark	54.2	Avoca	49.1	Lynchburg	56.0
New Mexico		Erie	47.5	Norfolk	59.5
Albuquerque	56.2	Harrisburg	53.0	Richmond	57.7
Clayton	52.9	Philadelphia	54.3	Roanoke	56.1
Roswell	61.4	Pittsburgh	50.3	Washington	
New York		Williamsport	50.1	Olympia	49.6
Albany	47.2	Rhode Island		Quillayute	48.7
Binghamton	45.7	Block Island	50.2	Seattle (City)	52.7
Buffalo	47.6	Providence	50.3	Seattle International Airport	51.4
New York (Central Park)	54.6	South Carolina		Spokane	47.2
New York (JFK Airport)	53.2	Charleston (City)	66.1	Stampede Pass	59.3
New York (La Guardia Airport)	54.3	Charleston Airport	64.8	Walla Walla	54.1
Rochester	48.0	Columbia	63.3	Yakima	49.7
Syracuse	47.7	Greenville-Spartanburg	60.1	West Virginia	
North Carolina		South Dakota		Beckley	50.9
Asheville	55.5	Aberdeen	43.0	Charleston	54.8
Cape Hatteras	61.9	Huron	44.7	Elkins	49.3
Charlotte	60.0	Rapid City	46.7	Huntington	55.2
Greensboro	57.8	Sioux Falls	45.3	Wisconsin	
Raleigh	59.0	Tennessee		Green Bay	43.6
Wilmington	63.4	Bristol-Johnson City	55.9	La Crosse	46.1
North Dakota		Chattanooga	59.4	Madison	45.2
Bismarck	41.3	Knoxville	58.9	Milwaukee	46.1
Fargo	40.5	Memphis	61.8	Wyoming	
Williston	40.8	Nashville	59.2	Casper	45.2
Ohio		Oak Ridge	57.5	Cheyenne	45.7
Akron	49.5	Texas		Lander	44.4
		Abilene	64.5	Sheridan	44.6

Note: The data in this table are taken from *Comparative Climatic Data Through 1984*, National Oceanic and Atmospheric Administration, Asheville, North Carolina, 1986.

Table 10—Average Annual Stock Storage Temperature (T_s) as a Function of Tank Paint Color

Tank Color	Average Annual Stock Storage Temperature, T_s (degrees Fahrenheit)
White	$T_a + 0$
Aluminum	$T_a + 2.5$
Gray	$T_a + 3.5$
Black	$T_a + 5.0$

Note: T_a = average annual ambient temperature, in degrees Fahrenheit.

Table 11—Average Clingage Factors, C (Barrels per 1000 Square Feet)

Product Stored	Shell Condition		
	Light Rust	Dense Rust	Gunite Lining
Gasoline	0.0015	0.0075	0.15
Single-component stocks	0.0015	0.0075	0.15
Crude oil	0.0060	0.030	0.60

Note: If no specific information is available, the values in this table can be assumed to represent the most common or typical condition of tanks currently in use.

SECTION 3—COMPONENTS OF EXTERNAL FLOATING-ROOF TANKS

3.1 External Floating-Roof Tanks

External floating-roof tanks are cylindrical vessels that have a roof that floats on the surface of the liquid stock. In addition to a cylindrical shell, the basic components include (a) a floating roof, (b) an annular rim seal attached to the perimeter of the floating roof, and (c) roof fittings that penetrate the floating roof and serve operational functions. General types of these components, which are available in a range of commercial designs, are described in this section. Included in these descriptions are comments on the potential for evaporative loss, as well as some design and operational characteristics. Other factors, such as tank maintenance and safety, are important in designing and selecting tank equipment but are outside the scope of this publication.

3.2 Floating Roofs

Floating roofs are used to control evaporative stock loss. The basic design concept is to reduce the liquid surface exposed to evaporation to a minimum by placing a floating roof in direct contact with the liquid surface. Evaporative loss during standing storage is then limited to the rim-seal system and roof fittings. Floating roofs are used in volatile stock service, for stocks with a true vapor pressure at storage conditions below atmospheric pressure (that is, nonboiling). They are available in virtually all commercial tank sizes, from about 20 to 400 feet in diameter. Methods and materials have been developed to properly seal the annular rim space, which is located between the tank shell and the floating-roof rim, and to seal around the fittings that penetrate the floating roof.

Floating roofs are currently constructed of welded steel plate and are of three general types: pan, pontoon, and double deck. Although numerous pan-type floating

roofs are currently in use, the present trend is toward pontoon and double-deck floating roofs. Figures 19 and 20 show an external floating-roof tank with a pontoon floating roof and a double-deck floating roof, respectively. Manufacturers supply various versions of these basic types of floating roofs, which are tailored to emphasize particular features, such as full liquid contact, load-carrying capacity, roof stability, or pontoon arrangement.

3.3 Rim Seals

3.3.1 GENERAL

All types of floating roofs have an annular space between the tank shell and the floating-roof rim to permit travel of the floating roof within the tank. A rim-seal system is used with all types of floating roofs to control evaporative loss from the rim space. Effective rim-seal systems close the rim space, accommodate irregularities between the floating roof and the tank shell, and help to center the roof, yet permit normal roof movement.

A rim-seal system can consist of one or two separate seals: (a) the primary seal and (b) the secondary seal, which is mounted above the primary seal.

Three basic types of primary seals are currently in widespread use: (a) mechanical shoe (metallic), (b) resilient filled (nonmetallic), and (c) flexible wiper. Two basic configurations of secondary seals are currently available: shoe mounted and rim mounted. In addition, some rim-seal systems include a weather shield. Other types of primary and secondary seals have been or are being developed, but these rim seals are not presently in wide use. A number of specific types of rim seals and weather shields, which represent most of the rim-seal systems currently in use, are described in 3.3.2 through 3.3.6.

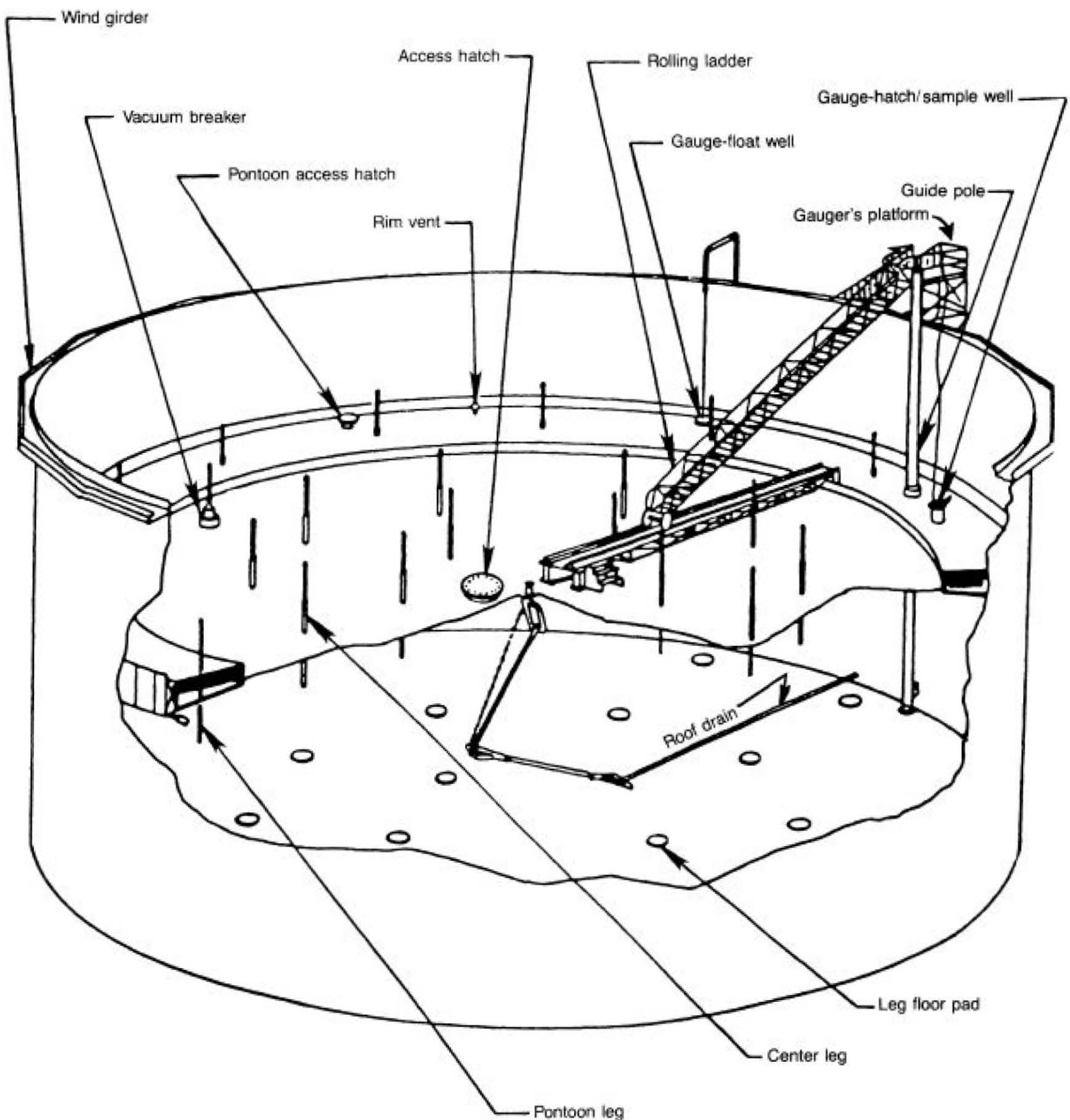


Figure 19—External Floating-Roof Tank With Pontoon Floating Roof

Factors used to determine evaporative loss (see 2.2.2.1) have been developed only for rim-seal systems with mechanical-shoe and resilient-filled primary seals.

Proper attention should be given to the selection of the materials used in the construction of rim-seal systems because of the potential for chemical incompatibility with the stored product.

3.3.2 MECHANICAL-SHOE PRIMARY SEALS

Mechanical-shoe (or metallic) primary seals have been in wide use for many years. Figure 21 shows a typical mechanical-shoe primary seal. The identifying characteristic of this rim seal is that it uses a light-gauge metallic band as the sliding contact with the tank shell.

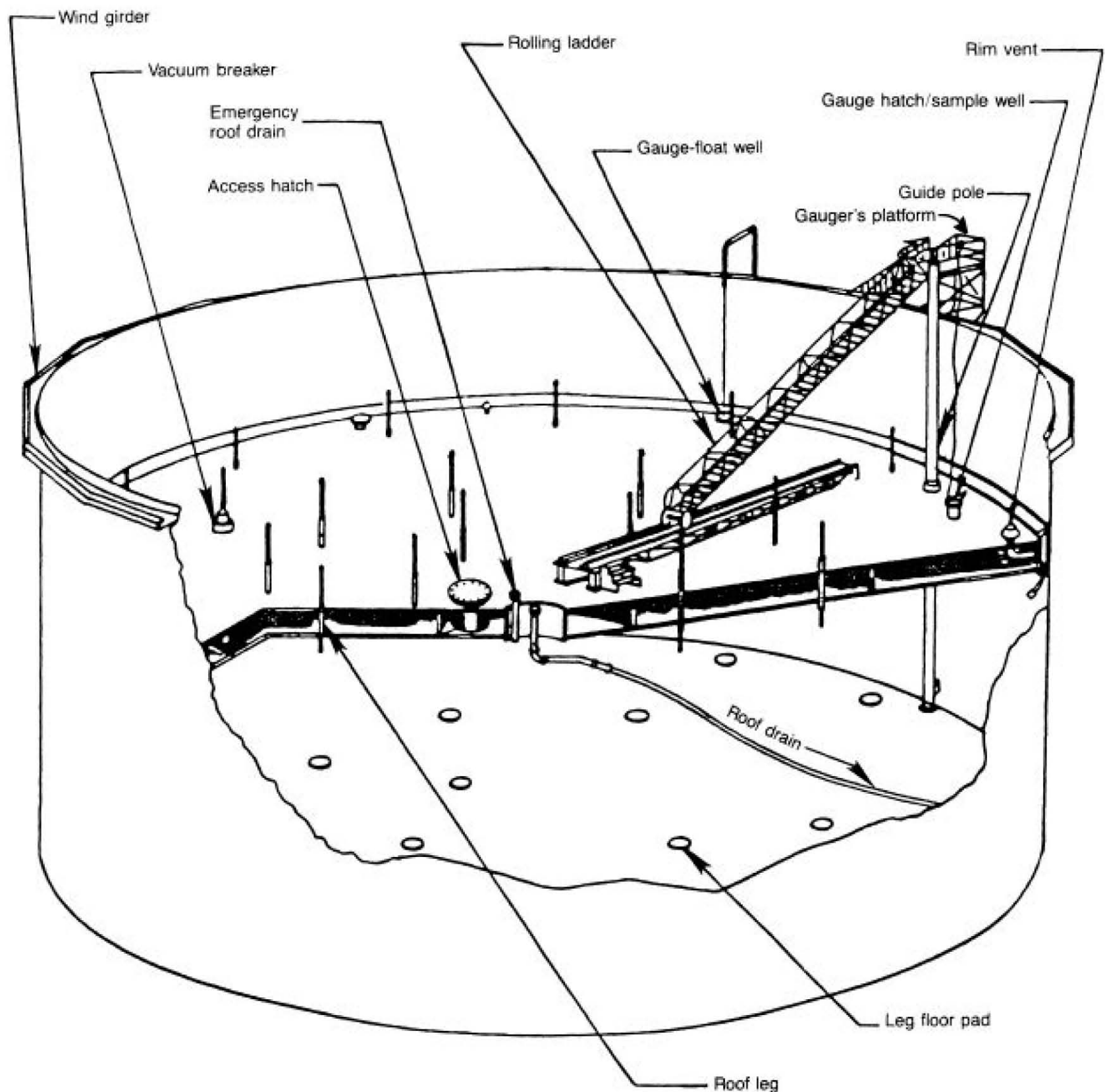


Figure 20—External Floating-Roof Tank With Double-Deck Floating Roof

The metallic band is supported and held against the tank shell by a mechanical device. The mechanical device varies with different manufacturers. The band is formed of sheets (shoes) and may vary in size with different manufacturers. The shoes are joined together to form a ring. The shoes are normally 3–5 feet deep and thus provide a potentially large contact area with the tank shell. Expansion and contraction of the ring is provided for as the ring passes over shell irregularities or rivets.

This is accomplished by jointing narrow pieces of fabric into the ring or by crimping the shoes at intervals. The bottoms of the shoes extend below the liquid surface to confine the rim vapor space between the shoe and the floating-roof rim.

The rim vapor space, which is bounded by the shoe, the floating-roof rim, and the liquid surface, is sealed from the atmosphere by bolting or clamping a coated fabric, called the primary-seal fabric, that extends from

the shoe to the rim. The specific type of fabric used varies with the tank manufacturer and the type of service.

Two locations are used for attaching the primary-seal fabric. With the most commonly used method, the fabric is attached to the top of the shoe and the floating-roof rim. With the reduced-rim-vapor-space method, the fabric is attached to the shoe and the floating-roof rim near the surface of the stored stock. These two positions of the primary-seal fabric are shown in Figure 21. Rim vents (see 3.4.10) can be used to relieve any excess pressure or vacuum in the rim vapor space.

Mechanical-shoe seals are usually designed to accommodate a local variation of ± 5 inches in a normal 8-inch-wide rim space. Different design details are available for tanks with large diameters or with rim spaces wider than 8 inches. The shoe sealing ring and mechanism ordinarily provide sufficient flexibility to accommodate nominal irregularities in the tank shell. Mechanical-shoe seals can easily be fitted with wear plates for longer service life in riveted tanks.

In normal use (that is, when the floating roof is kept continuously floating) mechanical-shoe seals have a good service life. In general, the primary-seal fabric begins to show signs of aging before the metallic parts show wear. Where mechanical-shoe seals are used with a corrosive product or with unusual operating practices, such as when the underside of the floating roof is frequently exposed to air, corrosion may be severe. In such service, the use of corrosion-resistant metals or special coatings can be advantageous.

Since the integrity of the enclosed rim vapor space is important with respect to controlling evaporative loss, repair of holes and other defects in the rim-seal system is desirable.

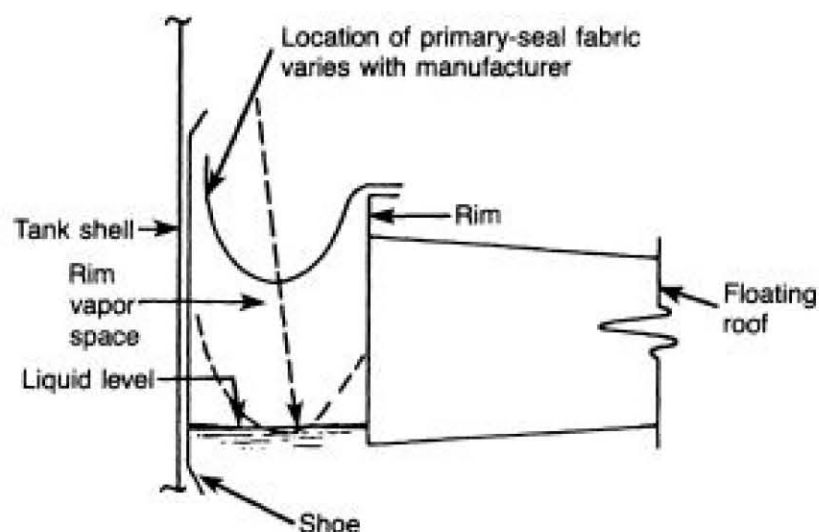


Figure 21—Mechanical-Shoe Primary Seal

3.3.3 RESILIENT-FILLED PRIMARY SEALS

Resilient-filled (or nonmetallic) primary seals have increased in popularity over the years. The identifying characteristic of this type of rim seal is the use of an elastomer-coated fabric envelope as the sliding contact with the tank shell, as shown in Figure 22. The envelope is expanded by being filled with liquid, resilient foam, or gas, thus providing contact with the tank shell. The seal is attached to the rim of the floating roof so that it either touches the liquid surface (liquid mounted) or allows for a rim vapor space between the liquid and the seal (vapor mounted). Tanks with resilient-filled seals are often equipped with a weather shield or a secondary seal.

The main advantage of the resilient-filled seal is its flexibility. The fabrics used for the envelope are much more flexible than are mechanical-shoe seals, so there is better conformity to the tank shell. Most resilient-filled seals are designed to accommodate a normal variation of ± 4 inches in a normal 8-inch-wide rim space. Different design details are available for tanks with large diameters or with rim spaces wider than 8 inches.

Since they are less abrasive than mechanical-shoe seals, resilient-filled seals are typically used if an interior coating has been applied to the tank shell. However, since the envelope rubs against the tank shell, projections from the shell, such as rivet heads or weld burrs, may cause wear and reduce the service life of this seal. Projections that might damage the envelope should be removed.

Vapor-mounted seals have an associated rim vapor space, which tends to contribute to evaporative loss. Also, since these rim seals have a relatively short vertical area in contact with the tank shell (compared with mechanical-shoe seals), gaps between the rim seal and the tank shell that communicate with the rim vapor space

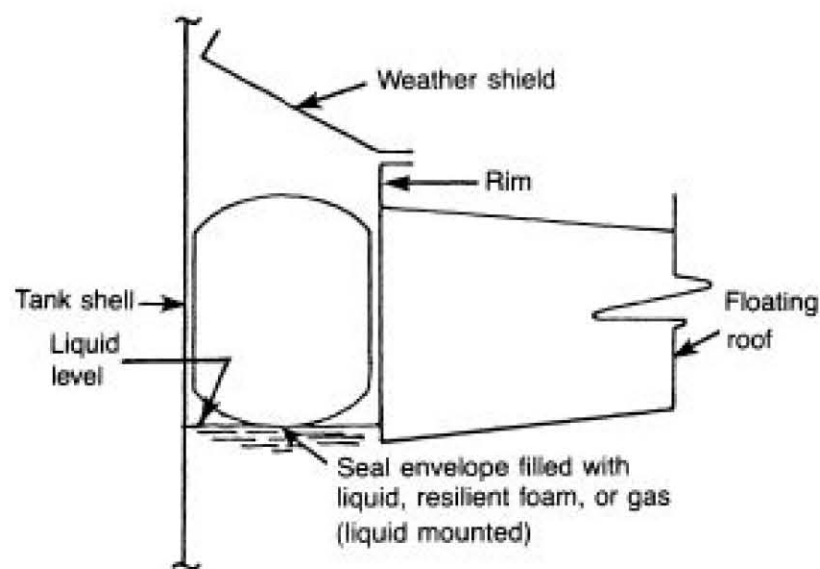


Figure 22—Resilient-Filled Primary Seal

permit additional evaporative loss. On the other hand, vapor-mounted seals are not subject to deterioration from contact with the liquid stock surface.

Liquid-mounted seals, which touch the liquid surface, significantly reduce evaporative loss. However, coated fabrics in contact with hydrocarbon products, especially those with high aromatic content, have in some cases experienced reduced life or required increased maintenance. Recent advances in synthetic compounding have resulted in fabrics with increased compatibility with hydrocarbon products. Seal manufacturers can recommend the most suitable envelope fabric for particular applications.

Although resilient-filled seals have not been in service as long as mechanical-shoe seals, they too are known to have a good service life. Unlike mechanical-shoe seals, resilient-filled seals have only a few metallic parts that are subject to corrosion.

3.3.4 FLEXIBLE-WIPER PRIMARY SEALS

Flexible-wiper primary seals have been developed in recent years. The identifying characteristic of this type of rim seal is its use of an elastomeric blade as the sliding contact with the tank shell, as shown in Figure 23. The flexible-wiper seal bridges the annulus between the floating-roof rim and the tank shell and uses its own stiffness or mechanical means to push the seal against the tank shell.

An advantage of this type of rim seal is its flexibility. The wiper is usually more flexible than are mechanical-shoe seals, so there may be better conformity to the tank shell. The flexible-wiper seal is usually mounted above the liquid to avoid any potential deterioration from liquid contact. Most flexible-wiper seals are designed to accommodate a local variation of about ± 4 inches in a normal 8-inch-wide rim space. Special details may be

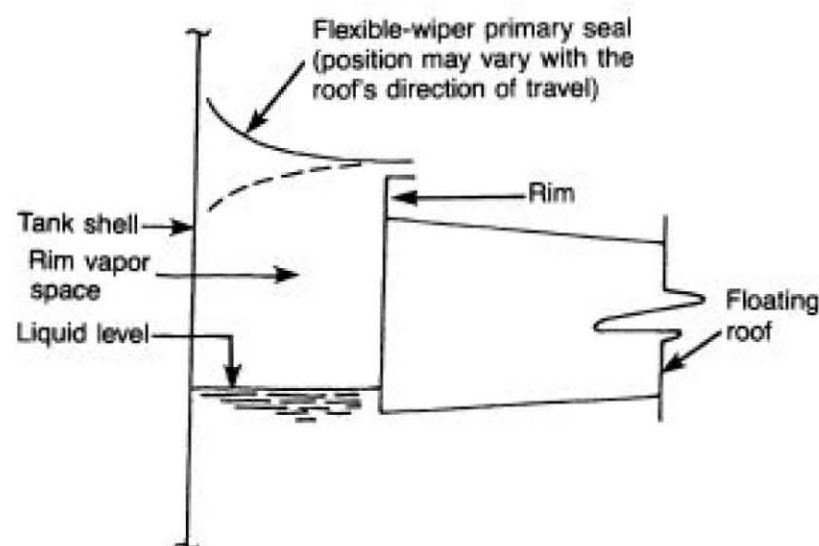


Figure 23—Flexible-Wiper Primary Seal

required for tanks with large diameters or with rim spaces wider than 8 inches. Some flexible-wiper seals are designed to reverse when the floating roof's direction of travel reverses, as shown by the dotted line in Figure 23.

Flexible-wiper seals have an associated rim vapor space, which tends to contribute to evaporative loss. Depending on the length of the vertical contact area between the flexible wiper and the tank shell, gaps between the rim seal and the tank shell permit additional evaporative loss, since they lead directly to the rim vapor space.

Because flexible-wiper seals have been used for a relatively short time, the expected service life is not well defined. As is the case for resilient-filled seals, the non-metallic parts of flexible-wiper seals are not subject to corrosion.

3.3.5 SECONDARY SEALS

Secondary seals can generally be divided into two categories: shoe mounted (see Figure 24) and rim mounted (see Figure 25). Rim-mounted secondary seals are more effective in reducing losses because they cover the entire rim vapor space. Shoe-mounted secondary seals, which are used only with mechanical-shoe primary seals, are effective in reducing losses from gaps between the shoe and tank shell but do not reduce losses caused by defects in the primary-seal fabric.

Secondary seals are usually made from fabric or elastomeric materials, sometimes reinforced with metallic or nonmetallic stiffeners or guided by external attachments. Some secondary seals are designed to reverse as the floating roof's direction of travel reverses, as shown by the dotted line in Figure 25. For secondary seals to be effective, they must maintain contact with the tank shell. Thus, the use of a secondary seal may reduce the effective capacity of the tank.

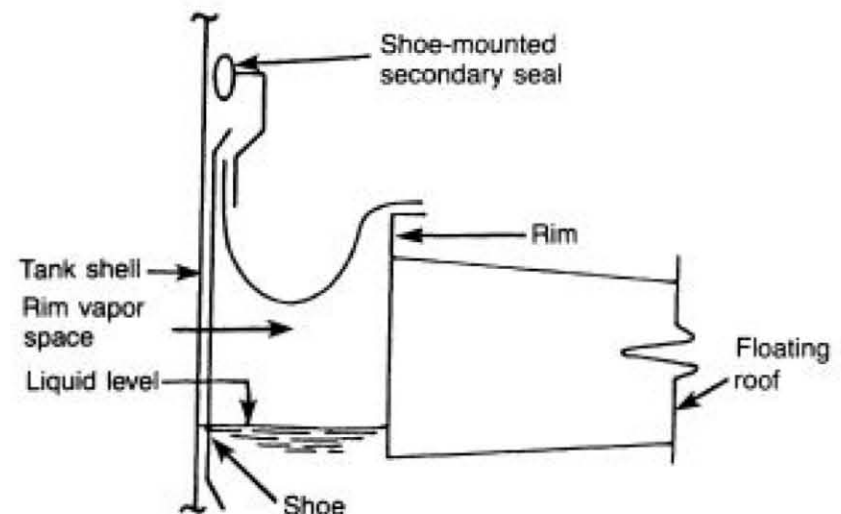


Figure 24—Mechanical-Shoe Primary Seal With Shoe-Mounted Secondary Seal

Properly fitted shoe-mounted secondary seals are known to provide a good service life. The service life of rim-mounted secondary seals has not yet been determined because of their recent use.

3.3.6 WEATHER SHIELDS

When floating roofs that have a resilient-filled primary seal are not equipped with a secondary seal, most are furnished with weather shields, as shown in Figure 22. Weather shields are usually of a leaf-type construction and have numerous radial joints to allow for movement of the floating roof and irregularities in the tank shell. Weather shields may be of metallic, elastomeric, or composite construction. They are normally attached to the floating roof with either a mechanical or a pliable-hinge connection. Weather shields generally provide the primary seal with longer life by protecting the primary-seal fabric from deterioration due to exposure to weather, debris, and sunlight.

3.4 Roof Fittings

3.4.1 GENERAL

Numerous fittings pass through or are attached to a floating roof to allow for operational functions. Roof fittings can be a source of evaporative loss when they require openings in the floating roof. Other accessories are used that do not penetrate the floating roof and are thus not sources of evaporative loss. The most common fittings that require openings in the floating roof are described in 3.4.2 through 3.4.10.

3.4.2 ACCESS HATCHES

Figure 26 shows a typical access hatch, which consists of an opening in the floating roof with a peripheral

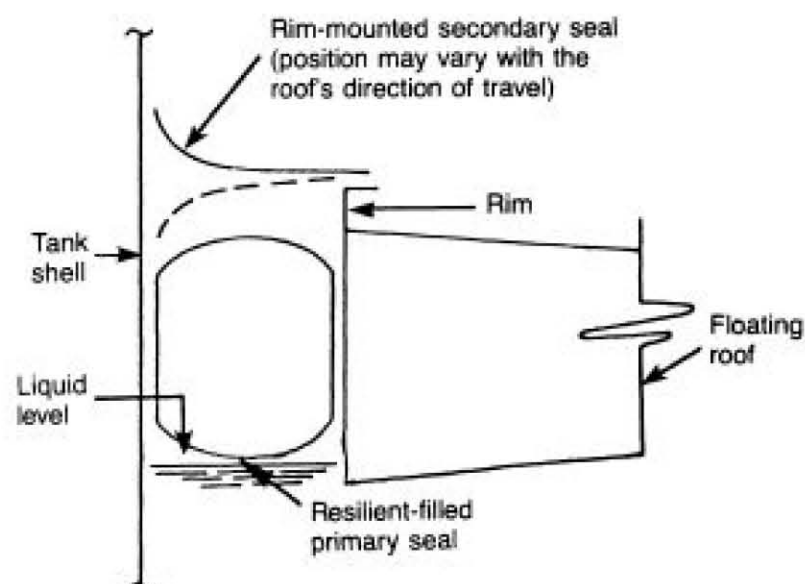


Figure 25—Resilient-Filled Primary Seal With Rim-Mounted Secondary Seal

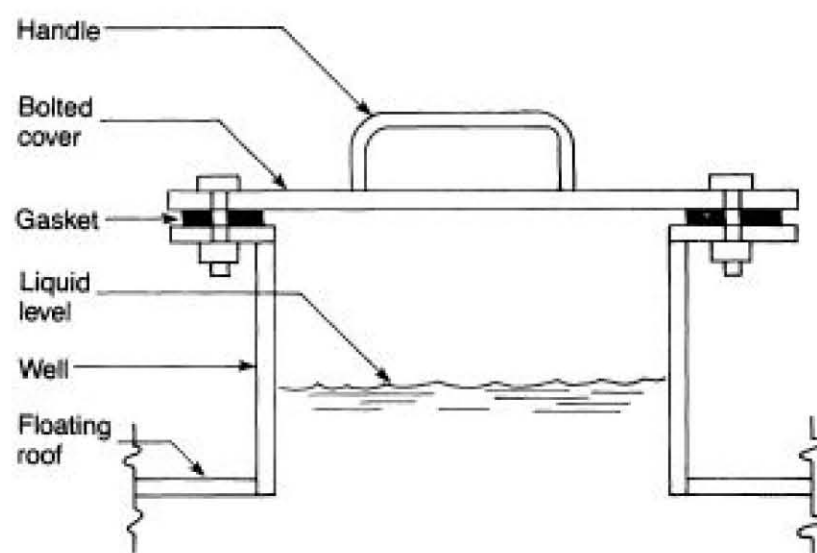


Figure 26—Access Hatch

vertical well attached to the roof and a removable cover. An access hatch is sized to provide for passage of workers and materials through the floating roof for construction and maintenance. The cover can rest directly on the well, or a gasket can be used between the cover and the well to reduce evaporative loss. Bolting the cover to the well further reduces evaporative loss.

3.4.3 UNSLOTTED GUIDE-POLE WELLS

Figure 27 shows a typical unslotted guide-pole well. Antirotation devices are used to prevent floating roofs from rotating and damaging rolling ladders, roof-drain systems, and rim seals and from interfering with float

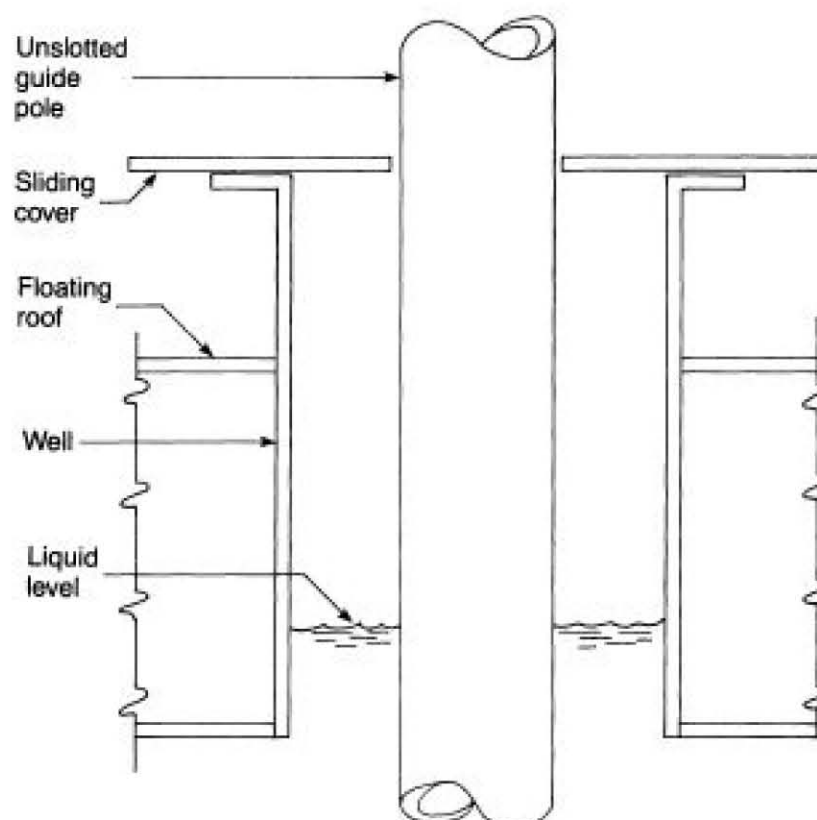


Figure 27—Unslotted Guide-Pole Well

gauges. One commonly used antirotation device is a guide pole that is fixed at the top and bottom of the tank. The guide pole passes through a well on the floating roof. Rollers attached to the top of the well ride on the outside surface of the guide pole to prevent rotation of the floating roof. The guide-pole well has a sliding cover to accommodate limited radial movement of the roof. The sliding cover can be equipped with a gasket between the guide pole and the cover to reduce evaporative loss. The guide-pole well can also be equipped with a gasket between the sliding cover and the top of the well to reduce evaporative loss. Openings at the top and bottom of the guide pole provide a means of hand gauging the tank level and of taking bottom samples.

3.4.4 SLOTTED GUIDE-POLE/SAMPLE WELLS

Figure 28 shows a typical slotted guide-pole/sample well. In this application, the wall of the guide pole is constructed with a series of holes or slots that allow the product to mix freely in the guide pole and thus have the same composition and liquid level as the product in the tank. To reduce evaporative loss caused by these openings, a removable float is sometimes placed inside the guide pole.

3.4.5 GAUGE-FLOAT WELLS

Figure 29 shows a typical gauge-float well. Gauge floats are used to indicate the level of stock within the tank. They usually consist of a float contained within a well that passes through the floating roof. The float is

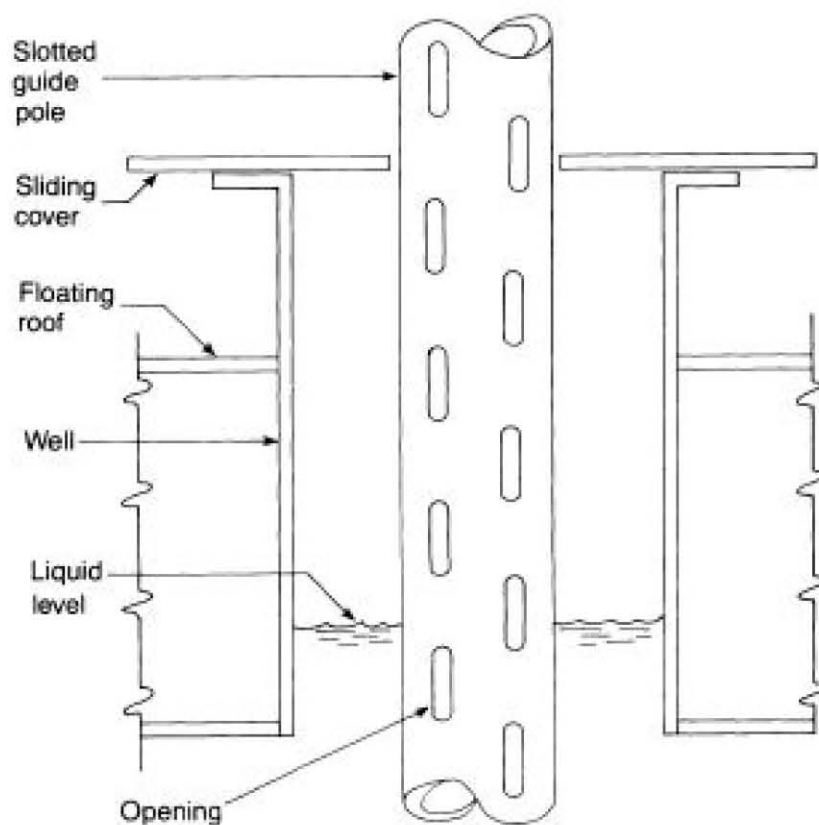


Figure 28—Slotted Guide Pole/Sample Well

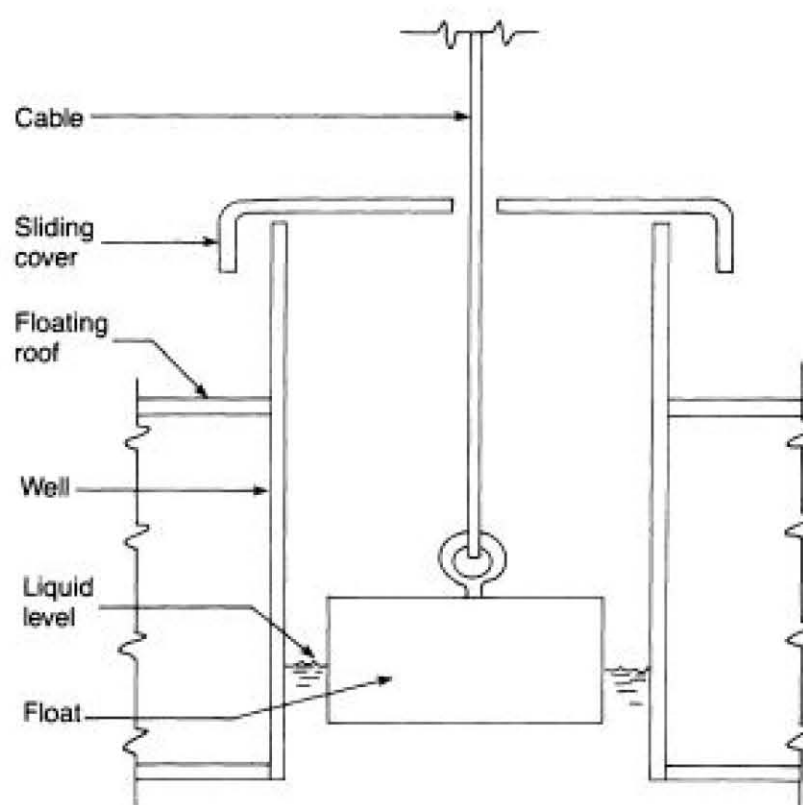


Figure 29—Gauge-Float Well

connected to an indicator on the exterior of the tank by a cable or tape that passes through a guide system. The well is closed by a cover that contains a hole through which the cable or tape passes. Evaporative loss can be reduced by gasketing and/or bolting the cover to the well.

3.4.6 GAUGE-HATCH/SAMPLE WELLS

Figure 30 shows a typical gauge-hatch/sample well. Gauge-hatch/sample wells provide access for hand gauging the level of stock in the tank and for taking thief samples of the tank contents. A gauge-hatch/sample well consists of a pipe sleeve through the floating roof and a self-closing gasketed cover. Gauge hatch/sample wells are usually located under the gauger's platform, which is mounted on the top of the tank shell. The cover may have a cord attached so that it can be opened from the gauger's platform. A gasketed cover will reduce evaporative losses.

3.4.7 VACUUM BREAKERS

Figure 31 shows a typical vacuum breaker. A vacuum breaker is used to equalize the pressure in the vapor space beneath the floating roof when the roof is either landed on its legs or floated off its legs. This is accomplished by opening a roof fitting, usually a well formed of pipe on which rests a cover. A guided leg is attached to the underside of the cover and comes in contact with the tank bottom just at the point when the roof floats freely

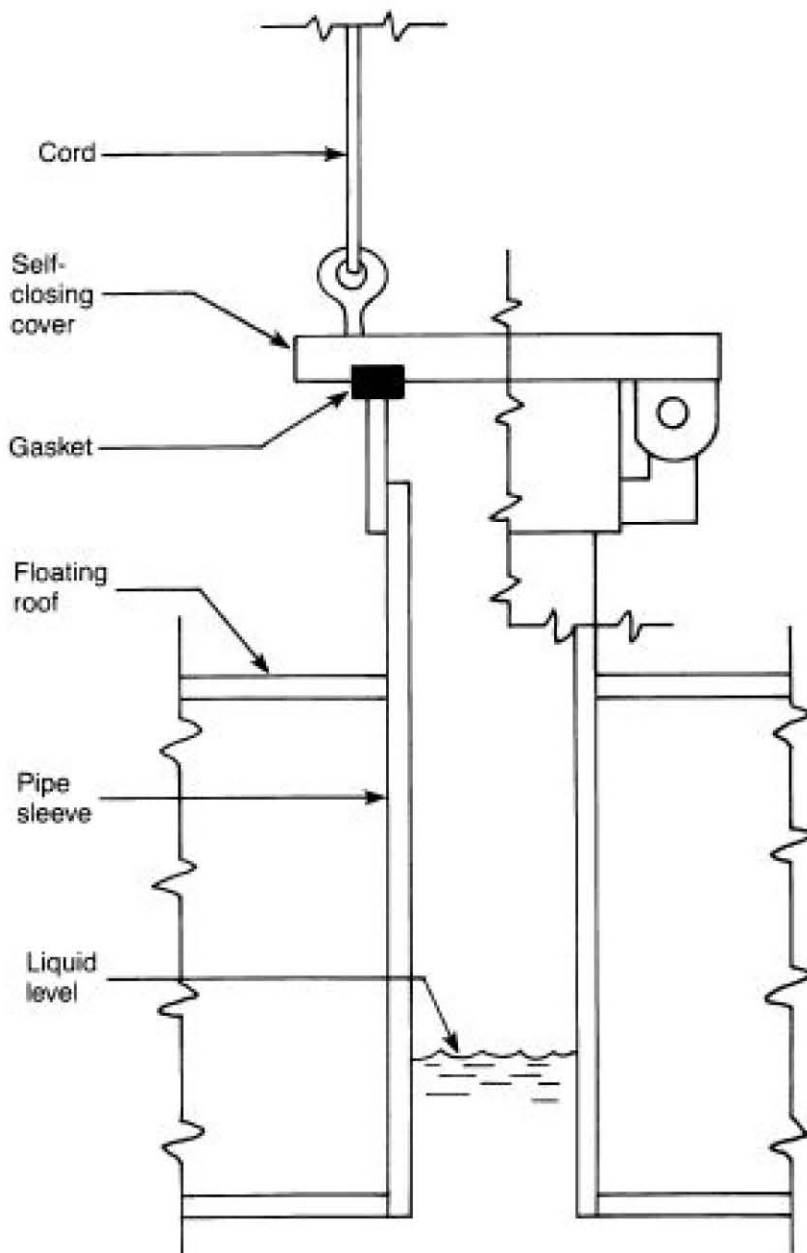


Figure 30—Gauge-Hatch/Sample Well

on the stock. When the leg is in contact with the tank bottom, it mechanically opens the vacuum breaker by lifting the cover off the well. When the leg is not in contact with the bottom, the opening is closed by the cover resting on the well. Some vacuum breakers have adjustable legs to permit changing the roof level at which the leg contacts the bottom. Since the purpose of the vacuum breaker is to allow the free exchange of air or vapor, the well does not extend appreciably below the bottom of the floating roof. A gasket can be used to reduce the evaporative loss when the cover is seated on the well.

3.4.8 ROOF DRAINS

Roof drains permit removal of rainwater from the surface of floating roofs. Two types of floating-roof drainage systems are currently used: closed and open.

Closed drainage systems carry rainwater from the surface of the floating roof to the outside of the tank

through a flexible or articulated piping system or through a flexible hose system located below the floating roof in the product space. Since product does not enter this closed drainage system, there is no associated evaporative loss.

Open drainage systems permit drainage of rainwater from the surface of the floating roof into the product. Roof drains in these systems consist of an open pipe that extends a short distance below the bottom of the floating roof. Since these drainpipes are filled with product to the product level in the tank, evaporative loss occurs from the top of the drainpipes. Open drainage systems can only be used on double-deck floating roofs.

Two types of roof drains are currently in common use in open drainage systems: flush drains and overflow drains. Flush drains have a drain opening that is flush with the top surface of the double deck. They permit rainwater to drain into the product. Overflow drains consist of a drain opening that is elevated above the top surface of the floating roof. Overflow drains limit the maximum amount of rainwater that can accumulate on the floating roof and are thus used to provide emergency

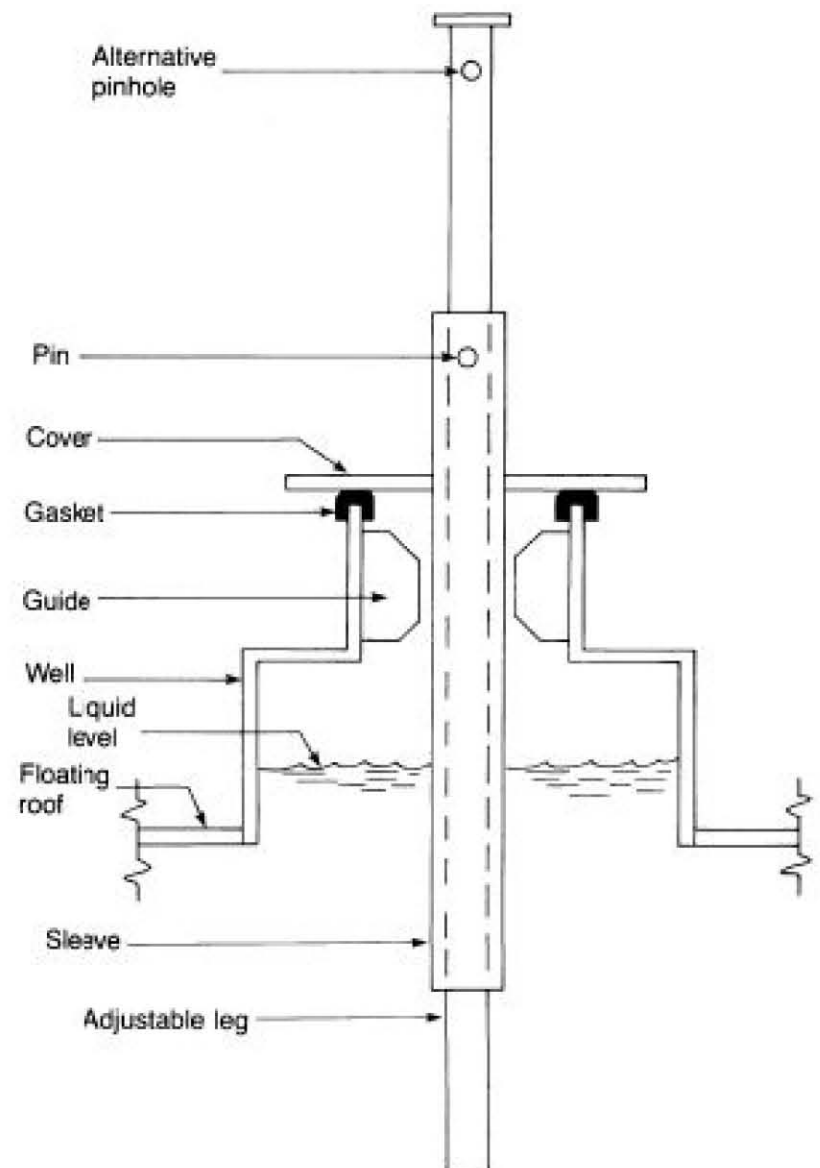


Figure 31—Vacuum Breaker

drainage of rainwater. They are normally used in conjunction with a closed drainage system to carry rainwater to the outside of the tank. Figure 32 shows a typical overflow roof drain.

For pontoon floating roofs, proprietary drain designs that employ manometer or membrane seals are available but are not commonly used.

Some open roof drains are equipped with an insert to reduce the evaporative loss. Care must be taken in the

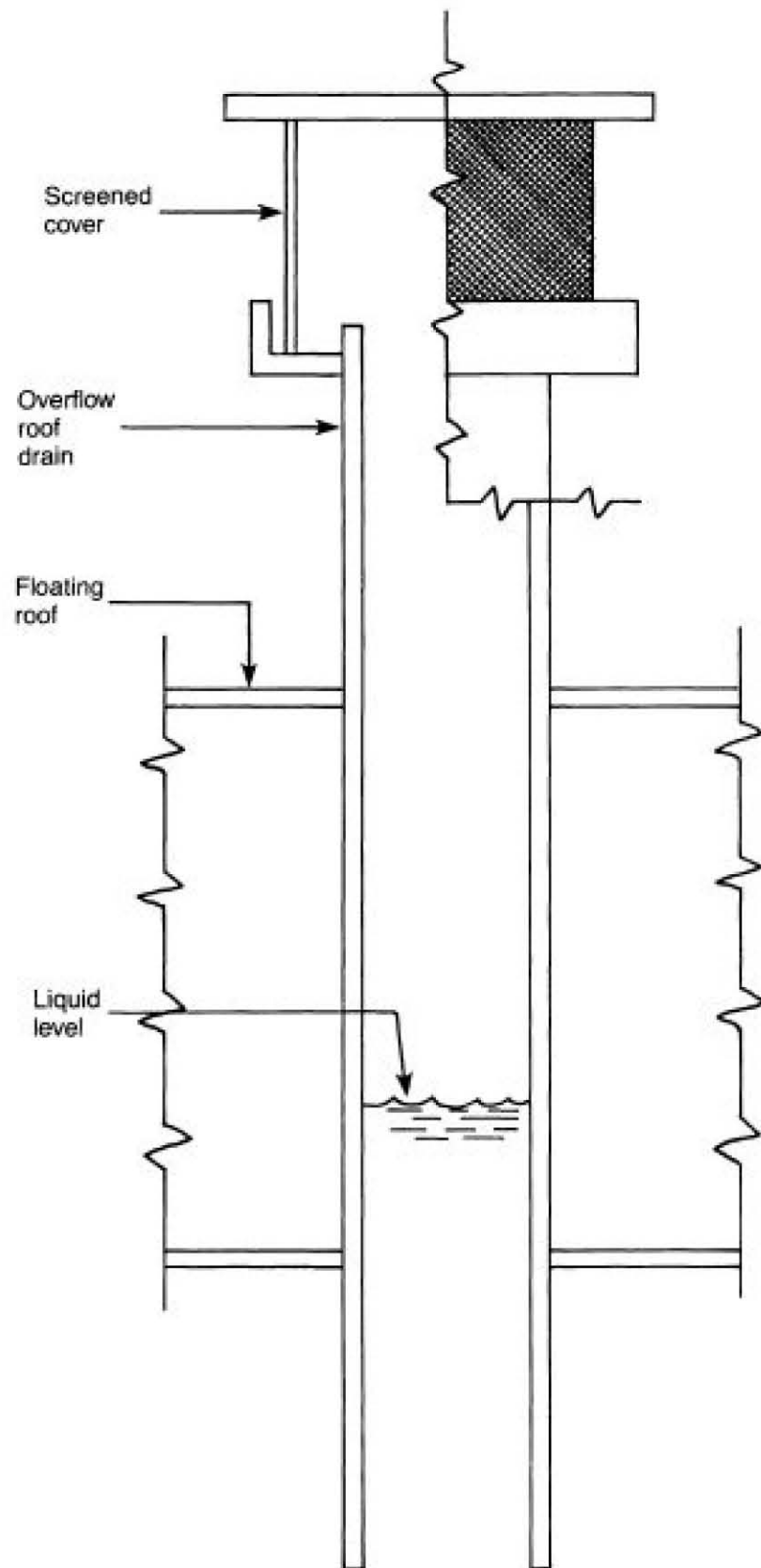


Figure 32—Overflow Roof Drain

design and use of the insert to avoid impairment of the fitting's drainage ability.

3.4.9 ROOF LEGS

Figure 33 shows a typical roof leg. To prevent damage to fittings located beneath the floating roof and to allow clearance for tank cleaning or repair, roof legs are provided to hold the floating roof at a predetermined distance above the tank bottom when the tank is emptied. The larger the diameter of the tank, the greater the number of legs required. Roof legs generally consist of an adjustable pipe leg that passes through a slightly larger diameter vertical pipe sleeve. The sleeve is welded

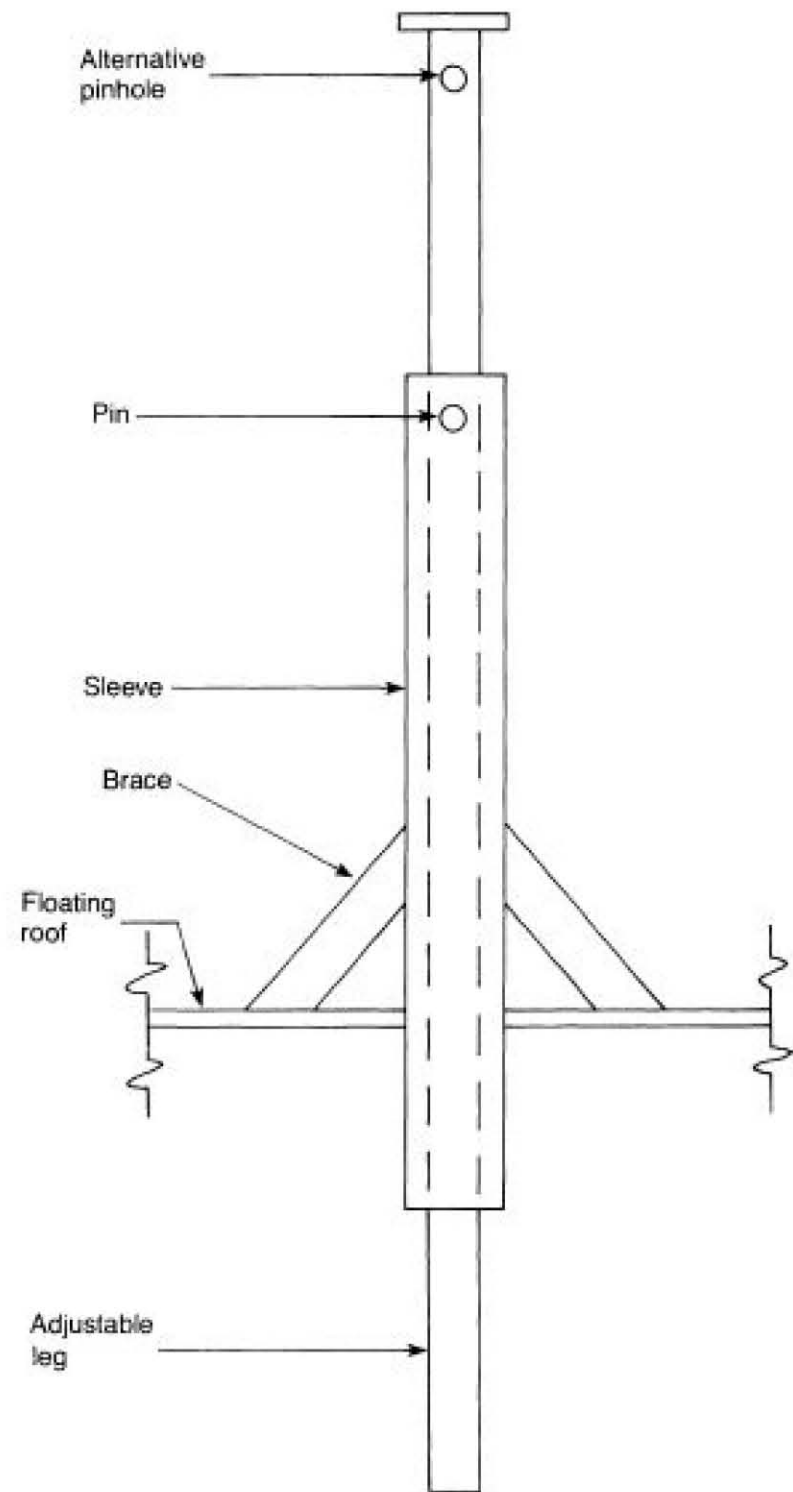


Figure 33—Roof Leg

to the floating roof, extending both above and below it. Steel pins are passed through holes in the sleeve and leg to permit height adjustment. The length of the sleeve above the floating roof varies, depending on its location on the roof. Evaporative loss occurs in the annulus between the leg and its sleeve.

3.4.10 RIM VENTS

Figure 34 shows a typical rim vent. Rim vents are normally supplied only on tanks equipped with a me-

chanical-shoe primary seal. The rim vent is connected to the rim vapor space by a pipe and releases any excess pressure or vacuum that is present. The rim vapor space is bounded by the floating-roof rim, the primary-seal shoe, the liquid surface, and the primary-seal fabric, as shown in Figure 34. Rim vents usually consist of weighted pallets that rest on gasketed surfaces.

SECTION 4—DETAILS OF LOSS ANALYSIS

4.1 Introduction

From 1976 through 1979, extensive tests were conducted to determine losses from external floating-roof tanks with various rim-seal systems. Losses were measured in a covered floating-roof test tank, 20 feet in diameter, designed and instrumented to study the independent effects of different rim-seal systems and their tightness, product types and vapor pressures, rim-space temperatures, atmospheric pressures, and ambient wind speeds on evaporative loss. Losses were measured directly by monitoring both the airflow rate induced over the floating roof and the hydrocarbon concentration in the inlet and outlet air, using an air velometer and a flame-ionization type of hydrocarbon analyzer, respectively.

To examine the effects of varying tank diameter and field conditions, losses were measured in external floating-roof field tanks. Losses from the field tanks were determined indirectly by measuring the change in liquid density over a long time period. Extensive work was performed that demonstrated the equivalence of the direct and indirect techniques for measuring evaporative loss. The test-tank and field-tank data were related by comparative studies of the test conditions.

Additional testing included measurement of losses from product clingage to the tank shell (using a test apparatus), laboratory and field investigations of wind-induced pressure differentials, thermal mixing of tank contents, and surveys of the field condition of existing rim seals.

From 1984 through 1985, evaporative-loss tests were performed on a large variety of general types of roof fittings. These tests were conducted using a bench-scale test apparatus that incorporated a wind tunnel to simulate ambient wind effects.

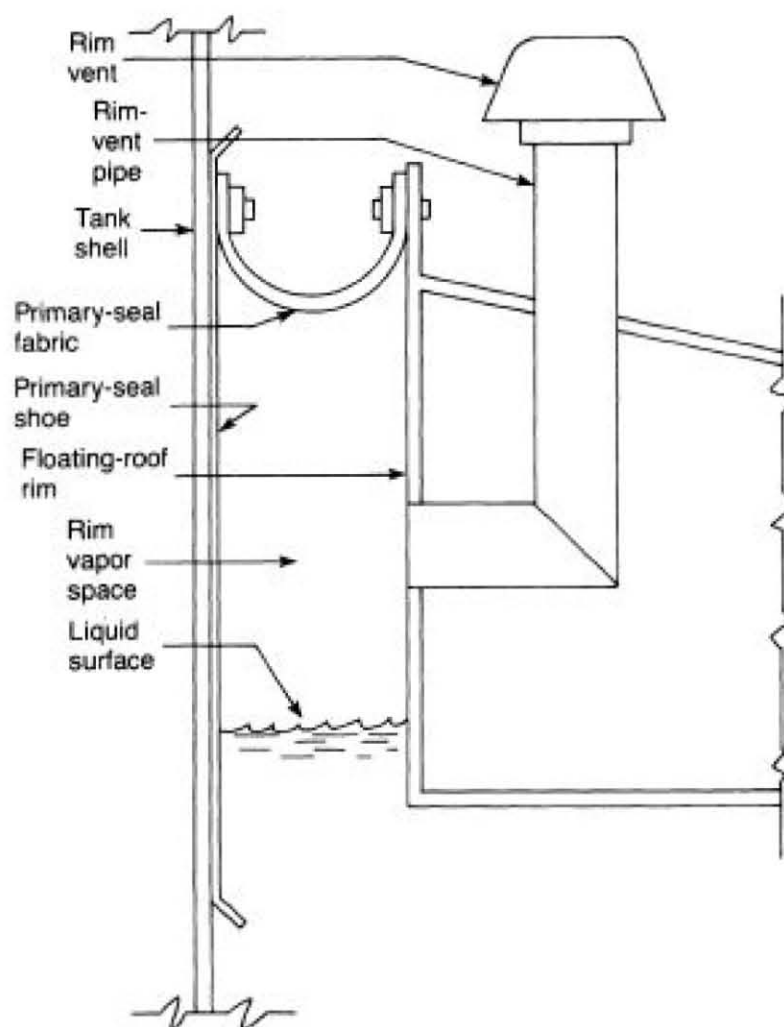
All of the work described above, in addition to relevant studies that were part of API's internal floating-roof test program, was considered in the development of

the loss-estimation methods and factors described in Section 2.

4.2 Loss Mechanisms

4.2.1 GENERAL

Every liquid stock has a finite vapor pressure, dependent on the surface temperature and composition of the



Note: Rim vents are normally supplied only on tanks equipped with a mechanical-shoe primary seal.

Figure 34—Rim Vent

liquid, that produces a tendency for the liquid to evaporate. Through evaporation, all liquids tend to establish an equilibrium concentration of vapors above the liquid surface. Under completely static conditions, an equilibrium vapor concentration would be established, after which no further evaporation would occur. However, external floating-roof tanks are exposed to dynamic conditions that disturb this equilibrium, leading to additional evaporation. These dynamic conditions are responsible for continued evaporation, resulting in stock loss and atmospheric emissions.

Evaporative losses from external floating-roof tanks primarily occur during standing storage. Sources of standing storage loss include the rim-seal system and fitting penetrations through the floating roof. Relatively minor losses result from evaporation of liquid that clings to the tank shell as stock is withdrawn from the tank. However, extremely frequent turnover of the stock in the tank can increase the significance of this withdrawal loss.

4.2.2 RIM-SEAL LOSS

The mechanisms of vapor loss from the rim seal are complex. However, wind has been found to be the dominant factor in inducing rim-seal vapor losses. Wind tunnel tests have shown that the air that flows up and over the top of a floating-roof tank produces a low-pressure zone above the floating roof on the upwind side of the tank. This results in air from the downwind side of the floating roof moving around the circumference of the floating roof above the rim seal. A steady wind thus establishes pressure differentials across the floating roof, with higher pressures on the downwind side and lower pressures on the upwind side. (Characterization of the wind-induced pressure differentials provided a means of converting airflow rates through the covered test tank into equivalent wind speeds for external floating-roof tanks, as discussed in Appendix B.)

The differential pressure and airflow patterns established across a floating roof are responsible for wind-induced losses in two basic ways: In one case, the pressure differentials cause air to enter any continuous rim vapor space beneath the rim seal on the downwind side of the floating roof. This air then flows circumferentially through the rim vapor space, flushing an air-hydrocarbon mixture out past the rim seal on the upwind (low-pressure) side of the floating roof. This action reduces the hydrocarbon concentration in the rim vapor space, so more liquid evaporates to reestablish more nearly equilibrium conditions. The magnitude of this wind-induced loss depends on the tightness of the rim-seal system and the presence of any gaps between the rim seal and the tank shell.

If no continuous rim vapor space exists between the rim seal and the liquid, the airflow pattern described

above does not apply. In this case, the wind flowing above the rim seal produces turbulence in the air that is present in any gaps between the rim seal and the tank shell. This turbulence causes fresh air to mix with the hydrocarbon vapor within the gap, resulting in a reduction in the hydrocarbon concentration within the gap and causing more liquid to evaporate to reestablish more nearly equilibrium conditions. The magnitude of this wind-induced loss depends on the area of the rim-seal gap and the depth of the vertical contact area between the rim seal and the tank shell. This mechanism can also contribute to losses from rim-seal systems that have a continuous rim vapor space. In general, lower wind-induced losses occur from rim seals with small gaps and from those with a large vertical contact area between the rim seal and the tank shell.

To a small extent, the wind-induced evaporative losses may be a function of the height of the floating roof in the tank. However, for operating field tanks, this loss variation is not considered significant.

Other potential loss mechanisms include the expansion of gas in the rim vapor space attributable to changes in temperature, pressure, or both (that is, breathing) and the varying solubility of gases, such as air, in the rim-space liquid as a function of temperature and pressure.

Breathing in the rim vapor space can occur as the pressure or temperature (or both) of the rim vapor changes. As the vapor temperature increases or the barometric pressure decreases, an air-hydrocarbon mixture can be expelled from the rim vapor space. As the vapor temperature decreases or the barometric pressure increases, fresh air can be drawn into the rim vapor space. This causes further evaporation and can also result in vapor being expelled from the rim vapor space. The degree to which the vapor is contained in or expelled from the rim vapor space during temperature and pressure changes is a function of the tightness of the rim-seal system and the pressure and vacuum settings of any rim vents on the floating roof.

Changes in the temperature of the liquid in the rim space or the barometric pressure can cause air to dissolve in or be evolved from the liquid. As the liquid temperature increases or the barometric pressure decreases (or both), the air solubility generally decreases, and air evolves from the liquid in the rim space. As air leaves the liquid, it carries with it some hydrocarbon vapor.

In the test tank, the wind speed was varied to determine the effect of wind-induced losses. The temperature of the vapor and liquid in the rim space and the atmospheric pressure were varied in some of the tests to examine the breathing and solubility loss mechanisms. The standing storage rim-seal loss factors presented in 2.2.2.1 were developed by averaging tests in which some or all of these loss mechanisms occurred. Therefore, all

of these loss mechanisms are accounted for in the loss factors used with the loss equation given in Section 2. Furthermore, when tests in which only the temperatures of the vapor and liquid in the rim space and the atmospheric pressure were varied were compared with tests in which these parameters were held constant, no significant differences in losses were observed. Therefore, the breathing and solubility loss mechanisms were judged to have a negligible effect on losses.

Other possible loss mechanisms include permeation of the sealing fabric by vapor and wicking of the liquid in the rim space up the tank shell into contact with the air above the rim seal. Seal fabrics are generally reported to have very low permeability with respect to typical hydrocarbon vapors, so this source of loss is not considered significant. However, if a seal material is used that is highly permeable to the vapor from the stored stock, the rim-seal loss could be significantly higher than that estimated from the rim-seal loss equation in 2.1.2. Wicking does not occur to any appreciable extent, and thus this loss is also negligible.

4.2.3 ROOF-FITTING LOSS

Fittings that penetrate the floating roof are potential sources of loss because they can require openings that allow for communication between the stored liquid and the open space above the floating roof. Although such openings are routinely sealed, the design details of roof fittings generally preclude the use of a completely vapor-tight seal. As a result, some of the mechanisms discussed in 4.2.2 for rim-seal losses can cause losses from roof-fitting penetrations. These mechanisms include vertical mixing, resulting from diffusion or air turbulence, of vapor through any gaps between the roof-fitting seal and the fitting; expansion of any vapor spaces directly below the fitting seal, resulting from temperature and pressure changes; varying solubility of gases in the liquid directly below the fitting seal; wicking of liquid up the roof fitting; and permeation of any fitting seal or gasket by vapor.

The extent to which any one of these mechanisms contributes to the total roof-fitting loss is not known. The relative importance of the various mechanisms probably depends on the type of roof fitting and the design of the fitting seal. Nevertheless, the roof-fitting loss factors in 2.2.2.1 account for the combined effects of all of these mechanisms.

4.2.4 WITHDRAWAL LOSS

As the floating roof descends during stock withdrawal, some of the liquid stock clings to the inside

surface of the tank shell and is exposed to the atmosphere. To the extent that this clingage evaporates before the exposed shell area is again covered by the ascending floating roof during a subsequent filling, evaporative loss results.

4.3 Data Base for Loss Correlations

4.3.1 STANDING STORAGE LOSS DATA

Of the test-tank data, 106 data sets had information relevant to an evaluation of the effects of tank construction and type of rim-seal system, wind speed, stock vapor pressure, and product type on the standing storage loss. Of these data sets, 44 could be used directly in the development of the rim-seal loss factors. Although the test tank was welded, some of the tests performed covered the gap-area ranges observed for rim seals in riveted tanks. The types of rim-seal systems that were used in these tests are listed below. These systems represent the vast majority of those currently in use.

- a. Mechanical-shoe seal:
 1. Primary only.
 2. Shoe-mounted secondary.
 3. Rim-mounted secondary.
- b. Liquid-mounted resilient-filled seal:
 1. Primary only.
 2. Weather shield.
 3. Rim-mounted secondary.
- c. Vapor-mounted resilient-filled seal:
 1. Primary only.
 2. Rim-mounted secondary.

During the tests conducted in the test tank, the airflow rate was varied to simulate equivalent wind speeds of 2–15 miles per hour. The stock true vapor pressure was varied from 0.75 to 9.25 pounds per square inch absolute. The stock liquid used in most tests was a mixture of *n*-octane and propane.

To evaluate the losses from various types of roof fittings, data from 52 bench-scale tests were evaluated. During these tests, the stock true vapor pressure ranged from 1.3 to 8.4 pounds per square inch absolute. Most of the tests were conducted with *n*-hexane, but mixtures of *n*-octane and propane were also used. In addition, survey information on the number of various types of roof fittings typically used as a function of tank diameter was compiled and evaluated.

To determine the effect of tank diameter on standing storage loss, data from a total of 16 field tanks were evaluated. Losses from three of these tanks, which ranged in diameter from 35 to 152 feet, were precisely measured, and extensive supporting data on tank construction, rim-seal system, and ambient conditions were collected. The other 13 field-tank tests used slightly less

precise instrumentation and included somewhat less complete data on the field tanks, which ranged in diameter from 55 to 153 feet.

To relate test-tank rim-seal conditions to actual field-tank rim-seal conditions, data from more than 400 measurements of field-tank rim-seal gap areas were analyzed. This analysis determined the frequency of occurrence of various ranges of rim-seal gap areas in operating external floating-roof field tanks.

Additional data analyzed included tank temperature data to determine the effects of paint color on stock liquid temperature relative to ambient temperatures [1]. Several loss-measurement tests were conducted with gasoline and crude oil in the test tank. Data from these tests were used to develop the product factors. In addition, vapor samples from both gasoline and crude oil stocks were analyzed, and these showed a large range of hydrocarbon components, including methane and ethane.

4.3.2 WITHDRAWAL LOSS DATA

Tests were conducted to determine the amount of liquid that clings to steel test plates as the test plates are drawn out of a stock liquid. These data were analyzed to develop clingage factors for gasoline and crude oil.

4.4 Development of Standing Storage Loss Correlation

4.4.1 GENERAL

The important parameters that affect standing storage loss were identified and separately evaluated to determine their independent effects on the total loss. These parameters include the type and condition of the rim-seal system (K_r , n , F_r); wind speed (V); tank diameter (D); the type, number, and general design of the roof fittings (K_{fa} , K_{fb} , m , N_f , F_f); stock vapor pressure (P); and type of stock (K_c). The methods used to develop the functional loss relationships involving these parameters are outlined in 4.4.2 through 4.4.7. The appendixes are referenced for more detailed discussions of some of the parameters.

4.4.2 RIM-SEAL LOSS FACTORS

As discussed in Appendix B, a regression analysis was used to develop equations to convert the airflow rate in the covered floating-roof test tank to the equivalent wind speed across an external floating-roof field tank. An analysis of the test-tank data indicated that straight-line plots are obtained when the logarithm of the losses is plotted against the logarithm of the wind speeds. There-

fore, loss, L , is related to wind speed, V , by an equation of the following general form:

$$L = KV^n$$

Where:

K , n = constants for a given rim-seal system and condition.

By regression analysis, values of K and n were directly calculated for each rim-seal system, as discussed in Appendix A. By considering the vapor pressure, vapor molecular weight, and test-tank diameter, the rim-seal loss factors, K_r and n , were directly calculated.

It should be noted that 2.2.2.1 recommends the use of wind-speed data from local airport weather stations if tank-site wind-speed data are not available. During two of the field-tank testing programs, National Weather Service wind-speed data were collected from the nearest airport and compared with wind speeds measured at the tanks. Tank wind speeds were expected to exceed the National Weather Service data, since the former measurements were made at greater distances above ground level. In all cases, however, tank wind speeds were lower than the National Weather Service data. For the four tank sites checked, tank wind speeds averaged about 50 percent of the wind speeds obtained from local airports. Airports are generally large flat areas; tank farms are characterized by local roughness caused by tanks, dikes, buildings, and other obstructions. These tank farm features contribute to turbulence that could conceivably decrease the local effective horizontal wind component, but the data were too limited to develop general conclusions. However, the data indicate that use of wind-speed data from local airports will generally provide conservative loss estimates. Calculated losses based on airport wind-speed data will generally be higher than those calculated using wind-speed data from the tank site.

4.4.3 TANK DIAMETER

The dependence of evaporative loss on tank diameter, D , was determined by comparing measured field-tank losses with predicted losses based on the test-tank data. As discussed in Appendix C, test-tank data were selected that most closely matched the conditions for the field-tank rim-seal systems. The data from these tests were used to predict expected field-tank losses as a function of the tank diameter raised to a variable exponent. The predicted losses were then plotted against varying values of the exponent. The exponents that resulted in the predicted losses being equivalent to the measured losses were read directly from these graphs. For the three field tests used as the primary data base, within the accuracy of the measured results, an exponent of 1 was

observed. Although a similar analysis of the other 13 field-tank tests showed significantly more variability, it too supported an exponent of 1.

4.4.4 ROOF-FITTING LOSS FACTORS

As described in Appendix D, losses from various types and designs of roof fittings were directly measured on a bench-scale test apparatus that used a wind tunnel to simulate the ambient wind speed at an external floating-roof tank site. Using the bench test apparatus, losses from several selected fitting types were determined by measuring the loss of liquid stock weight over time. These data were analyzed to obtain the roof-fitting loss factors, K_{fa} , K_{fb} , and m , for each fitting type.

These loss factors are applicable to average wind speeds from 2 to 15 miles per hour for typical roof-fitting conditions. This assumes a gap of approximately $1/8$ inch between a roof penetration (for example, a guide pole) and the sealing material on the well's sliding cover. Loss factors for roof-fitting types or conditions not addressed in this publication can be derived from the roof-fitting loss data, using the analysis procedures included in the documentation file for Appendix D.

Survey information from manufacturers was compiled to determine typical values for the number of each type of roof fitting generally installed, N_f , as a function of tank diameter.

To arrive at a total roof-fitting loss factor, F_f , for a given tank, roof-fitting loss factors K_{fa} , K_{fb} , and m can be combined either with information on the specific number of each roof-fitting type included in the tank under consideration or with typical N_f values.

4.4.5 VAPOR PRESSURE FUNCTION

As detailed in Appendix E, test-tank data in which the only variable was stock true vapor pressure were analyzed to determine how the standing storage loss varies with vapor pressure, P . Two proposed functional relationships were tested by correlation analysis techniques. Both functions were found to correlate about equally well with the data. However, one function becomes infinite as P approaches atmospheric pressure, P_a , and the other does not. Therefore, the latter function, P^* (as defined in 2.2.2.3), was selected to determine the effect of stock true vapor pressure on standing storage loss.

4.4.6 PRODUCT FACTORS

A product factor, K_c , was included in the equation for standing storage loss to account for the effects of different types of liquid stocks on evaporative loss. These effects (such as weathering) are in addition to those

accounted for by consideration of differences in stock true vapor pressure and vapor molecular weight. Since the loss equation was developed primarily from tests of mixtures of n -octane and propane, the product factors quantify the relative loss from a given stock type, compared with the loss from mixtures of n -octane and propane.

Tests were performed in the test tank to compare mixtures of n -octane and propane with both a midcontinent crude oil and gasoline. As a first approximation, it was assumed that the only differences would be the vapor pressure, P , and the molecular weight of the emitted vapors, M_v . However, after the data were normalized for these factors, the losses from crude oil were observed to be consistently less than those from the mixtures of n -octane and propane at all wind speeds, whereas the losses from gasoline were approximately equal to those from the mixtures of n -octane and propane.

As outlined in Appendix F, an analysis of the crude oil and gasoline data resulted in a crude oil product factor of 0.4 and a gasoline product factor of 1.0. The product factor for single-component stocks was developed in other API studies, as documented in Publication 2519 [2].

4.4.7 TANK PAINT COLOR

The tank paint color influences the amount of solar heat absorbed and thus the average stock liquid temperature. If the stock liquid temperature in a floating-roof storage tank has been measured, this measured value should be used to calculate the stock's true vapor pressure. In this case, no consideration of the tank paint color is needed. However, if the stock liquid temperature is not known, it can be estimated from the average ambient temperature at the tank site and the tank paint color, as shown in Table 10.

4.5 Development of Withdrawal Loss Correlation

Tests were conducted to determine the amount of stock that clings to the exposed tank wall as stock is withdrawn from a tank. In these tests, a lightly rusted steel test plate was alternately raised out of and lowered into a liquid. Sections of a floating-roof rim seal were placed above the liquid surface so that they provided a wiping action against the steel test plate as it was withdrawn. Measurements were made of the change in liquid level after many withdrawal cycles. These data were analyzed to calculate clingage factors, C , for different stocks and tank shell conditions. This analysis is discussed in more detail in Appendix G.

SECTION 5—REFERENCES

1. Publication 2518, *Evaporation Loss from Fixed-Roof Tanks*, 1st edition, American Petroleum Institute, Washington, D.C., June 1962.
2. Publication 2519, *Evaporation Loss from Internal Floating-Roof Tanks*, 3rd edition, American Petroleum Institute, Washington, D.C., June 1983.
3. "Gap Criteria for External Floating-Roof Seals" (Docket OAQPS 78-2, "Petroleum Liquid Storage Vessels," Part 4-B-7, from L. Hayes of TRW), Research Triangle Park, North Carolina, December 4, 1979.
4. "Western Oil and Gas Association Metallic Sealing Ring Emission Test Program" (Interim Report, Research Contract R-0136), Chicago Bridge & Iron Company, Plainfield, Illinois, January 19, 1977.
5. "Western Oil and Gas Association Metallic Sealing Ring Emission Test Program" (Final Report, Research Contract R-0136), Chicago Bridge & Iron Company, Plainfield, Illinois, March 25, 1977.
6. "Western Oil and Gas Association Metallic Sealing Ring Emission Test Program" (Supplemental Report, Research Contract R-0136), Chicago Bridge & Iron Company, Plainfield, Illinois, June 30, 1977.
7. "Hydrocarbon Emission Loss Measurements on a 20 Foot Diameter Floating-Roof Tank With a Type SR-1 Seal for a Product at Various Vapor Pressures" (Report 2, Research Contract R-0134), Chicago Bridge & Iron Company, Plainfield, Illinois, October 25, 1977.
8. R. J. Laverman, "Floating Roof Seal Development, Emission Test Measurements on Proposed CBI Wiper Type Secondary Seal for SR-1 Seals" (Letter Report, Research Contract R-0134), Chicago Bridge & Iron Company, Plainfield, Illinois, February 23, 1977.
9. W. N. Cherniwchan, "Hydrocarbon Emissions from a Leaky SR-1 Seal With a Mayflower Secondary Seal" (Report 1, Research Contract R-0177), Chicago Bridge & Iron Company, Plainfield, Illinois, September 20, 1977.
10. "Hydrocarbon Emission Loss Measurements on a 20 Foot Diameter External Floating-Roof Tank Fitted With a CBI SR-5 Liquid Filled Seal" (Final Report, Research Contract R-0167), Chicago Bridge & Iron Company, Plainfield, Illinois, August 31, 1978.
11. "SOHIO/CBI Floating Roof Emission Test Program" (Interim Report, Research Contract R-0101), Chicago Bridge & Iron Company, Plainfield, Illinois, October 7, 1976.
12. "SOHIO/CBI Floating-Roof Emission Test Program" (Final Report, Research Contract R-0101), Chicago Bridge & Iron Company, Plainfield, Illinois, November 18, 1976.
13. "Wind Speed Versus Air Flow Rate Calibration of 20 Foot Diameter Floating-Roof Test Tank" (Final Report, Research Contract R-0177), Chicago Bridge & Iron Company, Plainfield, Illinois, October 5, 1977.
14. J. F. Marchman, "Wind Effects on Floating Surfaces in Large Open-Top Storage Tanks," Paper presented at the Third Conference on Wind Effects on Buildings and Structures, Tokyo, 1971.
15. J. F. Marchman, "Surface Loading in Open-Top Tanks," *Journal of the Structural Division, American Society of Civil Engineers*, November 1970, Volume 96, Number ST11, pp. 2551-2556.
16. Publication 2517, *Evaporation Loss from Floating-Roof Tanks*, 1st edition, American Petroleum Institute, Washington, D.C., 1962.
17. A. K. Runchal, "Hydrocarbon Vapor Emissions from Floating-Roof Tanks and the Role of Aerodynamic Modifications," *Air Pollution Control Association Journal*, Volume 28, Number 5, May 1978, pp. 498-501.
18. J. G. Zabaga, "API Floating-Roof Tank Test Program," Paper presented at the 72nd Air Pollution Control Association Meeting, Cincinnati, Ohio, June 26, 1979.
19. Radian Corporation, "Field Testing Program to Determine Hydrocarbon Emissions from Floating-Roof Tanks," Report prepared for the Floating-Roof Tank Subcommittee, Committee on Evaporation Loss Measurement, American Petroleum Institute, Washington, D.C., May 1979.
20. "Measurement of Emissions from a Tubeseal Equipped Floating-Roof Tank," Pittsburgh-Des Moines Steel Company, Pittsburgh, Pennsylvania, December 4, 1978 (including supplemental report issued January 16, 1979).
21. Engineering Science, Inc., "Phase I, Test Program and Procedures," Report prepared for the Floating-Roof Tank Subcommittee, Committee on Evaporation Loss Measurement, American Petroleum Institute, Washington, D.C., November 1977.
22. Chicago Bridge & Iron Company, "Development of Laboratory Procedures for Use in the Field Testing Program to Determine Hydrocarbon Emissions from Floating-Roof Tanks," Report prepared for the Floating-Roof Tank Subcommittee, Committee on Evaporation Loss Measurement, American Petroleum Institute, Washington, D.C., May 18, 1978.
23. Chicago Bridge & Iron Company, "Hydrocarbon Emission Measurements of Crude Oil on the 20 Foot Diameter Floating-Roof Pilot Test Tank," Report prepared for the Floating-Roof Tank Subcommittee, Committee on Evaporation Loss Measurement, American Petroleum Institute, Washington, D.C., August 15, 1978.
24. Engineering Science, Inc., "Hydrocarbon Emissions from Floating-Roof Storage Tanks," Report prepared for the Western Oil and Gas Association, Los Angeles, January 1977.
25. CBI Industries, Inc., "Testing Program to Measure Hydrocarbon Evaporation Loss from External Floating-Roof Fittings" (CBI Contract 41851), Final report prepared for the Committee on Evaporation Loss Measurement, American Petroleum Institute, Washington, D.C., September 13, 1985.
26. R. L. Russell, "Analysis of Chicago Bridge & Iron Co. External Floating-Roof Tank Fitting Loss Data," Report prepared for Task Group 2517, Committee on Evaporation Loss Measurement, American Petroleum Institute, Washington, D.C., October 17, 1985.
27. R. J. Laverman, "Emission Measurements on a Floating Roof Pilot Test Tank," *1979 Proceedings—Refining Department*, Volume 58, American Petroleum Institute, Washington, D.C., 1979, pp. 301-322.
28. "SOHIO/CBI Floating-Roof Emission Test Program" (Supplemental Report, Research Contract R-0101), Chicago Bridge & Iron Company, Plainfield, Illinois, February 15, 1977.

APPENDIX A—DEVELOPMENT OF RIM-SEAL LOSS FACTORS

A.1 Mathematical Development of Rim-Seal Loss Factors

Test-tank data were analyzed to determine relative loss rates. Direct measurements of hydrocarbon concentration and airflow rate were converted to a mass loss rate, and the airflow rate was converted to wind speed (as described in Appendix B). The entire data base was reviewed and all relevant test data were analyzed. The logarithm of the losses from the selected tests was plotted as a function of the logarithm of wind speeds; linear regressions were performed on each set of loss versus wind-speed data. From the regression analyses, constants were obtained that were directly related to rim-seal loss factors K_r and n (as defined in 2.2.2.1).

K_r and n values were determined for the following cases, representing specific types of tank construction and types of primary rim seals:

- a. Welded tanks with (1) mechanical-shoe primary seals, (2) resilient-filled primary seals mounted with the rim seal in contact with the liquid (liquid mounted), and (3) resilient-filled primary seals mounted so that a vapor space exists between the rim seal and the liquid surface (vapor mounted).
- b. Riveted tanks with mechanical-shoe primary seals.

For each of these four tank-construction/primary-rim-seal cases, three rim-seal system configurations were included:

- a. Primary seal only.
- b. Primary seal plus shoe-mounted secondary seal (or a weather shield for a resilient-filled primary seal).
- c. Primary seal plus rim-mounted secondary seal.

K_r and n are interdependent; therefore, relative loss rates are not represented solely by a comparison of K_r values. A comparison of the F_r values, which are the products $K_r V^n$, is the proper measure of relative loss rates. Figures 1–4 may be used to compare the loss-control effectiveness of different rim-seal systems.

Two sets of K_r and n values were developed for the different cases of tank construction and rim-seal system. These two sets of rim-seal loss factors represent average-fitting and consistently tight-fitting rim-seal conditions. Their development is outlined in A.2 and A.3.

A.2 Development and Applicability of Average Rim-Seal Loss Factors

In many cases, but not all, losses were observed to increase as the tightness of fit of the rim seal against the tank shell decreased. This seal fit was characterized by the total area of the gap between the rim seal and the tank shell per foot of tank diameter. However, this measure of rim-seal tightness is not the only rim-seal condition that affects loss. Other conditions, such as relative location of the rim-seal gap, also affect loss, but these could not be quantified. Because of the effects of such randomly varying rim-seal conditions in field tanks, an explicit correlation between loss and area of the rim-seal gap will not exist. Therefore, to develop average rim-seal loss factors for each type of tank construction and rim-seal system described in A.1, the test-tank data selected for analysis included a wide range of rim-seal conditions marked by varying rim-seal gap areas and relative rim-seal gap locations.

In general, three categories of rim-seal gap areas were defined:

- a. Tight seals, with no gaps greater than $\frac{1}{8}$ inch.
- b. Small gap areas, which are commonly encountered in operating tanks.
- c. Large gap areas, which occur only infrequently.

For each type of tank construction and rim-seal system, all of the applicable loss data in each category were averaged together to determine representative factors for each category. To determine average factors for each type of tank construction and rim-seal system representative of a typical operating tank, the loss factors for each category were averaged. Categories were averaged by weighting according to the frequency with which each category occurs in operating tanks.

Field-tank gap measurement data collected by an air regulatory agency [3] were used to determine the frequency with which operating tanks exhibit specific rim-seal gap areas. Data from more than 400 tank inspections were analyzed by tank construction and rim-seal system. These data were interpreted as an indication of the percentage of time that a typical operating tank will exhibit a specific gap area. Since operating tanks generally have gap areas that vary as the roof height changes,

no one gap area is representative of an average tank. A typical tank is assumed to have a range of gap areas that corresponds to the distribution of gap areas determined from the tank inspection data.

The average rim-seal loss factors (see Table 3) are judged to be applicable to all typical operating tanks. These loss factors are based on distributions of rim-seal gap areas measured in operating tanks between 1976 and 1977. The difference in rim-seal loss factors between riveted and welded tanks with the same rim-seal system reflects the fact that the average rim-seal gap area in riveted tanks is greater than that in welded tanks. If future design or maintenance practice causes a significant change in gap area distributions, these average loss factors could be modified accordingly.

The average rim-seal loss factors developed are applicable to average wind speeds from 2 to 15 miles per hour.

A.3 Development and Applicability of Tight Rim–Seal Loss Factors

From the tank inspection data, rim-seal systems are tight (that is, have no gaps greater than $\frac{1}{8}$ inch) a significant percentage of the time (depending on tank construction and rim-seal system). Loss data from tests representing only a tight primary-seal condition were averaged to determine the rim-seal loss factors for tight primary-seal systems given in Table 3. Because the presence of small gaps in the primary seal below a tight secondary seal does not significantly influence loss, the rim-seal loss factors for tight secondary-seal systems given in Table 3 are based on data from both tight systems and those with small gaps in the primary seal under a tight secondary seal.

The tight rim-seal loss factors are applicable to welded tanks with rim-seal systems that remain consistently tight throughout the range of operating roof heights. No information is available on the extent to which it is possible to maintain consistently tight-fitting seals.

The tight rim-seal loss factors developed are applicable to average wind speeds from 2 to 15 miles per hour.

A.4 Data Base for Rim–Seal Loss Factors

Eighteen test-tank data sets were used to develop the average and tight rim-seal loss factors for mechanical-shoe primary seals in welded tanks [4–9]. In this case, the loss rate from primary seals did not vary with rim-seal gap area from tight-fitting seals to those with the rim-seal gap areas found approximately 90 percent of the time. Twenty test-tank data sets were used to develop the average and tight rim-seal loss factors for mechanical-shoe primary seals in riveted tanks [4–9]. In addition to variable gap areas and relative gap locations, a wide range of variability in the tightness of the primary-seal fabric is represented by the selected tests of mechanical-shoe primary seals for both welded and riveted tanks.

Six test-tank data sets were used to develop the loss factors for liquid-mounted resilient-filled primary seals [10], and eighteen test-tank data sets were used to develop the loss factors for vapor-mounted resilient-filled seals [11, 12]. The vapor-mounted rim-seal tests were conducted with a vertical vapor space of approximately 8 inches between the bottom of the rim seal and the liquid stock, representing the upper end of the range of rim vapor space sizes typical of vapor-mounted seals. Loss rates should decrease as this vapor space becomes smaller, approaching those from liquid-mounted seals. However, the effect of rim vapor space size on loss rates could not be quantified with currently available data.

A complete summary of the test conditions for the more than 100 test-tank data sets considered in the analysis of rim-seal loss factors is included in the documentation file for Appendix A. This file also includes graphs of loss rate versus wind speed for all the tests used to develop the rim-seal loss factors for each category. A summary of the field-tank inspection data is also included.

APPENDIX B—DEVELOPMENT OF RELATIONSHIP BETWEEN AIRFLOW RATE AND WIND SPEED

A test tank with a diameter of 20 feet was used to determine relative evaporative-loss levels. This test tank was fitted with an external floating roof (minus all roof fittings) and several different rim-seal systems. However, unlike an external floating-roof tank in the field, the test tank was covered to allow direct loss measurements. Air was blown into the test tank through a duct and exited through another duct 180 degrees from the inlet. This permitted direct measurements of flow rate and concentration from which losses could be calculated. The airflow rate was varied to simulate varying wind speeds above an external floating-roof tank. To relate losses from the test tank to those expected from field tanks, it was necessary to develop a relationship between the test-tank airflow rate and the corresponding wind speed at a tank site.

The approach taken was to relate the measured airflow-induced pressure differentials around the perimeter of the test tank's floating roof [13] to wind-induced pressure differentials that had been measured in wind-tunnel tests [14, 15] and on an actual field tank [11, 12]. A review of these results showed that the patterns of pressure differentials obtained in the test tank were similar to those obtained in both the wind-tunnel and field tests. It was therefore concluded that wind effects on losses from external floating-roof tanks were adequately simulated in the test tank.

A series of tests was conducted in which the pressures at various positions around the perimeter of the floating roof were measured as a function of airflow rate. Using these data, a regression analysis was performed to relate the measured test-tank airflow rate to the corresponding wind speed at a tank site, as outlined below.

Wind speed is related to pressure differentials by the following equation:

$$V = \left[\frac{(P_1 - P_j)2g}{(C_{p1} - C_{pj})\gamma} \right]^{0.5} \quad (\text{B-1})$$

Where:

- V = wind speed.
- $P_1 - P_j$ = differential pressure between Positions 1 and j around the perimeter of the floating roof.

- g = acceleration due to gravity.
- $C_{p1} - C_{pj}$ = difference in pressure coefficients between Positions 1 and j .
- γ = specific weight of air.

A value of 1 for $C_{p1} - C_{pj}$ was determined from wind-tunnel and field tests [11, 12, 15].

Pressures, P_j , at varying circumferential positions, j , around the perimeter of the floating roof, relative to a reference pressure at the leeward position on the floating roof, P_1 , were found to be related to the airflow rate, G , by the following equation:

$$P_1 - P_j = A_j G^b \quad (\text{B-2})$$

Where:

- A_j = position-dependent constant.
- G = airflow rate.
- b = airflow rate exponent.

Values for A_j and b were calculated by linear regression of $\log(P_1 - P_j)$ versus $\log G$.

Because the data analysis supported a value of 2 for b , Equations B-1 and B-2 were combined to result in the following relationship between the test-tank airflow rate, G , and the corresponding wind speed, V , at a tank site:

$$V = B_j G \quad (\text{B-3})$$

Where:

- B_j = constant evaluated for the case where Position j is on the windward side of the roof.

Equation B-3 was used to calculate the wind speed that corresponds to the test-tank airflow rate.

The wind-tunnel tests indicated that the pressure differentials did not vary significantly with the height of the roof in the tank. Since wind-induced losses are proportional to wind speed, and thus to the pressure differentials, these losses should not vary significantly with roof height.

The mathematical analysis and all supporting data used to develop the relationship between airflow rate and wind speed are in the documentation file for Appendix B.

APPENDIX C—DEVELOPMENT OF DIAMETER FUNCTION

The API correlation for estimating evaporative losses from floating-roof tanks in the first edition of Publication 2517 [16] indicated that losses are proportional to diameter raised to the 1.5 power. However, more recent aerodynamic studies [17] of wind effects on tank losses concluded that the diameter exponent should be 1 (that is, that losses are directly proportional to tank diameter).

To determine an empirical value for the diameter exponent, test programs were conducted to measure evaporative losses from field tanks that varied from 35 to 152 feet in diameter. The 1977–79 API field-test program is summarized in Reference 18.

Losses from the field tanks were determined by the density change method. Increases in stock bulk density were examined in two tanks tested by API [19] and one tank tested independently [20]. The increases in stock density were related to the decrease in stock volume (evaporative loss) [19, 21, 22, 23].

Field-tank rim-seal conditions were analyzed and compared with the test-tank data base, as described in 4.3.1. Loss predictions for the field tanks were developed from the test-tank data. These predictions, which incorporated the properties of the stock and climatic conditions at the field tanks, were used to evaluate the influence of tank diameter on evaporative loss.

Field-tank losses were calculated as a function of a variable exponent of tank diameter. These calculated values were plotted to determine the relationship between loss and diameter exponent, as shown in Figure C-1. Measured losses from the field tests were then compared with the predicted losses. Based on this comparison, a diameter exponent of 1 was established for the loss equation.

Data from a floating-roof tank test program sponsored by the Western Oil and Gas Association (WOGA) in 1976 [24] were evaluated in a similar manner. The WOGA tests involved 13 tanks in gasoline or volatile stock service, for which losses were measured with similar techniques. The WOGA program was the first in which sophisticated density-measurement instrumentation was used. Data scatter in this developmental program was higher than in the test programs discussed above. Wind speeds at the tank sites were not measured, and less information about the rim-seal conditions was obtained. Nevertheless, the average diameter exponent developed from the WOGA results supports the conclusion that the diameter exponent in the loss equation is 1.

The mathematical analysis and all supporting data used to develop the diameter exponent are in the documentation file for Appendix C.

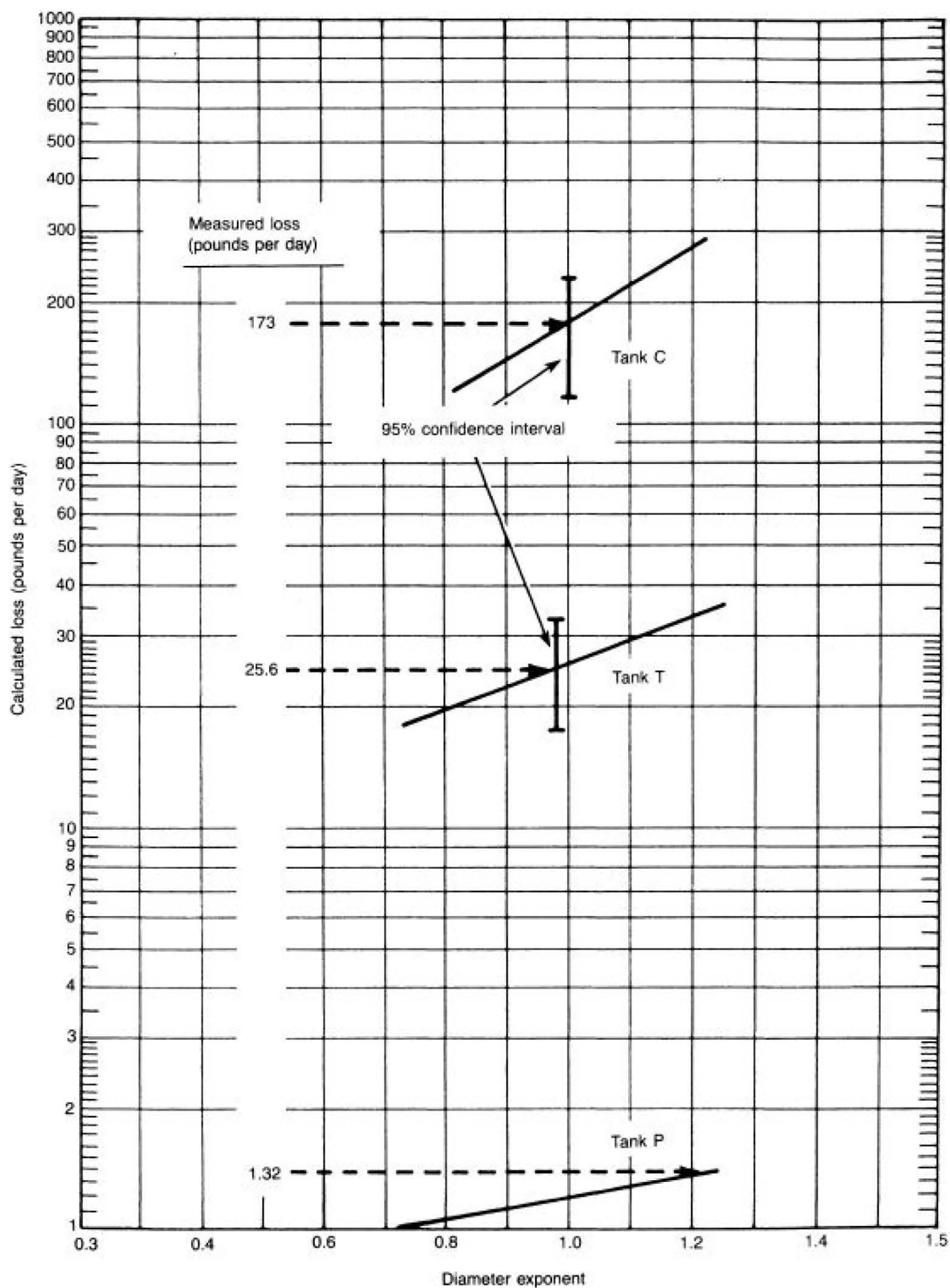


Figure C-1—Calculated Losses as a Function of Diameter Exponent

APPENDIX D—DEVELOPMENT OF ROOF-FITTING LOSS FACTORS

D.1 Mathematical Development of Roof-Fitting Loss Factors

The evaporative loss from the roof fittings on an external floating roof is the sum of the losses from each type of roof fitting. The losses for each type of fitting can be estimated as follows:

$$L_f = N_f K_f P^* M_v K_c \quad (\text{D-1})$$

Where:

- L_f = evaporative loss from the type of roof fitting being considered, in pounds per year.
- N_f = number of roof fittings of the type being considered (dimensionless).
- P^* = vapor pressure function (dimensionless).
- M_v = average stock vapor molecular weight, in pounds per pound-mole.
- K_c = product factor (dimensionless).
- K_f = roof-fitting loss factor, in pound-moles per year.

The roof-fitting loss factor, K_f , for each type of fitting can be estimated as follows:

$$K_f = K_{fa} + K_{fb} V^m \quad (\text{D-2})$$

Where:

- K_{fa} = loss factor for a particular type of roof fitting, in pound-moles per year.
- K_{fb} = loss factor for a particular type of roof fitting, in pound-moles per (miles per hour)^{*m*}-year.
- m = loss factor for a particular type of roof fitting (dimensionless).
- V = wind speed, in miles per hour.

After each roof fitting has been considered, the total roof-fitting loss is the sum of the losses from each type of roof fitting.

D.2 Data Base for Roof-Fitting Loss Factors

Experimental data [25] were used to determine roof-fitting loss factors. Tests were performed in a wind tunnel constructed for this test program. Four roof fittings could be tested simultaneously in this facility. Each roof fitting was mounted on an independent product reservoir that rested on a digital platform scale. The top of each roof fitting extended into the wind tunnel. Air passed over the roof fitting at a known velocity to simulate the wind on an actual external floating roof. Evaporation loss was measured by a weight-change method, using a computer-controlled data acquisition system that

would automatically record the weight of each test fixture, the product temperature, the air temperature, and the wind speed at specified time intervals. The wind tunnel was operated at wind speeds of 0, 5, and 14 miles per hour.

To be consistent with the mathematical formulations used in the development of rim-seal losses, the resulting loss data for each roof fitting were fitted to an equation assumed to have the form of Equation D-2.

The wind speeds measured in the wind tunnel were assumed to represent both the local wind speed at a particular roof fitting and the wind speed at the tank location. A literature search found no data to alter this assumption. This assumption is considered conservative in that the wind speed at any fitting on a floating roof will be less than the wind speed at the tank location. Both single-component hydrocarbons (*n*-hexane) and mixtures of propane and *n*-octane were tested. The data did not show a weathering effect for mixtures.

D.3 Roof Fittings Tested

Eight series of tests were performed, with four generic types of roof fittings tested in each series. These fittings were chosen as being representative of the most common roof fittings on existing external floating-roof tanks. The following fittings were tested:

- a. An 8-inch-diameter, Schedule 40 slotted guide pole and well, with the liquid level 18 inches below the level of the sliding plate and a 16-gauge sliding cover over the guide plate at the top of the 21³/₁₆-inch-inside-diameter well. The following features were varied:
 1. The guide-pole slots (2 inches wide × 10 inches long) were oriented at 0, 45, and 90 degrees from the wind-tunnel axis (wind direction) by rotating the pole about its vertical axis.
 2. The guide pole was tested with and without a float. The float was a tube with an outside diameter of 7.5 inches and a length of 28.5 inches, with sealed end covers. A wiper seal 8 inches in diameter was attached to the upper cover.
 3. The well was tested with the sliding plate sealed and unsealed.
- b. A 15-inch-diameter covered well with an unbolted sliding cover, with the liquid level 18 inches below the cover. The well was tested with and without a preformed sponge-foam gasket.
- c. A 6-inch-diameter, Schedule 40 open roof drain, with the liquid level 18 inches below the top of the drainpipe. The following features were varied:

1. The roof drain was tested with and without an insert in the upper end of the drainpipe. The insert was a 20-gauge galvanized sheet with triangular notches cut so that the remaining area represented 90-percent closure of the open roof drain.
 2. The roof drain was tested with *n*-hexane product and with product that was a mixture of propane and *n*-octane.
- d. A 2-inch-diameter, Schedule 80 open pipe, with the liquid level of the *n*-hexane product 18 inches below the top of the pipe.
- e. A 1-inch-diameter, Schedule 40 open pipe, with the liquid level of the *n*-hexane product 18 inches below the top of the pipe.
- f. A 4-inch-diameter, Schedule 40 pipe sleeve with a 3-inch-diameter, Schedule 40 pipe roof leg held in position by a 1.250-inch-diameter pin through a 1.375-inch-diameter pinhole located 3 inches below the top of the pipe sleeve. The closed upper end of the pipe roof leg was kept 15 inches above the top of the pipe sleeve. The following features were varied:
1. The fitting was tested with *n*-hexane product and with product that was a mixture of propane and *n*-octane.
 2. The liquid levels used were 18 inches and 36 inches below the top of the pipe sleeve.
- g. A 3-inch-diameter, Schedule 40 pipe sleeve with a 2.5-inch-diameter, Schedule 40 pipe roof leg held in position by a 1.250-inch-diameter pin through a 1.375-inch-diameter pinhole located 3 inches below the top of the pipe sleeve. The closed upper end of the pipe roof leg was kept 15 inches above the top of the pipe sleeve. The fitting was tested with *n*-hexane product and with product that was a mixture of propane and *n*-octane.

The data obtained from the 15-inch-diameter covered well were used to calculate losses from similar covered fittings. This calculation was based on a ratio of well diameters. Loss factors for the following roof fittings were calculated in this manner:

- a. A 20-inch-diameter gauge-float well.
- b. A 24-inch-diameter access hatch.
- c. A 6-inch-diameter rim vent.
- d. A 10-inch-diameter vacuum breaker.
- e. An 8-inch-diameter gauge-hatch/sample well.

Similarly, the test data for the 6-inch-diameter open roof drain were used to calculate losses from a 3-inch-diameter open roof drain by the ratio of the internal cross-sectional areas of the drainpipes.

D.4 Analysis of the Roof-Fitting Loss Data

The computer-controlled data acquisition system recorded the specified information from the wind tunnel.

The test data were stored on computer disks. The data were presented in the form of plots of product loss versus net time. The stored data were directly reduced by the computer, using regression techniques. The tests were documented in the form of plots of product loss versus net time.

In addition, when two-component mixtures were tested, initial, intermediate, and final samples were taken of the product, from which the compositions and vapor pressures were determined.

Least-squares regression was used on all of the test data to determine the slope of the data plots (which corresponds to the loss rate) for each roof fitting at time zero [26]. Whenever possible, the test data were fitted to a first-order polynomial, and the loss rate was determined by evaluating the first derivative of the polynomial. In several of the tests, however, the loss rate changed significantly as the test progressed. In these cases, the test data were fitted to a second-order polynomial at the start of the test, and the loss rate was determined by evaluating the first derivative of the polynomial at the start of the test. The second-order fit was used for all tests in which either the liquid level or the product vapor pressure changed significantly during the test. This method seemed reasonable, since it was only the initial loss rate that was used to calculate the roof-fitting loss factors.

The initial loss rate (in pound-moles per year) for each roof-fitting test was determined, and the recorded temperatures and measured vapor pressures were used to normalize the test data to a true vapor pressure of 1.91 pounds per square inch absolute.

These normalized test data represent the bulk of the data used to determine the roof-fitting loss factors. However, some additional data were obtained from the test data used to write API Publication 2519 [2]. Test data for the following roof fittings at a wind speed of 0 miles per hour were used:

- a. A 15-inch-diameter covered well, unbolted and gasketed.
- b. A 15-inch-diameter covered well, unbolted and un-gasketed.

With this information, a table of roof-fitting loss factors of the type used in Equation D-2 was developed.

The loss factors developed are applicable to average wind speeds from 2 to 15 miles per hour, which is the same range applicable to the rim-seal loss factors described in Appendix A. Although a few tests were made on certain roof fittings at a wind speed of 0 miles per hour, these were only for reference purposes.

The mathematical analysis and all supporting data used to develop the roof-fitting loss factors are in the documentation file for Appendix D.

APPENDIX E—DEVELOPMENT OF VAPOR PRESSURE FUNCTION

In the first edition of Publication 2517 [16], the evaporative-loss correlation included a vapor pressure function in the form of the following empirical relationship:

$$P' = \left(\frac{P}{14.7 - P} \right)^{0.7} = \left[\frac{P/14.7}{1 - (P/14.7)} \right]^{0.7} \quad (\text{E-1})$$

Where:

P = true vapor pressure, in pounds per square inch absolute.

This function has the undesirable property that when the stock true vapor pressure approaches 14.7 pounds per square inch absolute, the evaporative loss rate becomes infinite. Therefore, a new vapor pressure function was derived that approaches a finite value as the true vapor pressure approaches atmospheric pressure.

The following vapor pressure relationship was derived [27] based on theoretical considerations:

$$P^* = \frac{P/P_a}{\{1 + [1 - (P/P_a)^{0.5}]^2\}} \quad (\text{E-2})$$

Where:

P = true vapor pressure, in pounds per square inch absolute.

P_a = atmospheric pressure, in pounds per square inch absolute.

This vapor pressure function results in a finite evaporative loss rate as the true vapor pressure approaches atmospheric pressure. Therefore, this function is a more appropriate one to use in predicting evaporative loss.

To determine the effects of vapor pressure on evaporative loss and to evaluate the P^* relationship, a series of tests was performed in which only the stock true vapor pressure was varied [7]. During this series of tests, the stock was a mixture of propane and *n*-octane in which the propane content was varied to change the product vapor pressure from 0.75 to 9.25 pounds per square inch absolute. Test results were plotted as loss rate versus wind speed for each test and clearly showed increasing loss rate with increasing vapor pressure.

To choose the more appropriate vapor pressure function, the test results were normalized with respect to

each vapor pressure function. Curves for the loss functions versus wind speed were developed.

The evaporative-loss equation can be written as follows:

$$E = K_s M_v D \bar{P} V^n \quad (\text{E-3})$$

Where:

\bar{P} = some function of vapor pressure.

To normalize for vapor pressure (and molecular weight), the equation can be rewritten as follows:

$$\frac{E}{M_v \bar{P}} = K V^n \quad (\text{E-4})$$

Where:

K = constant equal to $K_s D$.

To evaluate a given vapor pressure function, the function can be substituted into Equation E-4. By plotting $\log (E/M_v \bar{P})$ versus $\log V$, the data can be analyzed with a linear regression technique to determine the values of K and n that yield the best-fitting curve. The correlation coefficient calculated for each curve can then be used to evaluate how well the vapor pressure function accounts for changes in loss with varying vapor pressure.

Such an analysis was done for both vapor pressure functions, P' and P^* . It was found that both functions were approximately equally good predictors within the range 2.50–9.25 pounds per square inch absolute. No tests were made at higher vapor pressures. One test was made below this range, at 0.75 pounds per square inch absolute; neither function predicted the results of this test as accurately as it predicted the results of the other tests.

It was concluded that the theoretically derived vapor pressure function, P^* (Equation E-2) is the most appropriate function to use in the evaporative-loss equation, since it approaches a finite value as P approaches P_a . This function is judged to be applicable for nonboiling stocks down to a true vapor pressure of approximately 1.5 pounds per square inch absolute.

The mathematical analysis and all supporting data used to select the vapor pressure function are in the documentation file for Appendix E.

1. The roof drain was tested with and without an insert in the upper end of the drainpipe. The insert was a 20-gauge galvanized sheet with triangular notches cut so that the remaining area represented 90-percent closure of the open roof drain.
 2. The roof drain was tested with *n*-hexane product and with product that was a mixture of propane and *n*-octane.
- d. A 2-inch-diameter, Schedule 80 open pipe, with the liquid level of the *n*-hexane product 18 inches below the top of the pipe.
 - e. A 1-inch-diameter, Schedule 40 open pipe, with the liquid level of the *n*-hexane product 18 inches below the top of the pipe.
 - f. A 4-inch-diameter, Schedule 40 pipe sleeve with a 3-inch-diameter, Schedule 40 pipe roof leg held in position by a 1.250-inch-diameter pin through a 1.375-inch-diameter pinhole located 3 inches below the top of the pipe sleeve. The closed upper end of the pipe roof leg was kept 15 inches above the top of the pipe sleeve. The following features were varied:
 1. The fitting was tested with *n*-hexane product and with product that was a mixture of propane and *n*-octane.
 2. The liquid levels used were 18 inches and 36 inches below the top of the pipe sleeve.
 - g. A 3-inch-diameter, Schedule 40 pipe sleeve with a 2.5-inch-diameter, Schedule 40 pipe roof leg held in position by a 1.250-inch-diameter pin through a 1.375-inch-diameter pinhole located 3 inches below the top of the pipe sleeve. The closed upper end of the pipe roof leg was kept 15 inches above the top of the pipe sleeve. The fitting was tested with *n*-hexane product and with product that was a mixture of propane and *n*-octane.

The data obtained from the 15-inch-diameter covered well were used to calculate losses from similar covered fittings. This calculation was based on a ratio of well diameters. Loss factors for the following roof fittings were calculated in this manner:

- a. A 20-inch-diameter gauge-float well.
- b. A 24-inch-diameter access hatch.
- c. A 6-inch-diameter rim vent.
- d. A 10-inch-diameter vacuum breaker.
- e. An 8-inch-diameter gauge-hatch/sample well.

Similarly, the test data for the 6-inch-diameter open roof drain were used to calculate losses from a 3-inch-diameter open roof drain by the ratio of the internal cross-sectional areas of the drainpipes.

D.4 Analysis of the Roof-Fitting Loss Data

The computer-controlled data acquisition system recorded the specified information from the wind tunnel.

The test data were stored on computer disks. The data were presented in the form of plots of product loss versus net time. The stored data were directly reduced by the computer, using regression techniques. The tests were documented in the form of plots of product loss versus net time.

In addition, when two-component mixtures were tested, initial, intermediate, and final samples were taken of the product, from which the compositions and vapor pressures were determined.

Least-squares regression was used on all of the test data to determine the slope of the data plots (which corresponds to the loss rate) for each roof fitting at time zero [26]. Whenever possible, the test data were fitted to a first-order polynomial, and the loss rate was determined by evaluating the first derivative of the polynomial. In several of the tests, however, the loss rate changed significantly as the test progressed. In these cases, the test data were fitted to a second-order polynomial at the start of the test, and the loss rate was determined by evaluating the first derivative of the polynomial at the start of the test. The second-order fit was used for all tests in which either the liquid level or the product vapor pressure changed significantly during the test. This method seemed reasonable, since it was only the initial loss rate that was used to calculate the roof-fitting loss factors.

The initial loss rate (in pound-moles per year) for each roof-fitting test was determined, and the recorded temperatures and measured vapor pressures were used to normalize the test data to a true vapor pressure of 1.91 pounds per square inch absolute.

These normalized test data represent the bulk of the data used to determine the roof-fitting loss factors. However, some additional data were obtained from the test data used to write API Publication 2519 [2]. Test data for the following roof fittings at a wind speed of 0 miles per hour were used:

- a. A 15-inch-diameter covered well, unbolted and gasketed.
- b. A 15-inch-diameter covered well, unbolted and un-gasketed.

With this information, a table of roof-fitting loss factors of the type used in Equation D-2 was developed.

The loss factors developed are applicable to average wind speeds from 2 to 15 miles per hour, which is the same range applicable to the rim-seal loss factors described in Appendix A. Although a few tests were made on certain roof fittings at a wind speed of 0 miles per hour, these were only for reference purposes.

The mathematical analysis and all supporting data used to develop the roof-fitting loss factors are in the documentation file for Appendix D.

APPENDIX E—DEVELOPMENT OF VAPOR PRESSURE FUNCTION

In the first edition of Publication 2517 [16], the evaporative-loss correlation included a vapor pressure function in the form of the following empirical relationship:

$$P' = \left(\frac{P}{14.7 - P} \right)^{0.7} = \left[\frac{P/14.7}{1 - (P/14.7)} \right]^{0.7} \quad (\text{E-1})$$

Where:

P = true vapor pressure, in pounds per square inch absolute.

This function has the undesirable property that when the stock true vapor pressure approaches 14.7 pounds per square inch absolute, the evaporative loss rate becomes infinite. Therefore, a new vapor pressure function was derived that approaches a finite value as the true vapor pressure approaches atmospheric pressure.

The following vapor pressure relationship was derived [27] based on theoretical considerations:

$$P^* = \frac{P/P_a}{\{1 + [1 - (P/P_a)^{0.5}]^2\}} \quad (\text{E-2})$$

Where:

P = true vapor pressure, in pounds per square inch absolute.

P_a = atmospheric pressure, in pounds per square inch absolute.

This vapor pressure function results in a finite evaporative loss rate as the true vapor pressure approaches atmospheric pressure. Therefore, this function is a more appropriate one to use in predicting evaporative loss.

To determine the effects of vapor pressure on evaporative loss and to evaluate the P^* relationship, a series of tests was performed in which only the stock true vapor pressure was varied [7]. During this series of tests, the stock was a mixture of propane and *n*-octane in which the propane content was varied to change the product vapor pressure from 0.75 to 9.25 pounds per square inch absolute. Test results were plotted as loss rate versus wind speed for each test and clearly showed increasing loss rate with increasing vapor pressure.

To choose the more appropriate vapor pressure function, the test results were normalized with respect to

each vapor pressure function. Curves for the loss functions versus wind speed were developed.

The evaporative-loss equation can be written as follows:

$$E = K_s M_v D \bar{P} V^n \quad (\text{E-3})$$

Where:

\bar{P} = some function of vapor pressure.

To normalize for vapor pressure (and molecular weight), the equation can be rewritten as follows:

$$\frac{E}{M_v \bar{P}} = K V^n \quad (\text{E-4})$$

Where:

K = constant equal to $K_s D$.

To evaluate a given vapor pressure function, the function can be substituted into Equation E-4. By plotting $\log (E/M_v \bar{P})$ versus $\log V$, the data can be analyzed with a linear regression technique to determine the values of K and n that yield the best-fitting curve. The correlation coefficient calculated for each curve can then be used to evaluate how well the vapor pressure function accounts for changes in loss with varying vapor pressure.

Such an analysis was done for both vapor pressure functions, P' and P^* . It was found that both functions were approximately equally good predictors within the range 2.50–9.25 pounds per square inch absolute. No tests were made at higher vapor pressures. One test was made below this range, at 0.75 pounds per square inch absolute; neither function predicted the results of this test as accurately as it predicted the results of the other tests.

It was concluded that the theoretically derived vapor pressure function, P^* (Equation E-2) is the most appropriate function to use in the evaporative-loss equation, since it approaches a finite value as P approaches P_a . This function is judged to be applicable for nonboiling stocks down to a true vapor pressure of approximately 1.5 pounds per square inch absolute.

The mathematical analysis and all supporting data used to select the vapor pressure function are in the documentation file for Appendix E.

APPENDIX F—DEVELOPMENT OF PRODUCT FACTORS

F.1 General

The test-tank data used to determine relative losses were obtained with mixtures of propane and *n*-octane, using direct measurement of vapor losses. To apply these results to refined products, such as gasolines, and to crude oil stocks, it was necessary to relate direct measurements from gasoline and crude oil to the mixtures of propane and *n*-octane under the same rim-seal configuration and wind-speed conditions. It was expected that after the measurements were normalized for differences in true vapor pressure and vapor molecular weight, these different stocks would have the same loss. However, differences in losses were observed even after this normalization. Therefore, a product factor, K_c , was needed in the loss equation to account for this observed difference in losses from one stock to another.

F.2 Theoretical Considerations

Crude oil losses were significantly lower than the losses from the mixtures of propane and *n*-octane under the same conditions of rim-seal configuration and wind speed. This difference was attributed to mass transfer effects that would occur when the evaporation was taking place under nonequilibrium conditions. If the rate at which evaporation occurs exceeds the rate at which the evaporating light ends migrate from the liquid bulk to the liquid surface, the evaporation is occurring under a nonequilibrium condition. The migration rate of the light ends depends strongly on the viscosity of the liquid; that is, as stock viscosity increases, migration rate decreases, promoting nonequilibrium conditions. Therefore, under the same conditions, as a stock's viscosity increases compared with that of mixtures of propane and *n*-octane, the loss will be less.

F.3 Crude Oil Factor

Evaporative loss data for crude oil and mixtures of propane and *n*-octane at varying wind speeds and three different rim-seal configurations were compared to quantify a crude oil product factor [23]. The data were first analyzed as described in Appendix B and the documentation file for Appendix F. After the data were normalized for vapor pressure and vapor molecular weight, the average ratios of losses from crude oil to losses from mixtures of propane and *n*-octane were cal-

culated. For rim-seal systems tested with only a primary seal, the average ratio was approximately 0.3. For rim-seal systems that included a rim-mounted secondary seal, the ratio was approximately 0.6, although the absolute magnitude of the crude oil losses was lower.

The increase in the product factor when a secondary seal was present is consistent with a reduced loss rate (that is, more nearly equilibrium conditions) caused by the secondary seal. However, more data are necessary to confirm that these factors are generally applicable. By averaging all the data together, an average product factor of 0.4 was determined. Because of the limited data base, it was judged that 0.4 is the most appropriate product factor for all tanks used to store crude oil, irrespective of the tank rim-seal system.

The crude oil factor is judged to be conservative for crude oils in general, since a relatively light crude oil was tested and heavier crude oils would have lower product factors.

API Bulletin 2518 [1] on losses from fixed-roof tanks includes a product factor of 0.58 for crude oil losses compared with gasoline losses. Although the data on which this factor is based are not directly comparable with data for floating-roof tanks, they tend to support the crude oil product factor discussed above. Also, a theoretical determination [23] of the expected crude oil product factor resulted in an estimate of 0.5, which also supports the test results.

F.4 Gasoline Factor

Evaporative loss data for gasoline were also compared with the loss data for mixtures of propane and *n*-octane [21]. These data were available only for a single rim-seal condition at a single wind speed. By a similar analysis, a ratio of losses from gasoline to losses from mixtures of propane and *n*-octane of approximately 0.9 was calculated. However, because of the similarity in viscosity between gasoline and mixtures of propane and *n*-octane and the limited loss data available for comparison, a product factor of 1.0 was judged to be reasonable and conservative for predicting gasoline losses (that is, such calculated losses will be higher than losses calculated using a factor of 0.9).

The mathematical analysis and all supporting data used to develop the product factors are in the documentation file for Appendix F.

APPENDIX G—DEVELOPMENT OF CLINGAGE FACTORS

G.1 General

A number of shell-wetting tests were performed to estimate the amount of stock remaining on the tank shell as the floating roof descends while the tank is emptied. In these tests a steel test plate was immersed in stock and then slowly withdrawn past sections of rim seal to simulate roof travel inside a tank.

A container was filled with a known volume of the test liquid. The test plate was slowly pulled out of the liquid between a pair of resilient-foam-filled seals 2 feet in length at a rate roughly equivalent to that at which a tank would be emptied. The plate was then reimmersed after most of the liquid had evaporated, and the remaining volume of liquid was determined. Enough tests were made to determine an accurate volume change, from which the clingage factor, C , in barrels per 1000 square feet, was calculated.

A separate series of tests was conducted to determine the evaporation that would have occurred without movement of the test plate, so that the results could be adjusted to represent only the withdrawal loss due to stock clingage to the test plate.

G.2 Gasoline Tests

Four shell-wetting tests were conducted with *n*-octane stock [28], which has clingage characteristics representative of those of gasoline. A lightly rusted steel plate was

used, and the seal position was varied. The resulting clingage factors ranged from 0.0010 to 0.0019 barrels per 1000 square feet, with an average of approximately 0.0015 barrels per 1000 square feet. The test results are considered conservative, since rim-seal pressure was not introduced to produce a wiping action on the steel plate.

G.3 Crude Oil Tests

Five shell-wetting tests were conducted with a medium-volatility crude oil [23]. Again, a lightly rusted steel plate was used, and the seal position was varied. The resulting clingage factors ranged from 0.0032 to 0.0072 barrels per 1000 square feet, with an average of approximately 0.0060 barrels per 1000 square feet.

G.4 Other Shell Conditions

Clingage factors for dense rust were determined by multiplying the values for light rust by a factor of 5. This factor is based on data referred to in the first edition of API Publication 2517 [16]. This publication also referred to data which indicated that gunite-lined tanks have a clingage factor 100 times greater than the factor for a lightly rusted steel. The resulting clingage factors are summarized in Table 11.

The mathematical analysis and all supporting data used to develop the clingage factors are in the documentation file for Appendix G.

APPENDIX H—DOCUMENTATION RECORDS

The documentation records for this publication contain the following files:

- a. Documentation file for Appendix A, "Development of Rim-Seal Loss Factors."
- b. Documentation file for Appendix B, "Development of Relationship Between Airflow Rate and Wind Speed."
- c. Documentation file for Appendix C, "Development of Diameter Function."
- d. Documentation file for Appendix D, "Development of Roof-Fitting Loss Factors."
- e. Documentation file for Appendix E, "Development of Vapor Pressure Function."
- f. Documentation file for Appendix F, "Development of Product Factors."
- g. Documentation file for Appendix G, "Development of Clingage Factors."

The documentation records are maintained and are available for inspection at the Measurement Coordination Department, American Petroleum Institute, 1220 L Street, N.W., Washington, D.C. 20005.

Copies of some of the sections may be obtained from API on request for a copying fee.

Order No. 852-25170

American Petroleum Institute
1220 L Street, Northwest
Washington, D.C. 20005

